

Developing High-Affinity Protein Capture Agents
and Nanotechnology-Based Platforms for *In Vitro* Diagnostics

Thesis by
Rosemary Dyane Rohde
In Partial Fulfillment of the Requirements
for the Degree of
Doctor of Philosophy



California Institute of Technology
Pasadena, California
2009
(Defended May 27, 2009)

This thesis is dedicated to my Mom for her unconditional and everlasting love and support.

Acknowledgements

The work described in this thesis would not have been possible without guidance from many people. First, I would like to thank my advisor, Jim Heath. Jim is an inspiration— his intensity, creativity, and dedication to science is admirable. I never left his office without being motivated and excited to further my research. I am thankful for the space, funding, and intellectual support he has provided me. I am excited to continue to work with him at our new start-up called Integrated Diagnostics. Thank you to the rest of my faculty committee: Geoffrey Blake, Jack Beauchamp, and Christina Smolke. It has been an honor to work with such a distinguished group of scientists. I would especially like to thank my lab mate, Heather Agnew, who is a great scientist— hard working, passionate, and dedicated. I am truly grateful to have worked with her over the years. She is also an inspiration and has helped me grow into the scientist I am today. Special thanks to Arundhati Nag, Dr. Steven Millward, Dr. Woon-Seok Yeo, and Dr. Ryan Bailey for useful discussions, assistance with experiments, and support. I also want to thank all the bright undergraduates: Abdul Ahad Tariq, Vanessa M. Burns, Russell J. Krom, Marissa Barrientos, Eric M. Johnson, and Andreea D. Stuparu, who worked with me throughout the years. Thanks to everyone in the Heath group for caring about my graduate career and me. Your ideas, support, and suggestions are greatly appreciated. Thanks to Kevin Kan for fixing my computer several times. Thanks to Diane Robinson and Gabe Kwong for all their advice and support. I would like to thank the people at The Scripps Research Institute: Dr. Jason E. Hein, Dr. Suresh M. Pitram, Dr. Valery Fokin, Dr. M. G. Finn, and Dr. Barry K. Sharpless for our scientific conversations and collaborations. Special thanks to Dr. Michael McAlpine, Dr. Mario Blanco, Dr. Bert

Lai, and Dr. Bruce Brunschwig for their teachings and help with experiments.

I greatly appreciate the Bill and Melinda Gates Foundation for supporting my education, including my undergraduate studies at UCLA. I thank the Genomics Facility for use of the Genepix 4200 array scanner. ESI- and MALDI-MS analysis was completed by the Protein/Peptide MicroAnalytical Laboratory. Fluorescence polarization experiments were done in the Beckman Institute Laser Resource Center. SPR experiments were performed in the Protein Expression Center, under the direction of Jost Vielmetter. I thank Carl S. Parker for assistance with dot blot experiments.

Importantly, I thank my loved ones who are always a constant source of support. My wonderful mom, Lily Coloma, taught me the value of unconditional love. The sacrifices she made for me will never be forgotten. Thanks to George Porcari who has always been there for me, whether I needed help moving, a visit, or a phone call. I thank my aunts, Rosana Coloma-Diaz, Jenny Member, and Raquel Coloma, who are strong, hardworking beautiful women. I thank my uncles, Joe Diaz and Gregory Rohde, for their support. Thanks to all my family in Peru, especially my Abuelita Lily Coloma, for their love. I thank all my friends for their motivation and encouragement. I especially thank Moises Robles, Christine Baron, and Ronnie Bryan, who have helped me developed into the person I am today. Thanks to everyone who proofread my thesis. Thanks to all the GSC, Net Impact, and SASS students, staff, and administration that have worked with me over the years to help improve the quality of life at Caltech. I will miss Caltech and its community.

Abstract

Blood protein diagnostics has the potential to revolutionize health care by providing the relevant clinical measurements that can provide the foundation for predictive, preventive, and personalized medicine.¹ Blood bathes all organs in the body, with a circulation time of just a few minutes.² Those organs secrete proteins into the blood, some of which contain information relevant to the health or disease status of the organ.³⁻⁵ Thus, the blood potentially provides a window into the health state of each individual, and the organ-specific secreted proteins can provide a molecular fingerprint of disease. The hypothesis is that each organ (and its associated diseases) has a unique fingerprint that can be read from the blood with an appropriately multiplexed diagnostic platform. These fingerprints potentially provide insight that can be harnessed for early disease diagnostics, since the protein levels associated with the organ-specific fingerprint will be altered by the onset of disease and by the stages of disease progression. A challenge is that capturing each organ-specific blood fingerprint will require the assessment of the levels of many blood protein biomarkers. Capturing the fingerprint from all of the 50 or so major organs (or organ regions) may require the measurement of from several hundred to a thousand or more proteins. Meeting such a challenge requires new technologies at all levels— from devices designed to process and deliver the blood proteins for measurement,^{2,6,7} to sensitive measurement approaches,⁸⁻¹² to affinity agents that can be utilized to capture the relevant biomarker proteins,¹³⁻¹⁷ to computational approaches that can process large numbers of measurements into a result that can be interpreted by a physician.^{3,4,18-20}

To realize this vision of personalized healthcare, disease diagnostics measurements must be extremely inexpensive. Currently the assessment of blood-based protein biomarkers can take from between several hours to several days, depending upon the resources of a specific healthcare clinic. Consider, for example, a prostate-specific antigen (PSA) ELISA (enzyme-linked immunosorbent assay) test that helps detect prostate cancer in men.²¹ In this test, a patient's serum is diluted and applied to a plate to which PSA antigens have been attached. If antibodies to PSA are present in the serum, they may bind to these PSA antigens. The plate is then washed to remove all other components of the serum. A specially prepared "secondary antibody" — an antibody that specifically binds to human antibodies — is then applied to the plate, followed by another wash. Prior to this step, the secondary antibody is chemically linked to an enzyme. Thus, after application of the secondary antibody, the plate will contain immobilized enzyme in proportion to the amount of secondary antibody bound to the plate. A substrate for the enzyme is applied, and catalysis by the enzyme leads to a change in color or fluorescence. ELISA results are reported as a number; the most subjective aspect of this test is determining the "cut-off" point between a positive and negative result. This ELISA assay is representative of a typical test for a protein biomarker but it does have its disadvantages. First, it requires large amounts (~ 5–10 ml) of blood to be collected from the patient. Second, the long time period separating the point of blood collection from the time of measurement has associated costs in terms of both measurement accuracy (degradation of blood-based proteins) and labor costs. Third, the antibodies that serve as protein capture agents are expensive to develop, purchase, and store, and can be degraded by any number of subtle physical, chemical, and biological influences. Fourth, most

diagnostics measurements are pauciparameter. Fifth, the sensitivity, specificity, and/or dynamic range of the biomarker detection strategies are often limited.

In this thesis, I describe projects that were aimed at addressing specific aspects of some of these problems. Nanoelectronic sensors, such as silicon nanowires (SiNWs),^{12,22} can provide quantitative measurements of protein biomarkers in real time. Another advantage of SiNWs is that they are label-free sensors, so no secondary antibody is needed to detect the binding event. The goal is to fabricate large arrays of SiNW circuits, each of which can be individually functionalized by a different capture agent. When the blood protein binds to the specific capture agent, both the electrical conductance of the nanowire and the electrical capacitance between the nanowire and the serum is changed. These changes correlate to the amount of the protein in the blood, and thus permit a label-free, real-time measurement. One technical challenge for nanoelectronic protein sensors is to develop chemistry that can be applied for selectively encoding the nanowire surfaces with capture agents, thus making them sensors that have selectivity for specific proteins or other biomolecules. Furthermore, because of the nature of how the sensor works, it is desirable to achieve this spatially selective chemical functionalization without having the silicon undergo oxidation. The native oxide on silicon (SiO_2) has a low isoelectric point, meaning that under physiological conditions (= pH 7.4), surfaces are negatively charged.²³ These surface charges can potentially limit the sensitivity of certain nanoelectronic biomolecular sensor devices through Debye screening of the biomolecular probe/target binding event to be sensed. Furthermore, the native oxide of Si can detrimentally impact carrier recombination rates.²⁴ For high-surface-area devices, such as SiNWs, this can likely result in a degradation of electrical properties.

A general method for the non-oxidative functionalization of single-crystal silicon (111) is described in Chapter 1. The general approach is to start with a silicon-on-insulator (SOI) wafer. A SOI wafer is comprised of a thin, single-crystal silicon film (~ 30–50 nm) on top of a thick, insulating SiO₂ layer (on the order of microns). It is from this SOI layer that the nanowire sensors are fabricated. The silicon film, unless specially treated, is naturally passivated with a thin (1–2 nm thick) native oxide (SiO₂) layer as described above. To remove the native oxide, the silicon surface is fully acetylenylated (-C≡CH), thus preventing the growth of oxidation. Additionally, the -C≡CH group also provides a chemical handle for additional functionalization via the ‘click’ reaction^{25,26} between an azide containing benzoquinone (masked with a primary amine) and the surface-bound alkyne. The benzoquinone is electrochemically reduced, exposing the amine terminus. During this process, minimal oxidation is present. Molecules presenting a carboxylic acid have been immobilized to the exposed amine sites. This strategy provides a general platform that can incorporate organic and biological molecules on Si (111) with minimal oxidation of the silicon surface. This method can further be extended towards the selective biopassivation of capture agent arrays of nanoelectronic sensor devices.

The development of these devices is, in part, driven by early diagnosis, differential treatment, monitoring, and personalized medicine— all of which are increasingly requiring quantitative, rapid, and multiparameter measurement capabilities on ever smaller amounts of tissues, cells, serum, etc.^{1–5} To begin achieving this goal, a large number of protein biomarkers need to be captured and quantitatively measured to create a diagnostic panel. One of the greatest challenges towards making protein-

biomarker-based *in vitro* diagnostics inexpensive involves developing capture agents to detect the proteins. In the content of this thesis, a capture agent is a biochemical molecule that has specificity for a distinct target molecule and can be naturally derived and/or synthetic. A major thrust of this thesis is to develop multi-valent, high-affinity and high-selectivity protein capture agents using *in situ* click chemistry.²⁷⁻³⁰ *In situ* click chemistry is a tool that utilizes the protein itself to catalyze the formation of a biligand from individual azide and alkyne ligands that are co-localized. Large libraries of peptides are used to form the body of these ligands, also providing high chemical diversity and protease stability, with minimal synthetic effort. Peptide-based moderate-affinity lead compounds can be isolated from a 2-generation screen of the protein against a one-bead one-compound (OBOC) library. By modifying that peptide with appropriate alkyne or azide functionalities, that peptide becomes an anchor (1°) ligand, and part of the capture agent. Simultaneously screening the protein against this single anchor ligand and a large library of click-complementary secondary (2°) ligands constitutes our strategy for identifying biligand capture agents. The protein target holds the two peptide-units in close proximity promoting the covalent coupling between the azide and alkyne moieties. This process can be repeated—the biligand capture agent can serve as the new anchor unit and the same OBOC library can be employed to identify a triligand, tetraligand, and so forth. The addition of each ligand to the capture agent causes the affinity and selectivity to increase dramatically for its cognate protein. In particular, we describe the production of a triligand capture agent that exhibits 45 nM and 64 nM affinities against human and bovine carbonic anhydrase II (bCAII and hCAII) protein, respectively, and can be used in a dot blot test to detect those proteins at the ≥ 20 ng level from 10%

serum. *In situ* click chemistry screens are shown to yield results identical to more traditional OBOC screens, but the *in situ* screens permit orders of magnitude more chemical space to be sampled. Moreover, the resulting multiligand protein capture agents can be produced in gram-scale quantities using conventional synthetic methods with designed control over chemical and biochemical stability and water solubility.

Chapter 2 will cover the synthesis of the azide containing artificial amino acids at the multi-gram quantity scale. The construction of large (up to 20 million elements on 100 million beads) peptide libraries for screening, including bulk peptide synthesis and on-bead click reaction will be discussed. Bead-based library screening procedures will be reviewed. Analysis of lead compounds by Edman degradation will be introduced, including calibrating peptide-sequencing equipment so artificial amino acids can be identified.

Chapter 3 will cover screening procedures and results for the anchor ligand, biligand, and triligand in detail. Binding affinity measurements using fluorescence polarization and surface plasmon resonance (SPR) are reported. The sensitivity and selectivity of the multi-ligand (biligand and triligand) capture agents for CAII proteins in complex environments are demonstrated through the use of dot blot experiments in 10% serum. The advances of this approach are multifold and will be discussed in Chapter 3. This is a general and robust method for inexpensive, high-throughput capture agent discovery that can be utilized to capture the relevant biomarker proteins for blood protein diagnostics.

References:

1. Hood, L.; Heath, J. R.; Phelps, M. E.; Lin, B. Y. *Science* **2004**, *306*, 640–643.
2. Fan, R.; Vermesh, O.; Srivastava, A.; Yen, B.; Qin, L.; Ahmad, H.; Kwong, G.; Liu, C.; Gould, J.; Hood, L.; Heath, J. R. *Nature Biotechnology* **2008**, *26*, 1373–1378.
3. Davidson, E. H., et al. *Science* **2002**, *295*, (5560), 1669–1678.
4. Kitano, H. *Science* **2002**, *295*, (5560), 1662–1664.
5. Ludwig, J. A.; Weinstein, J. N. *Nature* **2005**, *5*, 845–856.
6. Toner, M.; Irimia, D. *Annu. Rev. Biomed. Eng.* **2005**, *7*, 77–103.
7. Yang, S.; Undar, A.; Zahn, J. D. *Lab Chip* **2006**, *6*, 871–880.
8. Fritz, J., et al. *Science* **2000**, *288*, 316.
9. Cui, Y.; Wei, Q.; Park, H.; Lieber, C. M. *Science* **2001**, *293*, 1289.
10. Chen, R. J., et al. *Proc. Natl. Acad. Sci. U.S.A.* **2003**, *100*, 4984.
11. Patolsky, F.; Lieber, C. M. *Mater. Today* **2005**, *8*, 20.
12. Bunimovich, Y. L.; Shin, Y.-S.; Yeo, W.-S.; Amori, M.; Kwong, G.; Heath, J. R. *J. Am. Chem. Soc.* **2006**, *128*, 16323–16331.
13. Lee, J. F.; Hesselberth, J. R.; Meyers, L. A.; Ellington, A. D. *Nucleic Acids Res.* **2004**, *32*, D95–D100.
14. Fabian, M. A., et al. *Nat. Biotechnol.* **2005**, *23*, 329–336.
15. Smith, G. P.; Petrenko, V. A. *Chem. Rev.* **1997**, *97*, 391–410.
16. Lam, K. S.; Lebl, M.; Krchňák, V. *Chem. Rev.* **1997**, *97*, 411–448.
17. Agnew, H. D.; Rohde, R. D.; Millward, S. W.; Nag, A.; Yeo, W.-S.; Hein, J. E.; Pitram, S. M.; Tariq, A.-A.; Burns, V. M.; Krom, R. J.; Fokin, V. V.; Sharpless, B. K.; Heath, J. R. *Angew. Chem. Int. Ed.* **2009**, *accepted*.
18. Cui, J., Liu, Q., Puett, D., Xu, Y. *Bioinformatics* **2008**, *24*, 2370–2375.
19. Davidson, E. H., et al. *Science* **2002**, *295*, 1669–1678.
20. Kitano, H. *Science* **2002**, *295*, 1662–1664.
21. Kuriyama M.; Wang, M.C.; Papsidero, L.D.; et al. *Cancer Research* **1980**, *40*, 4658–4662.

22. Zheng, G.; Patolsky, F.; Cui, Y.; Wang, W. U.; Lieber, C. M. *Nature Biotechnol.* **2005**, *23*, 1294, and references therein.
23. Hu, K.; Fan, F.-R. F.; Bard, A. J.; Hillier, A. C. *J. Phys. Chem. B* **1997**, *101*, 8298.
24. Yablonovitch, E.; Allara, D. L.; Chang, C. C.; Gmitter, T.; Bright, T. B. *Phys. Rev. Lett.* **1986**, *57*, 249.
25. Kolb, H. C.; Finn, M. G.; Sharpless, K. B. *Angew. Chem., Int. Ed.* **2001**, *40*, 2004.
26. Bock, V. D.; Hiemstra, H.; van Maarseveen, J. H. *Eur. J. Org. Chem.* **2006**, *51*, and references therein.
27. Lewis, W. G.; Green, L. G.; Grynszpan, F.; Radić, Z.; Carlier, P. R.; Taylor, P.; Finn, M. G.; Sharpless, K. B. *Angew. Chem. Int. Ed.* **2002**, *41*, 1053–1057.
28. Manetsch, R.; Krasinski, A.; Radić, Z.; Raushel, J.; Taylor, P.; Sharpless, K. B.; Kolb, H. C. *J. Am. Chem. Soc.* **2004**, *126*, 12809–12818.
29. Bourne, Y.; Kolb, H. C.; Radić, Z.; Sharpless, K. B.; Taylor, P.; Marchot, P. *Proc. Natl. Acad. Sci. USA* **2004**, *101*, 1449–1454.
30. Mocharla, V. P.; Colasson, B.; Lee, L. V.; Röper, S.; Sharpless, K. B.; Wong, C.-H.; Kolb, H. C. *Angew. Chem. Int. Ed.* **2005**, *44*, 116, and references therein.

Table of Contents

Acknowledgements	iv
Abstract	vi
References	xii
Table of Contents	xiv
List of Figures, Schemes, and Tables	xvii
Chapter 1: A Non-Oxidative Approach Towards Chemically and Electrochemically Functionalizing Si(111)	1
1.1 Introduction	2
1.2 Experimental Methods	5
1.2.1 Chemicals	5
1.2.2 Acetylenylation of Si(111)	6
1.2.3 Synthesis and Attachment of Electroactive Benzoquinone	7
1.2.4 Electrochemical Activation and Attachment	10
1.3 Surface Characterization Methods	12
1.3.1 X-Ray Photoelectron Spectroscopy	12
1.3.2 Contact Angle Measurements	12
1.3.3 Electrochemical Characterization of Surface Coverages	13
1.3.4 Infrared Surface Characterization	13
1.4 Results and Discussions	14
1.4.1 X-Ray Photoelectron Spectroscopy Measurements	14
1.4.2 Contact Angle Measurements	18
1.4.3 Electrochemical Characterization of Surface Coverages	18
1.4.4 Surface Coverages Summary	20

1.4.5 Infrared Surface Characterization	21
1.4.6 Biofunctionalization of Si(111) Surfaces	23
1.5 Conclusion	24
1.6 References	26
Chapter 2: Identifying Protein Capture Agent via <i>In Situ</i> Click Chemistry	30
2.1 Introduction	31
2.2 Artificial Amino Acid Synthesis	36
2.3 One-Bead One-Compound Peptide Library Construction	39
2.3.1 Materials	39
2.3.2 Library Construction	40
2.4 <i>On Bead</i> Click Reaction	42
2.4.1 Materials	42
2.4.1 Click Reaction	42
2.5 Bead-Based Library Screening Procedures	43
2.5.1 Proteins	43
2.5.2 Screening	44
2.6 Analysis of Lead Compounds by Edman Degradation	46
2.6.1 Method	46
2.6.2 Custom Edman Degradation	47
2.7 Bulk Peptide Synthesis	50
2.8 Conclusion	50
2.9 References	51
Chapter 3: Generating a High-Quality Triligand Capture Agent for bCAII.....	54
3.1 Introduction	55
3.2 Peptide Library Construction	56
3.3 Screening and Results for Anchor Ligand	57
3.3.1 First-Generation Screen for Anchor Ligand	58

3.3.2 Re-Screening for Anchor Ligand with a Focused Library.....	60
3.4 Binding Measurements for Anchor Ligand by Fluorescence Polarization	61
3.5 <i>In Situ</i> Click and <i>On Bead</i> Biligand Screens and Results	63
3.5.1 First-Generation <i>In Situ</i> Biligand Screen	63
3.5.2 First-Generation <i>On Bead</i> Biligand Screen	65
3.6 Binding Measurements for Biligand by Surface Plasmon Resonance (SPR)	68
3.7 <i>In Situ</i> Click and <i>On Bead</i> Triligand Screens and Results	69
3.7.1 First-Generation <i>In Situ</i> Triligand Screen	69
3.7.2 First-Generation <i>On Bead</i> Triligand Screen	71
3.7.3 Azide-Free <i>In Situ</i> Triligand Screen	72
3.7.4 Re-Screening for Triligand Ligand with Focused Libraries	73
3.8 Binding Measurements for Triligand using SPR	76
3.8.1 Protein	76
3.8.2 SPR	76
3.9 Dot Blot Selectivity/Sensitivity Assays in Serum	78
3.10 Conclusion	80
3.11 References	83
3.12 Future Directions	85
Appendix A. Structure of the Twenty D-Amino Acids.....	87
Appendix B. Complete Structures of Biligands and Triligands	88
Appendix C. Iterative <i>In Situ</i> Click Chemistry Creates Antibody-Like Protein-Capture Agents (paper)	95

List of Figures

- Figure 1.1** XPS data of H-C≡C-[Si(111)], collected in the Si 2p region, and taken after exposure to air for up to 160 hours. The peaks for SiO_x species should appear between 100 and 104 BeV. The amount of oxidation of the Si(111) can be estimated from this data to be < 0.25 equivalent monolayers. The Si 2p features are normalized to the same height for all three scans. The 37, 79, 160 hours scans are shown offset from the 0 hours scan to reveal the spectral detail. **15**
- Figure 1.2** High-resolution XPS spectra of H-C≡C-[Si(111)], and of that surface following the click reaction to form **1s** and the reduction of **1s** to **2s**. A) Si 2p region revealing the near absence of oxide growth during the Cu^I-catalyzed click reaction, and during the reductive transformation of **1s** to **2s**. B) Scan of the C 1s region of H-C≡C-[Si(111)]. The Si-C peak is unique to H-C≡C-[Si(111)] surfaces. The C-C peak contains contributions from the C≡C bond and adventitious carbon from the environment. The C-O peak present also arises from adventitious hydrocarbons. C) Scan of the N 1s region of **1s**, validating the click formation of **1s**. The area ratio of the three peaks is 1:2:1, respectively. D) Scan of the Fe 2p region showing the formation of **3s** via the amide coupling of ferrocene carboxylic acid to **2s**. The control plots are of **1s** (dark grey) and the H-C≡C-Si(111) surface (light grey) after exposure to ferrocene carboxylic acid under the same conditions. **16**
- Figure 1.3** Cyclic voltammetry (CV) results for **1s** and **3s**. A) The electrochemical activation of **1s** → **2s**. The black trace is of the first scan, and the grey traces are of two subsequent scans, indicating nearly complete conversion of benzoquinone to hydroquinone during the first scan. B) The reversible oxidation of **3s**. Two subsequent scans are shown. All voltages are relative to Ag/AgCl. **19**
- Figure 1.4** ATR-FTIR characterization of a H-[Si(111)] and of H-C≡C-[Si(111)] in the region of the 2083 cm⁻¹ Si-H mode **22**
- Figure 1.5** Demonstration of bioattachment to H-C≡C-[Si(111)], through reductive formation of **2s** followed by the **23**

amide coupling of biotin. A) XPS of the biotinylated Si(111) surface following exposure to strept-Au, but prior to the electroless Au amplification. The Au 4f region is comprised of two spin-orbit coupled peaks: Au 4f_{7/2} (~84 BeV) and Au 4f_{5/2} (~88 BeV). The dotted trace is from H-C≡C-[Si(111)], and the gray trace is from **1s**, each exposed to biotin and strept-Au as controls. The three SEM images (B, C, and D) are of the activated and biofunctionalized surface, plus two controls. All images were taken following the electroless amplification step. The scale bar is 1 μm. B) **2s**, incubated with biotin, and exposed to strept-Au. C) H-C≡C-[Si(111)] incubated with biotin, and exposed to strept-Au. D) **1s** incubated with biotin, and exposed to strept-Au. There are at least 500 Au nucleation sites on B, 5 on C, and 7 on D.

Figure 2.1	<i>In situ</i> click chemistry schematic. Azide-alkyne partners (represented by the green hemisphere and blue cylinder, respectively) can click together on bovine carbonic anhydrase II (bCAII). The expected affinity for the biligand could approach 1 x 10 ⁻¹⁴ M.	33
Figure 2.2	Azide- and acetylene-containing amino acids used in this study	35
Figure 2.3	Solid-phase mix-and-split combinatorial synthesis	40
Figure 2.4	Imaging hit beads	46
Figure 2.5	Pulsed-Liquid cLC extended method	48
Figure 2.6	Normal 1 cLC extended gradient	48
Figure 2.7	Final steps of flask normal extended flask cycle	48
Figure 2.8	Edman traces for artificial azide-containing amino acids	49
Figure 2.9	Edman sequencing calibration for the <i>in situ</i> click hit	49
Figure 3.1	Screening for anchor ligand	58
Figure 3.2	Histogram for 51 hit sequences isolated from screen An1 (first-generation anchor ligand screen)	59
Figure 3.3	Fluorescence polarization binding isotherm for the	62

anchor ligand **lklwfk-(D-Pra)**, showing $K_D \approx 500 \mu\text{M}$.

- Figure 3.4** A) Biligand chemical structure. B) SPR response sensorgrams obtained with increasing concentration of the biligand **kwlwGl-Tz2-kfwlkl** (2 nM to 5 μM) demonstrate a 3 - μM binding affinity to bCAII. **69**
- Figure 3.5** A) Triligand chemical structure. B,C) SPR response sensorgrams were obtained with increasing concentration of triligand (0.1 nM to 162 nM) and demonstrate 45 -nM and 64 -nM affinities for human (B) and bovine (C) CA II, respectively. **77**
- Figure 3.6** A) Dot blot illustrating the limit of detection by the triligand for bCAII and hCAII in 10% serum. B) When the biligand anchor is used as the capture agent in 0.1% serum, the sensitivity is reduced > ten fold. C) Dot blot illustrating the selectivity of the triligand, compared to a commercial antibody. **80**

List of Schemes

- Scheme 1.1** Click reaction, leading to the formation of a 1,2,3-triazole **4**
- Scheme 1.2** Strategy for the functionalization of Si(111) **6**
- Scheme 1.3** Synthesis of electroactive benzoquinone **8**
- Scheme 1.4** The chemical and electrochemical steps involved in non-oxidatively activating Si(111) surfaces. The molecules or molecular components are colored to highlight their different functions. **1s** represents the surface-bound benzoquinone that resulted from the click reaction of **1** to the acetylene-modified Si(111) surface (reacted acetylene group drawn in black). Upon reduction at -800 mV (vs Ag/AgCl) of the benzoquinone to the hydroquinone, an intramolecular cyclization reaction ensues to produce **2l** (red lactone leaving group) and **2s** (the green triazole ring with an amine terminus). This represents the activated surface. The ferrocene carboxylic acid (orange), a second electrochemically active molecule, is then coupled to the Si(111) surfaces. **11**
- Scheme 2.1** Identifying a protein capture agent via *in situ* click **34**

	screen	
Scheme 2.2	Synthesis for azide-containing artificial amino acids	36
Scheme 2.3	<i>On bead</i> ‘classic’ click reaction	42
Scheme 2.4	Edman Degradation method	47
Scheme 3.1	Preparation of protein-catalyzed, multi-ligand capture agents	55
Scheme 3.2	A) <i>In situ</i> biligand screen schematic, illustrating the <i>on bead</i> biligand synthesis catalyzed by bCAII. B) <i>On bead</i> biligand library schematic	63

List of Tables

Table 1.1	Measured contact angles for various Si(111) surface	18
Table 1.2	The measured molecular surface coverages for various Si(111) surfaces, as measured by XPS or electrochemistry (EC)	20
Table 2.1	Screening summary; pH=7.4 and T=25°C, unless otherwise noted	44
Table 3.1	Libraries used in this study	57
Table 3.2	First-generation anchor ligand screen An1 (100 nM) results	59
Table 3.3	Second-generation anchor ligand screen An2a (50 nM) results	60
Table 3.4	Second-generation anchor ligand screen An2b (8nM) results	60
Table 3.5	<i>In situ</i> biligand screen Bi1 (50 nM) results	64
Table 3.6	<i>On bead</i> biligand screen Bi2a (50 nM) results	66
Table 3.7	<i>On bead</i> biligand screen Bi2b (10 nM) results	67
Table 3.8	First-generation <i>in situ</i> triligand screen Tri1 (10 nM) results	70

Table 3.9	First-generation <i>on bead</i> triligand screen Tri2 (10 nM) results	71
Table 3.10	Azide-free <i>in situ</i> triligand screen TriX results (control)	72
Table 3.11	Table 3.11 Position-dependent histograms for the first-generation <i>in situ</i> click screens, for peptides with and without an azide-containing amino acid, to generate a triligand. The final, consensus triligand sequence is indicated by red font. For the <i>in situ</i> screen, 1/3 of the beads had no azide at the x ₁ or x ₇ positions, but all hit beads contained an azide. Sample size: <i>in situ</i> and <i>in situ no azide</i> n=24	73
Table 3.12	Second-generation <i>in situ</i> triligand screen Tri3 (500 pM) results	75
Table 3.13	Second-generation <i>on bead</i> triligand screen Tri4 (250 pM) results	75

**Chapter 1: A Non-Oxidative Approach Towards Chemically and Electrochemically
Functionalizing Si (111)**

The text of this chapter was taken in part from the following manuscripts:
Rohde, R. D.; Agnew, H. D.; Yeo, W.-S.; Bailey, R. C.; Heath, J.R. *J. Am. Chem. Soc.*,
2006, 128, 9518.

1.1 Introduction

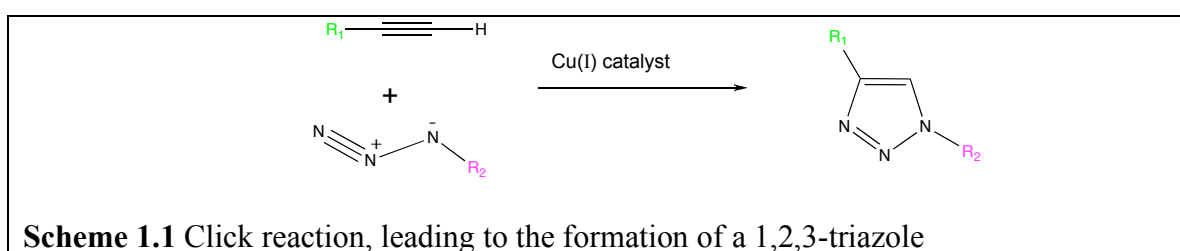
Semiconductor devices and semiconductor processing are playing an increasingly large role in biotechnology, with applications that include nanowires (NWs)¹ and nanocantilevers^{2,3} for label-free biomolecular sensors, nanofluidics for biomolecular separations,⁴⁻⁷ and a host of microfabricated lab-on-a-chip technologies.^{8,9} Coupled with these emerging nano- and microtechnologies has been the emergence of mechanical,¹⁰⁻¹² chemical, and electrochemical approaches for functionalizing and/or selectively activating surfaces. Electrochemical activation of surfaces is particularly relevant since it is shape conformal and is only limited by the size of electronically addressable features (which can be much denser than what can be spotted with an inkjet, for example). Electrochemical activation of metal surfaces has been pioneered by Mrksich,¹³⁻¹⁶ and applications of that chemistry towards the biofunctionalization of semiconductor nanowires has been demonstrated by at least two groups.^{17,18} For Si surfaces, the chemistry is particularly challenging: without protection, Si will form a native oxide that can prevent the use of silicon electrodes for electrochemical functionalization. The native oxide on silicon also has a low isoelectric point, meaning that under physiological conditions (= pH 7.4), SiO₂ surfaces are negatively charged.¹⁹ These surface charges can potentially limit the sensitivity of certain nanoelectronic biomolecular sensor devices through Debye screening²⁰ of the biomolecular probe/target binding event to be sensed. Furthermore, the native oxide of Si can detrimentally impact carrier recombination rates.²¹ For high-surface-area devices, such as Si NWs, this can likely result in a degradation of electrical properties. Thus, the ideal biofunctionalization strategy for electrochemically activating Si surfaces should begin with non-oxidized Si. The

approach should also provide continued protection of the Si surface against subsequent oxidation, and should limit the number of surface traps that can increase carrier recombination rates.

Several methods for attaching organic molecules onto non-oxidized Si surfaces have been reported. One class of schemes relies upon the direct covalent attachment of alkene-terminated molecules to H-terminated surfaces by thermal induction, ultraviolet (UV) light, or catalysis.²²⁻²⁹ These strategies have not been demonstrated as giving long-term protection to the Si surface against oxidation. Lewis' group has developed the two-step chlorination/alkylation procedure for Si(111) surfaces that is based upon Grignard chemistry.³⁰⁻³⁵ A limitation of these approaches is that only the methylated Si(111) surface (using Lewis' chemistry) can be 100% covered.^{31,36} For example, the coverage that can be achieved through the ethylation of Cl-terminated Si(111) is limited by steric effects and is about 80% of the atop sites.³⁷ For larger organic molecules, surface coverages will most certainly be lower, and resistance to oxidation reduced. In order to fully passivate the Si(111) surface, generate resistance to oxide growth, and provide for a chemically versatile surface, different surface chemistries are needed. Recently, J. J. Gooding has made passivated Si(100) surfaces using hydrosilylation and bis-alkyne for much more technologically relevant Si(100) surface against oxidation.³⁸

Chapter 1 describes a versatile and robust strategy for chemically passivating Si(111) surfaces in a manner that stabilizes the underlying Si against oxidation and allows for both chemical and electrochemical functionalization of the surface. Based upon our previous work on methylated and ethylated Si(111),³⁰⁻³⁷ we chose to explore the more chemically versatile acetylenylation ($-C\equiv CH$) of chlorine-terminated Si(111).

Work by Nemanick³⁹ and Lewis' group^{40,41} indicated that the chlorination/alkylation chemistry for acetylenylating Si(111) could proceed to completion. The footprint of the $-C\equiv CH$ on Si(111) should be as small or smaller than the $-CH_3$ group, and so a high surface coverage should be possible. Equally important is that the $-C\equiv CH$ group also provides a chemical handle for additional functionalization via the Cu(I) catalyzed Huisgen 1,3-dipolar cycloaddition ('click' reaction^{42,43}) between an azide and the surface-bound alkyne to form a 1,4-disubstituted 1,2,3-triazole (Scheme 1.1).



In particular, we designed an azide-functionalized, modified benzoquinone for attachment, via the click reaction, to the surface-bound acetylenyl groups to form a 1,2,3-triazole. The click reaction is useful because azides and acetylenes are synthetically easy to introduce, compatible with a variety of solvents and species, and tolerant against other functionality (highly specific, coupling can only occur between these two groups). Our work here follows reports that have demonstrated that different molecules can be clicked onto gold and SiO₂ surfaces in a variety of solvent and pH conditions.^{44–52}

We previously reported on the electrochemistry of hydroquinones on Si(111) and Si(100) surfaces, attached via the UV-activation of H-terminated Si.¹⁷ In that work, the hydroquinones could be reversibly oxidized to form benzoquinones (the 'activated' surface) which could then react by way of either Diels-Alder cycloaddition^{13,15} or Michael addition chemistries,^{53,54} leading to a selectively biofunctionalized Si microwire

or nanowire surface. However, while the hydroquinone coverage on the Si(111) surface did yield at least some protection for that surface against oxidation, the electrochemical step to oxidize the hydroquinone also led to oxidation of the underlying Si(111). Thus, in this work, we have designed and synthesized a benzoquinone that can be clicked onto the acetylenylated Si surface. The surface-bound benzoquinone may be then activated via electrochemical *reduction* to produce an amine terminus. We demonstrate that the entire chemical process may be accomplished in a fashion that greatly reduces the oxidation of the underlying Si. We also demonstrate the selective attachment of ferrocene onto an electrochemically activated Si(111) surface, as well as the model biomolecule, biotin.

1.2 Experimental Methods

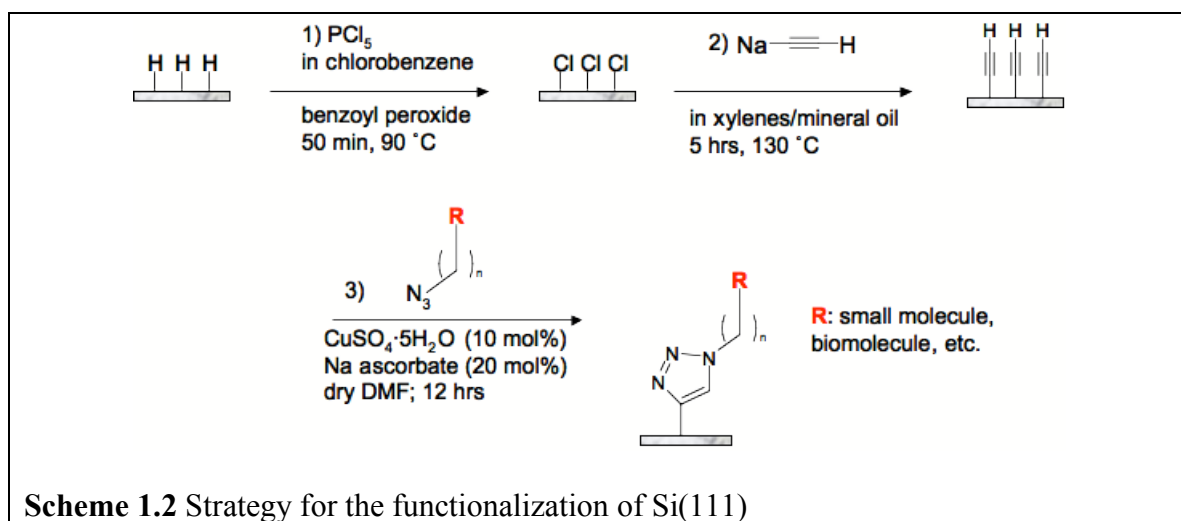
1.2.1 Chemicals

Anhydrous methanol and anhydrous tetrahydrofuran (THF, inhibitor-free) were obtained from Aldrich and exclusively stored and used in a N₂(g)-purged glove box. Chlorobenzene, benzoyl peroxide, and sodium acetylide (18 wt% in xylenes/light mineral oil) were purchased from Aldrich and were stored and used in the glove box. Phosphorus pentachloride (PCl₅) was acquired from Riedel-de Haën (Seelze, Germany). The 40% NH₄F(aq) solution was obtained from Transene Co. (Rowland, MA) and was used as received. The CuSO₄·5H₂O was obtained from Spectrum Chemical Mfg. Corp. (Gardena, CA). Sodium ascorbate, ferrocene carboxylic acid, and anhydrous *N,N*-dimethylformamide (DMF) were obtained from Aldrich. *N,N'*-Diisopropylcarbodiimide (DIC) was purchased from Anaspec (San Jose, CA). Dulbecco's Phosphate Buffered Saline (DPBS) (2.7 mM KCl, 1.5 mM KH₂PO₄, 137 mM NaCl, 8 mM Na₂HPO₄) pH 7.4 was purchased from Sigma. EZ-Link NHS-Biotin was obtained from Pierce

Biotechnology, Inc. (Rockford, IL). Nanogold Streptavidin was purchased from Invitrogen (Carlsbad, CA). GoldEnhance-EM kit for Nanogold amplification was bought from Nanoprobes (Yaphank, NY).

1.2.2 Acetylenylation of Si(111)

Scheme 1.2 shows the strategy used for functionalization of Si(111), using a two-step chlorination/alkylation method followed by Cu(I)-catalyzed click chemistry. The acetylene passivation leads to a high coverage of atop sites on an unreconstructed Si(111) surface ($97 \pm 5\%$), which resists native oxidation of the surface.^{40,41} Another advantage is the ability to use the terminal alkyne to attach a variety of molecules via click chemistry.



The starting surfaces used in these experiments were single-crystal, polished Si(111) wafers, that were 500–550 μm thick, phosphorus-doped (n-type), with 0.005–0.02 $\Omega\text{-cm}$ resistivity, and a miscut angle of 3–4° (Montco Silicon Technologies, Spring City, PA). Prior to use, the Si wafers (1 cm \times 1 cm) were cleaned by successive sonications in acetone, methanol, and isopropanol. Substrates were then rinsed with

Millipore (18 MW) water and then placed into basic piranha solution (5:1:1 = H₂O:H₂O₂:NH₄OH *warning: caustic!*) at 80 °C for 5 min. The samples were removed from piranha solution, rinsed with copious amounts of Millipore water and dried under streaming N₂(g). The samples were immediately placed in degassed NH₄F(aq) solution for 15 min. The samples were subsequently removed from the NH₄F(aq), rinsed copiously with water, dried under streaming N₂(g), and immediately loaded into a glove box.

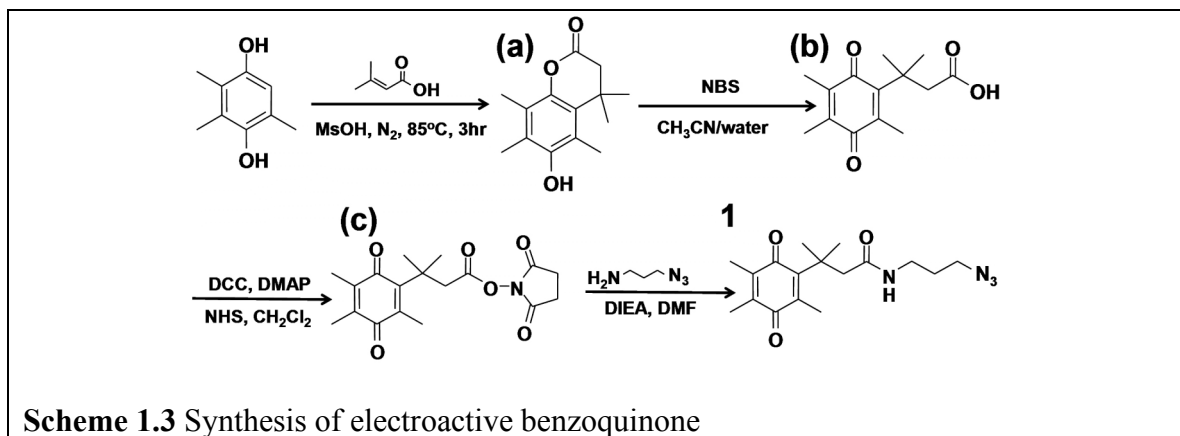
Chlorination of the Si(111) surfaces (Scheme 1.2, Step 1) was carried out in a N₂(g)-purged glove box, according to published methods.³⁰⁻³⁷ A saturated solution of PCl₅ in chlorobenzene was prepared and heated for one hour prior to use to ensure complete dissolution of the PCl₅. To 2 ml of this PCl₅ solution, the Si substrate was added with a grain of benzoyl peroxide. The solution was heated to 90 °C for 50 min. Subsequently, the samples were rinsed with anhydrous THF several times and immediately used for the acetylenylation step.

Acetylenylation of the chlorinated Si(111) surfaces (Scheme 1.2, Step 2) was performed inside the N₂(g)-purged glove box. The chlorinated wafers were immersed in a sodium acetylide (18 wt% in xylenes/light mineral oil) suspension and heated to 130 °C for 5 hours.⁴¹ After reaction, the samples were removed from solution, rinsed copiously with anhydrous THF, and then rinsed with anhydrous methanol. The samples were then immersed into a fresh volume of anhydrous methanol, taken out of the glove box into air, sonicated for 10 min, and then dried in a stream of N₂(g).

1.2.3 Synthesis and Attachment of Electroactive Benzoquinone

Scheme 1.3 describes the synthetic procedure for making the electroactive benzoquinone **1** used for all surface click reactions. A 2,3,5-trimethylhydroquinone was

treated with dimethylacrylic acid to give a lactone **(a)** by a Friedel-Crafts type addition reaction. The quinone acid **(b)** was prepared by oxidation of the resulting lactone **(a)** with aqueous N-bromosuccinimide (NBS). The acid was activated with an N-hydroxysuccinimidyl (NHS) group to give **(c)**, which was then subjected to 3-azidopropylamine to afford **1**.



6-Hydroxy-4,4,5,7,8-peptamethyl-chroman-2-one (a). 2,3,5-

Trimethylhydroquinone (2 g, 13.1 mmol) was mixed with 3,3-dimethylacrylic acid (1.45 g, 14.5 mmol) and methanesulfonic acid (10 ml). The mixture was stirred at 85 °C under nitrogen for 3 hours and then cooled to room temperature. To the mixture was added 100 g of ice with stirring. The precipitate was extracted with ethyl acetate (4 × 50 ml). The combined organic layer was washed with saturated NaHCO₃ (2 × 50 ml) and water (2 × 50 ml), and dried over MgSO₄. After filtration and evaporation, an obtained residue was recrystallized from hexane and ethyl acetate (2:1, v/v) to give 2.6 g (84%) of the desired product as a white solid. ¹H NMR 300 MHz (CDCl₃) δ 4.69 (s, 1H), 2.56 (s, 2H), 2.37 (s, 3H), 2.23 (s, 3H), 2.9 (s, 3H), 1.46 (s, 6H).

3-Methyl-3-(2,4,5-trimethyl-3,6-dioxocyclohexa-1,4-dienyl)butanoic acid (b).

To a solution of the lactone **a** (1.58 g, 6.74 mmol) in a mixture of acetonitrile (15 ml) and water (3 ml) was added N-bromosuccinimide (1.26 g, 7.08 mmol) in portions with stirring at room temperature. After 30 min, the organic solvents were evaporated under reduced pressure, and the remaining solution was extracted with CH₂Cl₂ (2 × 30 ml). The combined organic layer was dried over MgSO₄, and reduced solvent to give 1.65 g (98%) of a yellow oily product, which was used without further purification. ¹H NMR 300 MHz (CDCl₃) δ 3.04 (s, 2H), 2.15 (s, 3H), 1.96 (m, 3H), 1.94 (m, 3H), 1.45 (s, 6H).

3-Methyl-3-(2,4,5-trimethyl-3,6-dioxocyclohexa-1,4-dienyl)butanoic acid, N-hydroxysuccinimidyl ester (c). To a solution of acid **b** (326 mg, 1.30 mmol) and N-hydroxysuccinimide (152 mg, 1.32 mmol) in CH₂Cl₂ (15 ml), was added 1,3-dicyclohexylcarbodiimide (DCC, 270 mg, 1.31 mmol) portionwise, followed by a catalytic amount of *N,N*-dimethylaminopyridine (DMAP). The reaction mixture was stirred for 1 hour. The white precipitate was filtered and the filtrate was concentrated. The residue was redissolved in cold ethyl acetate (5 ml) and insoluble impurities were filtered. Solvent was removed to give 419 mg (93%) of a yellow foamy solid product. ¹H NMR 300 MHz (CDCl₃) δ 3.27 (s, 2H), 2.77 (s, 4H), 2.15 (s, 3H), 1.94 (s, 6H), 1.51 (s, 6H).

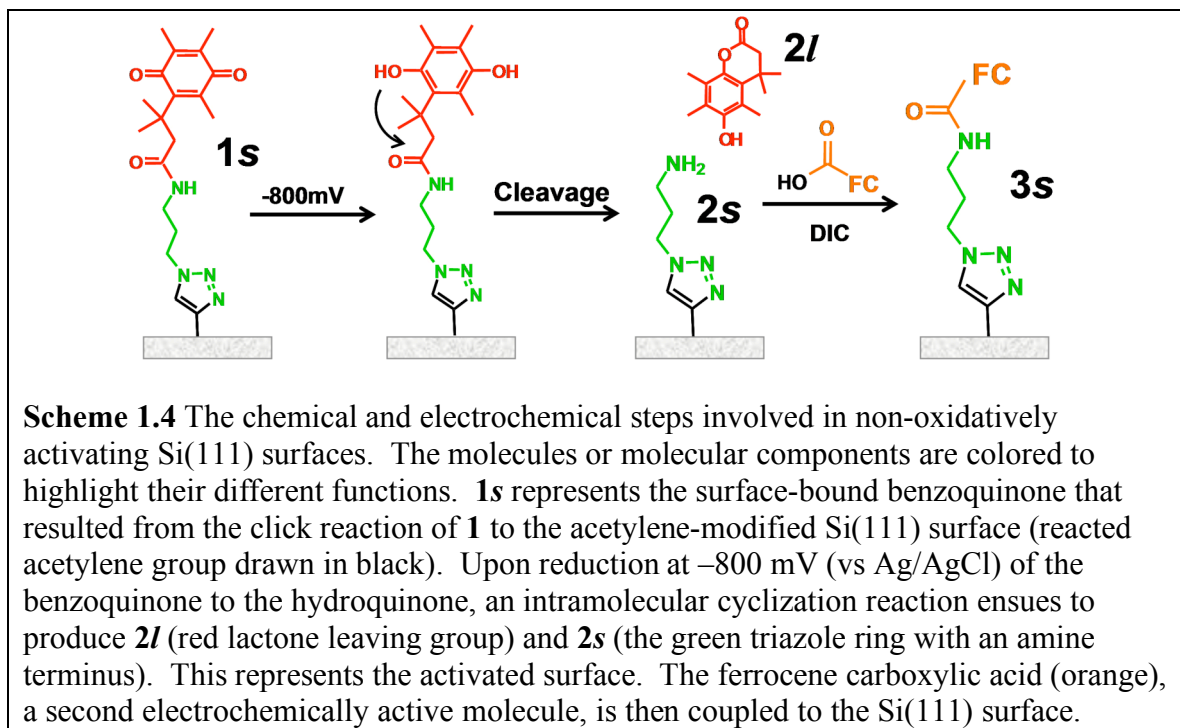
N-(3-azidopropyl)-3-methyl-3-(2,4,5-trimethyl-3,6-dioxocyclohexa-1,4-dienyl)butanamide (1). To a solution of **c** (443 mg, 1.28 mmol) in DMF (5 ml) was added diisopropylethylamine (DIEA, 523 ml, 3.06 mmol), followed by 3-azidopropylamine (153 mg, 1.53 mmol). The reaction mixture was stirred overnight at 50 °C, diluted with ethyl acetate (30 ml), washed with NH₄Cl and brine, and dried over MgSO₄. Solvent was

reduced and the residue was purified by silica gel chromatography (hex/EtOAc, 2:1) to give 370 mg (87%) of product as a yellow solid. ^1H NMR 300 MHz (CDCl_3) δ 3.30 (t, $J = 6.6$, 2H), 3.23 (q, $J = 6.6$, 2H), 2.81 (s, 2H), 2.12 (s, 3H), 1.96 (m, 3H), 1.94 (m, 3H), 1.70 (quint, $J = 6.6$, 2H), 1.41 (s, 6H). Mass (ES) m/z 333.0 ($[\text{M}+1]^+$).

Click reaction to attach **1 onto acetylene-terminated Si(111).** The click reaction of acetylene-terminated Si(111) (Scheme 1.2, Step 3) with **1** (Scheme 1.3) was carried out in anhydrous DMF. Relative to the azide, 20 mol% sodium ascorbate was added, followed by 10 mol% of $\text{CuSO}_4 \cdot 5\text{H}_2\text{O}$, and a 10 mM azide solution of **1** in DMF. The reaction was run for 12 hours in the glove box. After the reaction, the surface was sonicated in DMF for 5 min three times and then rinsed with methanol and blow dried under $\text{N}_2(\text{g})$.

1.2.4 Electrochemical Activation and Attachment

Ferrocene. **1** was attached to acetylene-terminated Si(111) using the Cu(I)-catalyzed click reaction (Scheme 1.2, Step 3), to form **1s** (Scheme 1.4). Reductive electrochemistry (-800 mV referenced to Ag/AgCl) was performed to convert the modified benzoquinone to hydroquinone in degassed DPBS (pH 7.4). The hydroquinone then underwent an intramolecular cyclization reaction leaving a free amine on the surface (**2s**) and releasing a lactone species (**2l**). This amine terminus allows for a variety of subsequent reactions, including amide coupling chemistry, which is commonly utilized to attach biomolecules to surfaces. We first illustrated the use of this electrochemical reduction process to attach ferrocene carboxylic acid to the surface, to form **3s**, via amide coupling chemistry.



Ferrocene carboxylic acid (0.02 M) and *N,N'*-diisopropylcarbodiimide (DIC) (0.13 M) in DMF were added to the free amine surface. The amide coupling reaction was run overnight covered in an N_2 -purged glove box. The surface was then sonicated three times in DMF, then MeOH, and then blown dry.

Biotin. Biotin (0.02 M) and DIC (0.13 M) in DMF were added to the free amine surface **2s**. The amide coupling reaction was run overnight in an N_2 -purged glove box at $50\text{ }^\circ\text{C}$. The surface was then sonicated three times in DMF, then MeOH, and blown dry. Subsequently, the Nanogold streptavidin (10 pM in 0.05% Tween20/DPBS) was introduced for 15 min. The surface was sonicated in 0.05% Tween20/DPBS for 25 min and then water for 5 min. The gold particles were then amplified with gold enhancement reagents for 10 min and then sonicated in water for 5 min.

1.3 Surface Characterization Methods

1.3.1 X-Ray Photoelectron Spectroscopy

X-ray photoelectron spectroscopy (XPS) was utilized to characterize many of the steps of both Schemes 1.2 and 1.4. All XPS measurements were performed in an ultra-high vacuum chamber of an M-probe surface spectrometer that has been previously described.⁵⁴ All measurements were taken on the center of the sample at room temperature. Monochromatic Al K α X-rays (1486.6 eV) were incident at 35° from the sample surface and were used to excite electrons from samples. The emitted electrons were collected by a hemispherical analyzer at a take-off angle of 35° from the plane of the sample surface.

ESCA-2000 software was used to collect and analyze the data. To get an overview of the species present in the sample, survey scans were run from 0 to 1000 binding eV (BeV). The Si 2p (97–106 BeV), Cl 2p (196–206 BeV), C 1s (282–292 BeV), N 1s (393–407 BeV), Fe 2p (695–745 BeV), and Au 4f (77–97 BeV) regions were investigated in detail.

1.3.2 Contact Angle Measurements

The sessile contact angle of water on the functionalized Si(111) surface was used to check the fidelity of the monolayer for all surfaces of Schemes 1.2 and 1.4 except H- and Cl-terminated Si(111). Contact angle measurements were obtained with an NRL C.A. Goniometer Model #100-00 (Rame-Hart, Inc.) at room temperature. Contact angles, θ , were measured from sessile drops by lowering a 1 μ l drop from a syringe

needle onto the surface. This was repeated three times and averaged to obtain the θ for the surface.

1.3.3 Electrochemical Characterization of Surface Coverages

Electrochemistry was performed in a custom-made cell using a VMP Multi-Potentiostat (Princeton Applied Research, Oak Ridge, TN). Dulbecco's Phosphate Buffered Saline (DPBS) was used as the electrolyte, with silicon as a working electrode, a Pt coil as a counter electrode, and an Ag/AgCl reference electrode. Molecular coverage was obtained by integrating the cathodic peak of the first scan in which all the modified benzoquinone was reduced to hydroquinone.

1.3.4 Infrared Surface Characterization

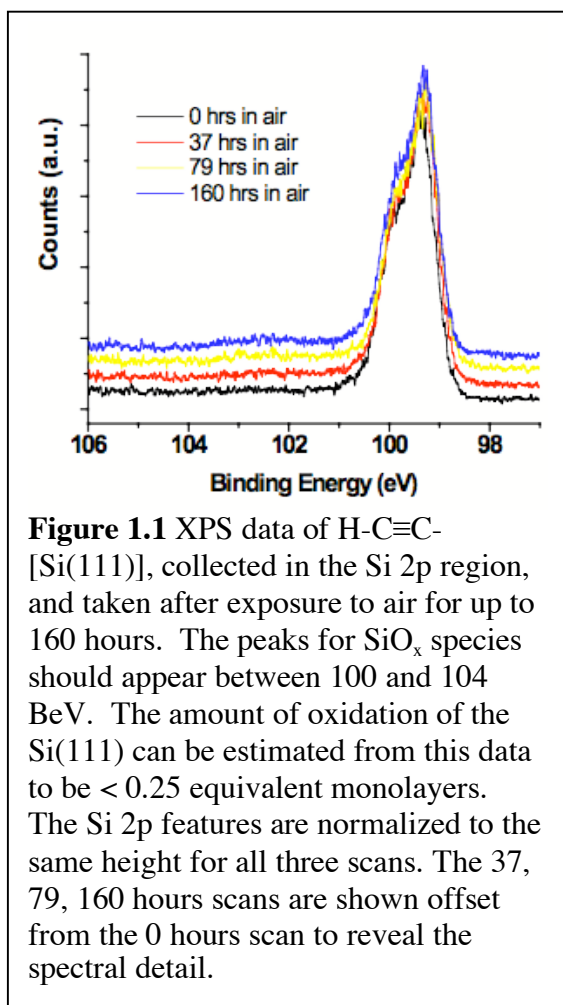
The H- and H-C \equiv C-terminated Si(111) surfaces were characterized by Attenuated Total Reflection Fourier Transform Infrared Spectroscopy (ATR-FTIR). The Si(111) surfaces were prepared from single-crystal, polished Si(111), miscut 3–4°, boron-doped (n-type), 500–550 μm thick, and with 4–20 $\Omega\text{-cm}$ resistivity (Addison Engineering, Inc., San Jose, CA). Samples were cut into (2 cm \times 2 cm) pieces and underwent the acetylenylation and click reactions as described above. Samples were mounted on a Germanium ATR crystal (GATR, Harrick Scientific Products, Inc.) for a grazing angle of 65°. The sample was placed in a Vertex 70 FT-IR spectrometer (Bruker Optics Inc.) for measurements. In an air-purged sample chamber, 512 or 1024 scans were taken, with background scans of air subtracted from the spectra. Spectra were fitted with a linear baseline prior to analysis.

1.4 Results and Discussions

1.4.1 X-Ray Photoelectron Spectroscopy Measurements

XPS survey scans revealed the progression of the acetylenylation and click chemistry steps. For a freshly prepared, H-terminated Si(111) surface (H-[Si(111)]), Si 2p and Si 2s peaks were observed, at 100 BeV and 150 BeV, respectively. Additional small C 1s and O 1s peaks, corresponding to adventitiously adsorbed carbon and oxygen on the surface, were also detected. After chlorination of H-[Si(111)] by PCl_5 , two new peaks at 200 BeV and 270 BeV appeared in the XPS spectrum, representing the Cl 2p and Cl 2s electrons, respectively. Upon a treatment with sodium acetylide, the chlorine peaks disappeared and a pronounced C 1s appeared at 285 BeV, verifying that the acetylene-terminated Si(111) surface (H-C \equiv C-[Si(111)]) has been generated. Other adsorbed carbon can contribute to the C 1s peak intensity for this scan. After the click reaction, a new N 1s peak appears at 400 BeV.

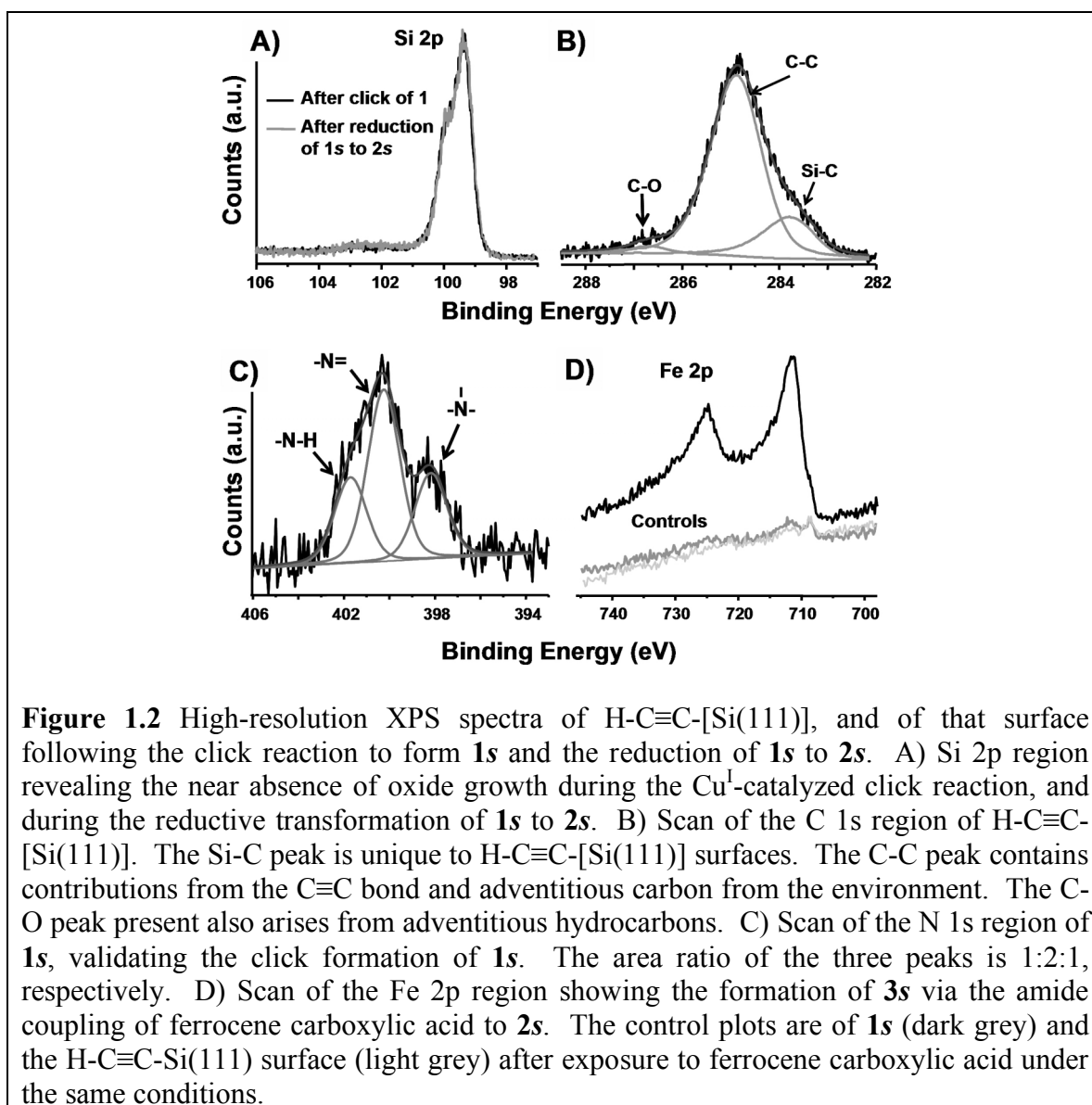
High-Resolution XPS Measurements. High-resolution XPS measurements were utilized to quantitate the chemical steps of Schemes 1.2 and 1.4. In particular, the Si 2p region was used to monitor the growth of silicon oxides as a function of exposure time to air (Figure 1.1) and as a function of the chemical and electrochemical steps of Scheme 1.4 (Figure 1.2A) in two sets of experiments. For both measurements, a Shirley baseline was applied to each spectrum before the peaks were fitted. Peak line shapes for bulk Si



2p_{3/2} and 2p_{1/2} were fitted to Voigt functions fixed at 95% Gaussian and 5% Lorentzian, with a 15% asymmetry. The Si 2p_{1/2} and 2p_{3/2} peaks were fitted with the two peaks held 0.6 BeV apart, the full width at half maximum (FWHM) was fixed at 1, and the integrated area ratio of the 2p_{1/2}/2p_{3/2} peaks was fixed at 0.51, as has been previously described.^{30–32,40} The broad peak between 100 and 104 BeV was assigned as Si⁺ to Si⁴⁺ oxides and was fitted to a third peak. The positions of the three peaks and the width of the third peak were optimized to get the best fit to the

experimental spectrum. For very thin oxide layers, the oxide coverage was calculated from the SiO_x:Si 2p peak area ratio. This was determined by dividing the area under the third peak by the total area of the Si 2p_{3/2} and 2p_{1/2} peaks.³² The SiO_x:Si 2p peak area ratio was then divided by a normalization constant of 0.21 for Si(111) to estimate the fraction of surface atoms that were oxidized.^{30–32} We estimated that there were < 0.25 equivalent monolayers of oxide on the acetylene-terminated Si(111) surface after 6 days exposure to air (Figure 1.1). This is consistent with other results that have shown stability towards oxidation for as long as 60 days in air.⁴⁰ Following the formation of 1s

and the reduction of $1s$ to $2s$ at -800 mV (Scheme 1.4), the amount of oxide was calculated to be 0.29 and 0.34 equivalent monolayers, respectively (Figure 1.2A).



The H-C≡C-[Si(111)] surface was also characterized using high-resolution XPS of the C 1s spectrum (Figure 1.2B). This spectrum was deconvoluted and fitted to three peaks, the silicon-bonded carbon at 283.8 BeV, the carbon-bonded carbon at 284.9 BeV, and the oxygen-bonded carbon at 286.8 BeV. As developed by Nemanick,^{39,40} peaks

were fitted to Voigt functions having 70% Gaussian and 30% Lorentzian line shapes. The peak center-to-center distances were fixed at 1.1 BeV between the Si-C and C-C peaks, and at 2.9 BeV between the Si-C and O-C peaks. To calculate the surface coverage of the acetylene the integrated area under the silicon-bonded carbon peak was ratioed to the total integrated area of the Si $2p_{3/2}$ and $2p_{1/2}$ peaks and normalized with respect to scan time. The ratio calculated was referenced to a methyl terminated Si(111) surface that was scanned under the same conditions. The effective coverage of acetylene on the Si surface was $97 \pm 5 \%$, consistent with other measurements of such surfaces.⁴¹ The statistical uncertainty in this number is largely determined by the signal-to-noise ratio of the XPS data ($\sim 30:1$).

The high-resolution N 1s spectrum of **1s** illustrates the attachment of the benzoquinone (**1**) via click chemistry (Figure 1.2C). The spectrum was deconvoluted and fitted to three peaks, each composed of 80% Gaussian and 20% Lorentzian line shapes.⁵⁶ The three peaks correspond to the amide nitrogen at 401.7 BeV, the doubly bonded nitrogen atoms (in the triazole ring) at 400.3 BeV, and the singly bonded nitrogen (in the triazole ring) at 398.2 BeV, respectively. The ratio of peak areas was found to be 1:2:1, consistent with the structure of **1s**. After electrochemical cleavage to **2s**, the N 1s region remained unchanged.

Figure 1.2D is a high-resolution scan of the Fe 2p region that demonstrates the attachment of ferrocene carboxylic acid onto **2s** to form **3s**. The Fe $2p_{3/2}$ and $2p_{1/2}$ peaks occur at 711.3 and 724.8 BeV, respectively. It is difficult to quantify the amount of iron from such data because the peak shape is highly asymmetric and hard to deconvolute with a single Gaussian/Lorentzian function due to the strong multiplet splitting.⁵⁶

However, as discussed below, the surface coverage of **3s** can be estimated from cyclic voltammetry measurements. Figure 1.2D also shows two control experiments. Although a trace amount of ferrocene residue is detected on the controls, this measurement does confirm that the large majority of ferrocene is the result of the covalent bond formation between carboxylic acid of the ferrocene and the free amine of **2s**.

1.4.2 Contact Angle Measurements

As the functionalized Si (111) surface changes and becomes more hydrophilic, the contact angle of water decreases. These results are listed in Table 1.1.

Table 1.1 Measured contact angles for various Si(111) surfaces

Surfaces	Contact Angle (°)
H-C≡C-[Si(111)]	77 ± 2
1s	68 ± 2
2s	60 ± 2
3s	59 ± 2

1.4.3 Electrochemical Characterization of Surface Coverages

Figure 1.3A depicts the cyclic voltammogram (CV) for **1s**. The prominent cathodic peak in the first scan confirms the presence of electroactive benzoquinone and, therefore, that the click reaction proceeded. Molecular coverage was obtained by integrating the cathodic peak of the first scan in which all the modified benzoquinone was reduced to hydroquinone. Complete conversion of **1s** to **2s** accompanied by the release of **2I** (Scheme 1.4) was achieved at potentials below -0.9 V. Consecutive CV scans show that no detectable benzoquinone remained. For the determination of coverage, the area

under the cathodic peak was obtained after subtracting the non-Faradaic current. This area was converted to the number of molecules by a stoichiometric ratio of 2 electrons to 1 electroactive molecule. Then the number of molecules was divided by the electrode surface area and then normalized to the Si atom surface density ($7.8 \times 10^{14} / \text{cm}^2$ for Si(111)).¹⁷ The coverage calculated for **1s** on the H-C≡C-[Si(111)] was $6.7 \pm 0.3 \%$.

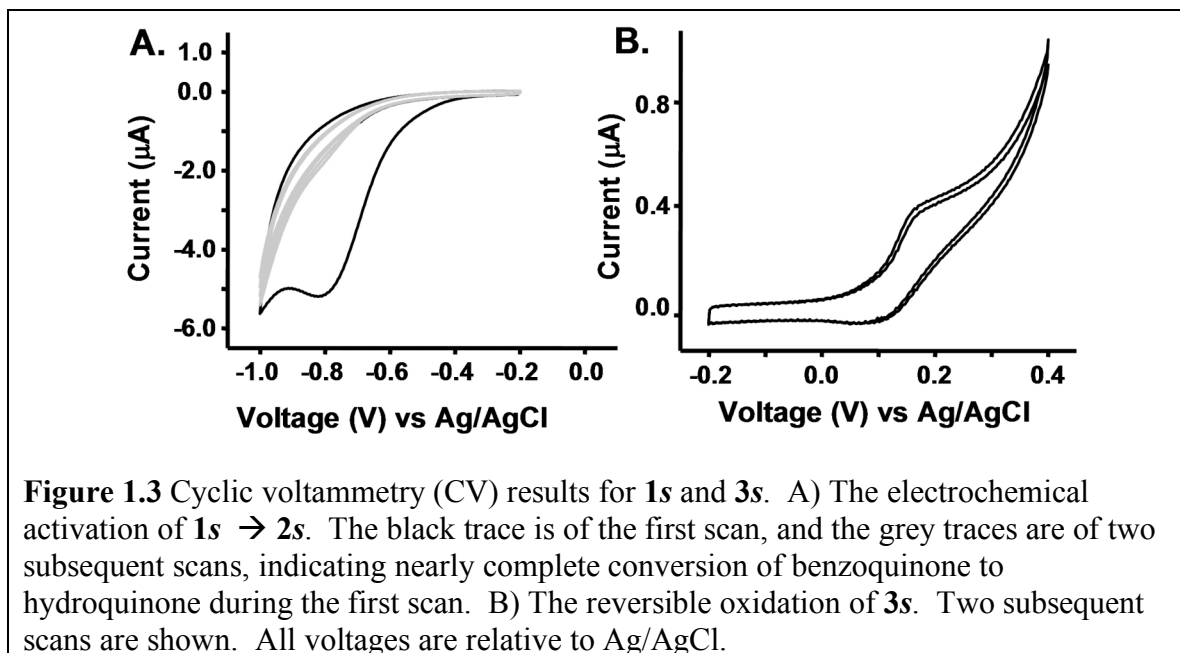


Figure 1.3B represents a CV of **3s**, the product of the amide coupling of ferrocene carboxylic acid with **2s**. The CV shows reversible $\text{Fc}^{0/+}$ redox behavior, as expected for ferrocene oxidation. The peak spacing confirms that ferrocene is covalently attached (but not adsorbed) onto the surface. The coverage was calculated by integrating the anodic peak after subtracting the non-Faradaic current. The number of molecules was divided by the electrode surface area and normalized to Si atom surface density which is $7.8 \times 10^{14} / \text{cm}^2$ for Si(111).¹⁷ The coverage calculated for **3s** was 0.5%.

1.4.4 Surface Coverages Summary

The coverage values for H-C≡C-[Si(111)], surface **1s**, and surface **3s** are summarized in Table 1.2, calculated with respect to all atop sites on an unreconstructed Si(111) surface.

Table 1.2 The measured molecular surface coverages for various Si(111) surfaces, as measured by XPS or electrochemistry (EC)

Surfaces	Coverage (%)
H-C≡C-[Si(111)]	97 ± 5 (XPS)
1s - benzoquinone	6.7 ± 0.3 (EC)
3s - ferrocene	0.5 (EC)

The 97% coverage of the H-C≡C-[Si(111)] surface is consistent with the Si 2p XPS in Figure 1.1 (and other studies⁴¹) that indicated little surface-bound SiO_x. The acetylene carbons are *sp*-hybridized, implying a perpendicular attachment to the Si(111) surface. The atomic radius for C is smaller than that for Si (0.70 Å vs 1.10 Å), and there is a 3.8 Å spacing between atop sites on Si(111). These values support the notion that a 100% passivation of Si(111) surfaces can be achieved using the approach we described here.

The coverage of the electroactive benzoquinone **1** on Si(111) to form **1s** was calculated to be ~ 7% of all available Si(111) atop sites. We previously reported on electrochemically activating Si(111) and Si(100) surfaces through the use of protected hydroquinones that were attached to H-terminated Si surfaces via UV activation.¹⁷ For those molecules, coverages of up to 23% were achievable on Si(111), although bulkier

protection groups on the hydroquinone led to slightly reduced surface coverages, implying steric interactions played at least some role in limiting coverage. It is likely that steric interactions play a dominating role in determining the efficiency of the click reaction to form **1s**. While the acetylene footprint may be approximated by the van der Waals radius of the carbon atom, the triazole ring formed upon the click reaction will obviously be much larger. In fact, it is possible that the click chemistry is only effective at the step edges of the Si(111) surface. We have extensively characterized various Si(111) surfaces that have been alkylated using the two-step chlorination/alkylation chemistry using high-resolution Scanning Tunneling Microscopy (STM). For both methylated^{31,36} and ethylated³⁷ Si(111), we find that about 10% of the Si surface atoms lie at step edges. This arises from etch pits that are apparently formed during the chlorination step⁵⁷, implying that the H-C≡C-[Si(111)] surface likely has a similar morphology. In that case, acetylene groups located at step edges would not have the steric constraints that would limit the formation of the triazole ring. It is interesting that the 7% coverage of **2s** is similar to the number of Si atop sites that would reside at step edges.

1.4.5 Infrared Surface Characterization

Additional support for 100% acetylenylation of Si(111) comes from the ATR-FTIR measurements of H-[Si(111)] and H-C≡C-[Si(111)] (Figure 1.4; black and grey traces, respectively).

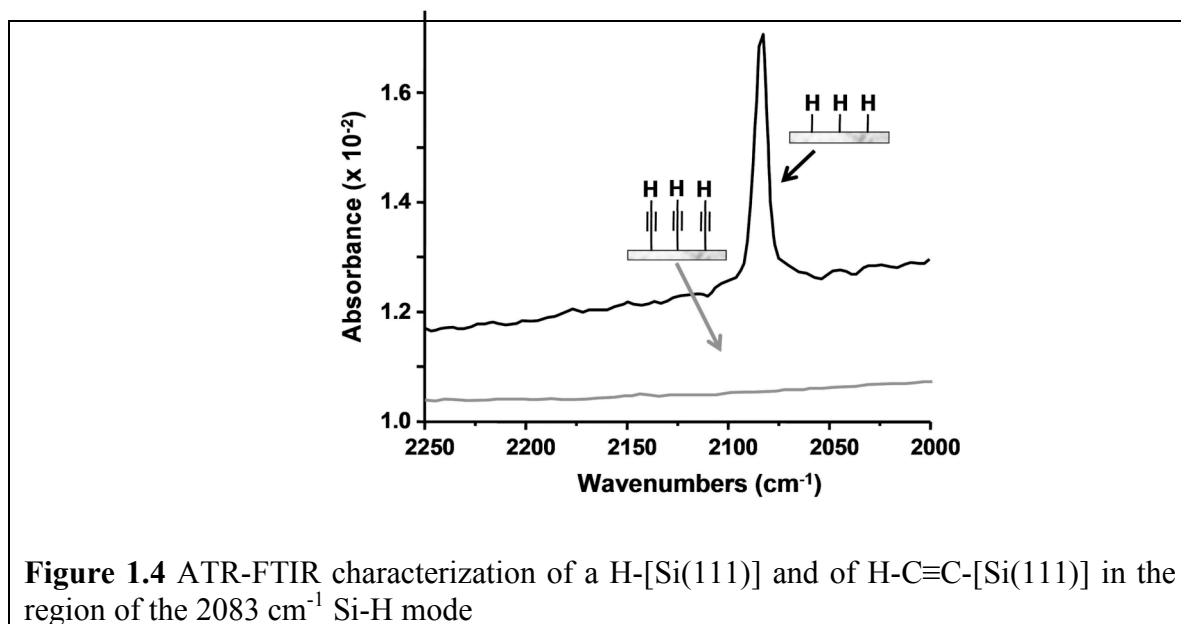


Figure 1.4 ATR-FTIR characterization of a H-[Si(111)] and of H-C≡C-[Si(111)] in the region of the 2083 cm⁻¹ Si-H mode

Whereas XPS allows analysis of the elemental composition of surfaces, infrared spectroscopy (IR) gives information about the types of chemical functionality on a surface. The spectra shown in Figure 1.4 are expanded to highlight the region containing the signature Si-H (2083 cm⁻¹) stretching frequency that is observed for the H-[Si(111)]. The Si-H stretch is strong and sharp, indicating that the surface sites are passivated with one hydrogen atom per atop site. This is expected for a H-[Si(111)] freshly prepared by an NH₄F(aq) etch.⁵⁸ For H-C≡C-[Si(111)], the 2083 cm⁻¹ vibration has quantitatively disappeared, again consistent with 100% acetylenylation and with other work.⁴¹ A weak C≡C stretch might be expected in this region (2120–2175 cm⁻¹),^{41,47} although we have not observed it. When H-[Si(111)] is ethylated through a similar chlorination/alkylation procedure, the coverage of ethyl groups on the atop sites of the Si(111) surface is limited by steric interactions to be approximately 80%.³⁷ Following the Grignard alkylation of Si(111), no Cl is detected on the surface,³⁰ and FTIR data indicates that the remaining Si(111) atop sites are hydrogenated.⁵⁹ For the ethylated surface, the 2083 cm⁻¹ feature is

broadened, shifted (to 2070 cm^{-1}), and reduced in intensity to 14% of that observed for the H-[Si(111)] surface.⁵⁹

1.4.6 Biofunctionalization of Si(111) Surfaces

The stated goal of this work was to develop a general strategy for electrochemically directing the biofunctionalization of Si(111) surfaces without oxidizing the underlying Si(111). To this end, we demonstrated the electrochemical activation and subsequent attachment of the model biomolecule, biotin, using a modification of the chemistry described in Scheme 1.4.

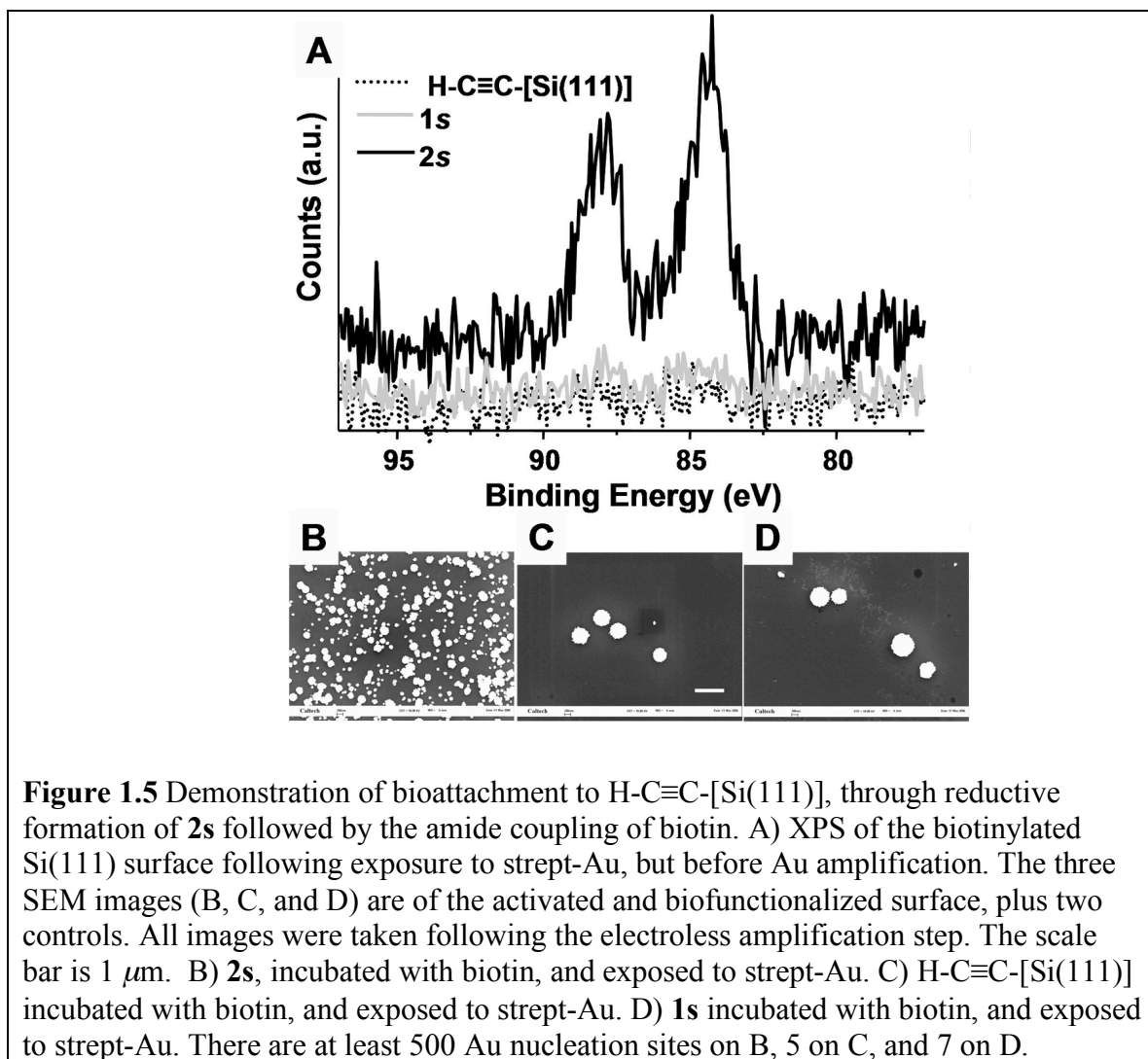


Figure 1.5A shows the XPS of the biotinylated Si(111) surface following exposure to strept-Au, but prior to the electroless Au amplification. The Au 4f region is comprised of two spin-orbit coupled peaks: Au 4f_{7/2} (~ 84 BeV) and Au 4f_{5/2} (~ 88 BeV). The dotted trace is from H-C≡C-[Si(111)], and the gray trace is from **1s**, each exposed to biotin and strept-Au as controls. To detect surface-bound biotin, we utilized Au nanoparticle-labeled streptavidin (strept-Au) and followed through with electroless amplification of the Au to produce particles that were imaged using Scanning Electron Microscopy (SEM). Representative data from this experiment, shown in Figure 1.5B, indicates that the selectivity for attachment of strept-Au onto **2s** is about 100-fold greater than on two control surfaces, H-C≡C-[Si(111)] and **1s**, both of which were also treated with biotin and exposed to strept-Au.

1.5 Conclusion

Acetylenylation of the Si(111) surface via the two-step chlorination/alkylation procedure was combined with click chemistry to provide a non-oxidative approach for adding chemical functionality to a silicon surface. Si(111) surfaces can be nearly 100% passivated with acetylene groups. A specifically designed, electroactive benzoquinone molecule has been immobilized to the H-C≡C-[Si(111)] surface. A 7% coverage of the benzoquinone was found, which implies that the click reaction likely occurred at step edges on the H-C≡C-[Si(111)] surface. The attachment of an electroactive benzoquinone was highly selective and was accomplished with only a minimal amount of oxidation of the underlying Si(111). The electroactive benzoquinone was reduced and cleaved from the surface to produce an amine terminus. In separate experiments, ferrocene carboxylic acid and biotin were selectively and covalently immobilized to the electrochemically

activated surface. X-ray photoelectron spectroscopy (XPS), Fourier transform infrared spectroscopy (FTIR), cyclic voltammetry (CV), and contact angle goniometry were utilized to characterize and quantitate each step in the functionalization process. As a result, the acetylene and click chemistries can modify silicon surfaces with minimal oxidation. This approach can be used as a general platform to prepare functional surfaces for various applications and can be extended towards the selective biopassivation of capture agents to nanoelectronic sensor devices.

1.6 References

1. Zheng, G.; Patolsky, F.; Cui, Y.; Wang, W. U.; Lieber, C. M. *Nature Biotechnol.* **2005**, *23*, 1294, and references therein.
2. Beckmann, N.; Zahnd, C.; Huber, F.; Bietsch, A.; Plückthun, A.; Lang, H.-P.; Güntherodt, H.-J.; Hegner, M.; Gerber, C. *Proc. Natl. Acad. Sci. U.S.A.* **2005**, *102*, 14587.
3. Yue, M.; Lin, H.; Dedrick, D. E.; Satyanarayana, S.; Majumdar, A.; Bedekar, A. S.; Jenkins, J. W.; Sundaram, S. *J. Microelectromech. Syst.* **2004**, *13*, 290.
4. Reccius, C. H.; Mannion, J. T.; Cross, J. D.; Craighead, H. G. *Phys. Rev. Lett.* **2005**, *95*, 268101.
5. Stavits, S. M.; Edel, J. B.; Li, Y. G.; Samiee, K. T.; Luo, D.; Craighead, H. G. *J. Appl. Phys.* **2005**, *98*, 044903.
6. Fan, R.; Karnik, R.; Yue, M.; Li, D. Y.; Majumdar, A.; Yang, P. D. *Nano Lett.* **2005**, *5*, 1633.
7. Karnik, R.; Castelino, K.; Fan, R.; Yang, P.; Majumdar, A. *Nano Lett.* **2005**, *5*, 1638.
8. Craighead, H. G.; James, C. D.; Turner, A. M. P. *Curr. Opin. Solid State Mater. Sci.* **2001**, *5*, 177.
9. Jung, D. R.; Kapur, R.; Adams, T.; Giuliano, K. A.; Mrksich, M.; Craighead, H. G.; Taylor, D. L. *Crit. Rev. Biotechnol.* **2001**, *21*, 111.
10. Piner, R. D.; Zhu, J.; Xu, F.; Hong, S.; Mirkin, C. A. *Science* **1999**, *283*, 661.
11. Lee, K.-B.; Park, S.-J.; Mirkin, C. A.; Smith, J. C.; Mrksich, M. *Science* **2003**, *295*, 1702.
12. Jung, H.; Dalal, C. K.; Kuntz, S.; Shah, R.; Collier, C. P. *Nano Lett.* **2004**, *4*, 2171.
13. Yousaf, M.; Mrksich, M. *J. Am. Chem. Soc.* **1999**, *121*, 4286.
14. Hodneland, C. D.; Mrksich, M. *J. Am. Chem. Soc.* **2000**, *122*, 4235.
15. Yeo, W.-S.; Yousaf, M. N.; Mrksich, M. *J. Am. Chem. Soc.* **2003**, *125*, 14994.

16. Yeo, W.-S.; Mrksich, M. *Adv. Mater.* **2004**, *16*, 1352.
17. Bunimovich, Y. L.; Ge, G.; Beverly, K. C.; Ries, R. S.; Hood, L.; Heath, J. R. *Langmuir* **2004**, *20*, 10630.
18. Curreli, M.; Li, C.; Sun, Y.; Lei, B.; Gundersen, M. A.; Thompson, M. E.; Zhou, C. *J. Am. Chem. Soc.* **2005**, *127*, 6922.
19. Hu, K.; Fan, F.-R. F.; Bard, A. J.; Hillier, A. C. *J. Phys. Chem. B* **1997**, *101*, 8298.
20. Israelachvili, J. *Intermolecular and Surface Forces*; Academic Press: London, **1985**.
21. Yablonovitch, E.; Allara, D. L.; Chang, C. C.; Gmitter, T.; Bright, T. B. *Phys. Rev. Lett.* **1986**, *57*, 249.
22. Sung, M. M.; Kluth, G. J.; Yauw, O. W.; Maboudian, R. *Langmuir* **1997**, *13*, 6164.
23. Sieval, A. B.; Demirel, A. L.; Nissink, J. W. M.; Linford, M. R.; van der Maas, J. H.; de Jeu, W. H.; Zuilhof, H.; Sudhölter, E. J. R. *Langmuir* **1998**, *14*, 1759.
24. Effenberger, F.; Gotz, G.; Bidlingmaier, B.; Wezstein, M. *Angew. Chem., Int. Ed.* **1998**, *37*, 2462.
25. Boukherroub, R.; Wayner, D. D. M. *J. Am. Chem. Soc.* **1999**, *121*, 11513.
26. Linford, M. R.; Fender, P.; Eisenberger, P. M.; Chidsey, C. E. D. *J. Am. Chem. Soc.* **1995**, *117*, 3145.
27. Cicero, R. L.; Linford, M. R.; Chidsey, C. E. D. *Langmuir* **2000**, *16*, 5688.
28. Buriak, J. M.; Allen, M. J. *J. Am. Chem. Soc.* **1998**, *120*, 1339.
29. Stewart, M. P.; Buriak, J. M. *J. Am. Chem. Soc.* **2001**, *123*, 7821.
30. Webb, L. J.; Nemanick, E. J.; Biteen, J. S.; Knapp, D. W.; Michalak, D. J.; Traub, M. C.; Chan, A. S. Y.; Brunschwig, B. S.; Lewis, N. S. *J. Phys. Chem. B* **2005**, *9*, 3930.
31. Yu, H. B.; Webb, L. J.; Ries, R. S.; Solares, S. D.; Goddard, W. A.; Heath, J. R.; Lewis, N. S. *J. Phys. Chem. B* **2005**, *109*, 671.
32. Webb, L. J.; Lewis, N. S. *J. Phys. Chem. B* **2003**, *107*, 5404.
33. Bansal, A.; Li, X. L.; Yi, S. I.; Weinberg, W. H.; Lewis, N. S. *J. Phys.*

- Chem. B* **2001**, *105*, 10266.
34. Royea, W. J.; Juang, A.; Lewis, N. S. *Appl. Phys. Lett.* **2000**, *77*, 1988.
35. Bansal, A.; Lewis, N. S. *J. Phys. Chem. B* **1998**, *102*, 4058.
36. Solares, S. D.; Yu, H.; Webb, L. J.; Lewis, N. S.; Heath, J. R.; Goddard, W. A., III. *J. Am. Chem. Soc.* **2006**, *128*, 3850.
37. Yu, H.; Webb, L. J.; Heath, J. R.; Lewis, N. S. *Appl. Phys. Lett.* **2006**, *88*, 252111.
38. Ciampi, S.; Böcking, T.; Kilian, K. A.; James, M.; Harper, J. B.; Gooding, J. J. *Langmuir*, **2007**, *23*, 9320.
39. Nemanick, E. J. *Chemical and Electrical Passivation of Single Crystal Silicon Surfaces through Covalently Bound Organic Monolayers*, Caltech Ph.D. Thesis, **2005**.
40. Nemanick, E. J.; Hurley, P. T.; Brunschwig, B. S.; Lewis, N. S. *J. Phys. Chem. B* **2006**, *110*, 14800–14808.
41. Hurley, P. T.; Nemanick, E. J.; Brunschwig, B. S.; Lewis, N. S., *J. Am. Chem. Soc.* **2006**, *128*, 9990–9991.
42. Kolb, H. C.; Finn, M. G.; Sharpless, K. B. *Angew. Chem., Int. Ed.* **2001**, *40*, 2004.
43. Bock, V. D.; Hiemstra, H.; van Maarseveen, J. H. *Eur. J. Org. Chem.* **2006**, *51*, and references therein.
44. Zhang, Y.; Luo, S.; Tang, Y.; Yu, L.; Hou, K.-Y.; Cheng, J. P.; Zeng, X.; Wang, P. G. *Anal. Chem.* **2006**, *78*, 2001.
45. Lummerstorfer, T.; Hoffmann, H. *J. Phys. Chem. B* **2004**, *108*, 3963.
46. Lee, J. K.; Chi, Y. S.; Choi, I. S. *Langmuir* **2004**, *20*, 3844.
47. Li, H.; Cheng, F.; Duft, A. M.; Adronov, A. *J. Am. Chem. Soc.* **2005**, *127*, 14518.
48. Zirbs, R.; Kienberger, F.; Hinterdorfer, P.; Binder, W. H. *Langmuir* **2005**, *21*, 8414.
49. Collman, J. P.; Devaraj, N. K.; Chidsey, C. E. D. *Langmuir* **2004**, *20*, 1051.
50. Collman, J. P.; Devaraj, N. K.; Eberspacher, T. P. A.; Chidsey, C. E. D. *Langmuir* **2006**, *22*, 2457.
51. Devaraj, N. K.; Dinolfo, P. H.; Chidsey, C. E. D.; Collman, J. P. *J. Am.*

- Chem. Soc.* **2006**, *128*, 1794.
52. Devaraj, N. K.; Miller, G. P.; Ebina, W.; Kakaradov, B.; Collman, J. P.; Kool, E. T.; Chidsey, C. E. D. *J. Am. Chem. Soc.* **2005**, *127*, 8600.
53. Giovanelli, D.; Lawrence, N. S.; Jiang, L.; Jones, T. G. J.; Compton, R. G. *Anal. Lett.* **2003**, *36*, 2941.
54. Rousell, C.; Rohner, T. C.; Jensen, H.; Girault, H. H. *ChemPhysChem* **2003**, *4*, 200.
55. Zheng, A.; Shan, D.; Binghe, W. *J. Org. Chem.* **1999**, *64*, 156.
56. Yeo, W.-S.; Hodneland, C. D.; Mrksich, M. *ChemBioChem* **2001**, 590.
57. Cao, P.; Yu, H.; Heath, J. R. *J. Phys. Chem. B*, **2006**, *110*, 23615.
58. Haber, J. A.; Lewis, N. S. *J. Phys. Chem. B* **2002**, *106*, 3639.
59. Babiæ-Samardzija, K.; Lupu, C.; Hackerman, N.; Barron, A. R.; Luttge, A. *Langmuir* **2005**, *21*, 12187.

Chapter 2: Identifying Protein Capture Agent via *In Situ* Click Chemistry

2.1 Introduction

In vitro diagnostic tests can be instrumental in the characterization of disease pathways and mechanisms of cancer, providing more-targeted treatment plans and better survival rates for patients. Quantitative, multi-parameter measurements of proteins in the blood, which monitor the changes in protein levels in a patient, will revolutionize *in vitro* diagnostics. A major challenge in realizing this goal is to find an efficient and general approach for producing protein capture agents for protein-biomarker-based detection that have positive attributes of antibodies, and exhibit a high level of chemical and biochemical stability. Antibodies are proteins and are, thus, unstable towards thermal shock, dehydration, pH variation, degradation and many chemical processes. In addition, developing a high affinity and selectivity antibody is very expensive and time consuming. Therefore, commercial antibodies do not exist for all proteins.¹ This is becoming an increasingly important problem as diagnostic measurements of proteins are quickly moving from single parameter to multi-parameter assays of large panels of biomarkers.²⁻⁴ Despite the drawbacks, antibodies remain the standard protein capture agent used in protein assays because of their high sensitivity and selectivity for their cognate proteins.

Nucleic acid aptamers, small molecules, and phage-display peptides are alternatives to antibodies. Nucleic acid aptamers⁵⁻⁷ are promising alternatives, with an extensive sequence space that can be screened in parallel ($\sim 10^{15}$ elements).⁸ However, the chemical diversity of aptamers is typically limited to 4 chemical constituents rather than 20 amino acids compared to peptides. Although, aptamers have been prepared as protein capture agents ($K_D \approx 10^{-8}$ - 10^{-9} M), the synthetic scale-up can be nontrivial as

aptamers are large (5–25 kDa) oligomers.⁹ Also, aptamer length does not directly translate to high three-dimensional diversity.¹⁰

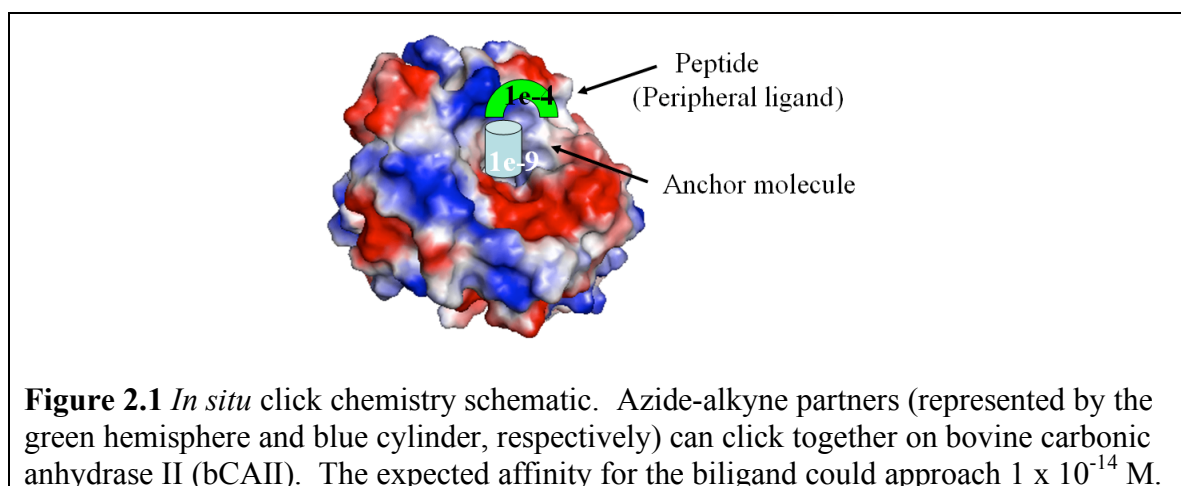
Small molecule inhibitors, while displaying very high-affinity binding ($K_D \approx 10^{-8}$ – 10^{-13} M), bind to just one epitope on the protein of interest, and that epitope may not be unique to the single protein against which the inhibitor is developed. This means that the inhibitor may exhibit cross-reactivity with other related proteins.¹¹ Moreover, small molecule libraries can be time-consuming to synthesize, and such libraries do not represent a generic platform for screening against all proteins.

Peptides selected by phage display methods also can offer reasonably high-affinity binding ($K_D \approx 10^{-8}$ – 10^{-9} M) to a protein target with a relatively low molecular mass.^{4,12} However, for phage display approaches, peptides are limited to linear sequences comprised of naturally occurring L-amino acids that provide poor bioavailability and enzymatic degradation. Other characteristics, such as water solubility, are inconsistent and dependent upon the amino acid composition of the peptide.

Peptide affinity agents can also be identified using one-bead one-compound (OBOC) libraries.^{13–15} This approach allows for the inclusion of broad classes of amino acids, including artificial and nonnatural amino acids,^{16,17} peptoids,¹⁸ and other peptidomimetics.¹⁹ However, serious trade-offs between peptide length and library diversity have to be made, since OBOC libraries are typically only 10^4 – 10^6 elements in size. Phage display, by contrast, produces $\sim 10^{12}$ element libraries. As a result, high quality protein capture agents are rarely identified from OBOC peptide libraries.

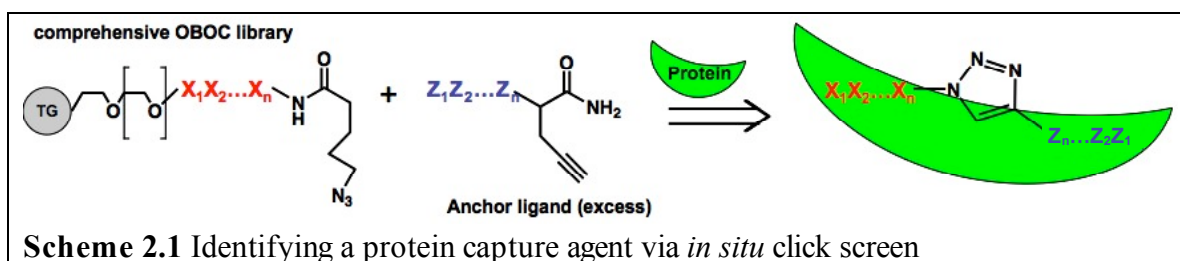
In situ click chemistry,^{20–23} as a target-guided^{24–26} approach, has been utilized previously for the identification of small molecule enzymatic inhibitors. For this method,

the protein target replaces the role of a Cu(I) catalyst for promoting the 1,3-dipolar ‘click’ cycloaddition reaction between two low-affinity molecules into a single high-affinity bivalent ligand or biligand. In these studies, a known small molecule inhibitor to a biological target is divided into parts, each part is expanded into a small library and engineered to have a terminal alkyne or azide functionality. The uncatalyzed click reaction, which is slow at room temperature, is accelerated when the azide and alkyne groups are held within close proximity by the biological target (for example, a protein). Under this condition, the azide and alkyne ‘click’ together irreversibly, creating a bivalent enzymatic inhibitor. This approach has been used to assemble small molecule inhibitors to acetylcholinesterase (AChE), carbonic anhydrase (CA), and HIV-1 protease with sub-pM binding affinities,²⁰⁻²⁶ and we have shown that peptide-based high-affinity lead compounds can be isolated with similar success. Furthermore, when a molecule with a 10^{-4} -M affinity is combined with a molecule with a 10^{-9} -M affinity, the ‘clicked’ product can exhibit an affinity as high as 10^{-13} M (Figure 2.1).²¹ While achieving the full product affinity may be rare, increasing the affinity by 2 to 3 orders of magnitude per additional ligand should be readily achievable.



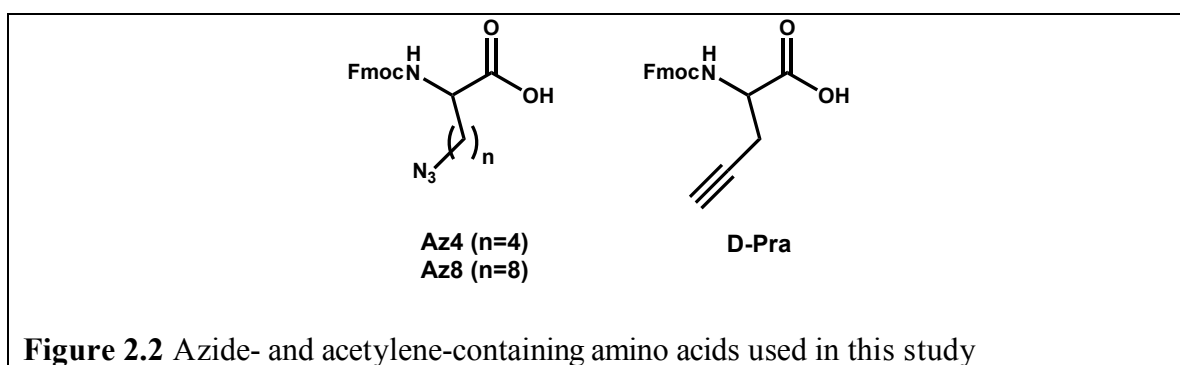
If the achieved affinity and selectivity of the biligand is not sufficient for the desired task, then the biligand itself may be treated as an anchor ligand, and the *in situ* click chemistry process may be repeated as needed to prepare triligands.^{27,28} This process can further be repeated to produce multi-ligands, such as tetraligands, pentiligands, etc., until the desired affinity is achieved. Thus, multi-valent binding agents can provide a potential shortcut to high affinity.²⁹ This approach is used here as a general platform for high-throughput peptide capture agent development.

We have generalized the *in situ* click chemistry strategy for producing protein capture agents by implementing peptides selected from OBOC libraries.¹³⁻¹⁵



OBOC libraries allow thousands to millions of compounds to be rapidly prepared on bead and screened concurrently for specific binding. For many biological targets, recognition of targets is effective using peptides as small as three-to-five amino acids in length.^{30,31} Therefore, penta- to heptapeptide libraries were expected to afford enough diversity to discriminate between weak and strong binders. OBOC libraries offer a distinct advantage in which nonnatural modifications are easily accomplished, allowing for incorporation of almost infinite diversity elements. Natural, nonnatural, and artificial amino acids are assembled together to form peptides using standard coupling chemistries.³² D-amino acids were chosen for the core of the library so that the synthesized peptides have an

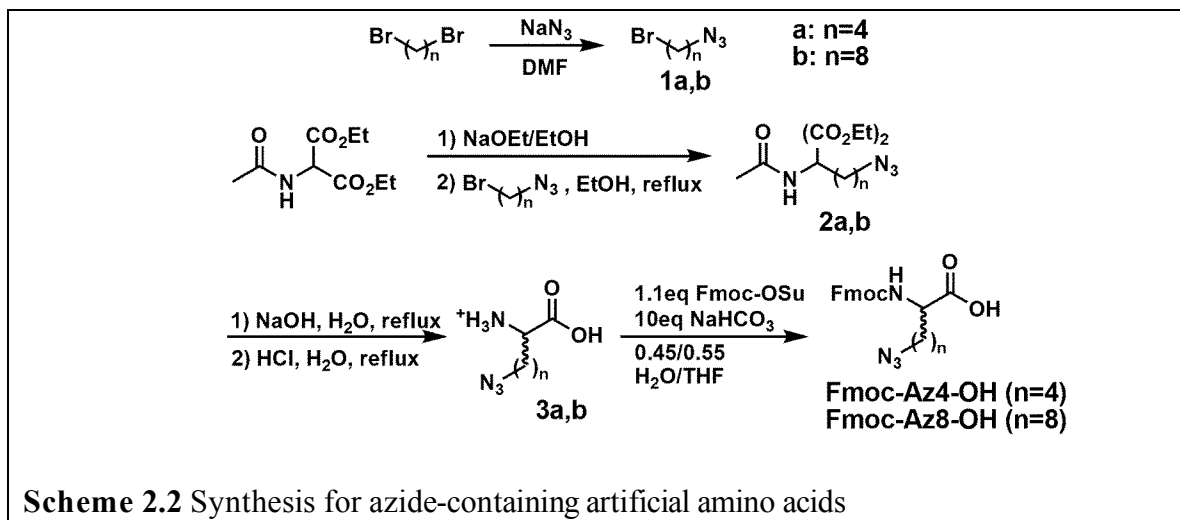
increased resistance to enzymatic degradation when applied to *in vivo* assays. Azide-containing amino acids displaying 4-carbon (**Az4**) or 8-carbon (**Az8**) azidoalkyl linkers and D-propargylglycine (**D-Pra**) are chosen as the azide and alkyne handles, respectively, for click chemistry (Figure 2.2). Azides and alkynes are also chemically attractive because they are synthetically convenient to introduce, compatible with a variety of solvents and species, and tolerant of other functionalities. The OBOC library technique also allows for desirable chemical and physical properties, such as water solubility, to be precisely tuned in the peptide capture agent. Scalability to gram quantities can be done straightforwardly and significantly cheaper than with antibodies.



Herein, I describe the use of *in situ* click chemistry as a general synthetic approach towards identifying high-quality, inexpensive protein capture agents. This chapter covers the synthesis of the azide-containing artificial amino acids, peptide library construction, *on bead* click reaction, and bead-based library screening procedures. Edman sequencing of lead compounds, including the custom gradient that was designed to allow for elution and verification of the artificial amino acids are also described in this section.

2.2 Artificial Amino Acid Synthesis

Azide-containing amino acids were synthesized and characterized, and used as handles for click chemistry following Scheme 2.2.



Azidobutylbromide (1a). To a solution of 1,4-dibromobutane (123 mmol) in N,N'-dimethylformamide (DMF), sodium azide (61.5 mmol) was added and stirred overnight at 50 °C. The reaction was diluted with ethyl acetate, and the organic layer was washed with water, then brine, and dried over MgSO₄. The crude residue was purified by silica gel chromatography (100% hexanes) to give a product (80%) as a clear oil. ¹H NMR (300 MHz, CDCl₃): δ 3.44 (2H, t, *J* = 6.3 Hz), 3.34 (2H, t, *J* = 6.6 Hz), 1.93–1.98 (2H, m), 1.74–1.79 (2H, m).

Azido-octylbromide (1b). Synthesis was carried out as described above, except 1,8-dibromobutane was used as the starting material. ¹H NMR (300 MHz, CDCl₃): δ 3.41 (2H, t, *J* = 6.9 Hz), 3.26 (2H, t, *J* = 6.6 Hz), 1.86 (2H, p, *J* = 6.9 Hz), 1.60 (2H, p, *J* = 8.7 Hz), 1.34–1.55 (4H, m).

Diethyl 2-acetamido-2-(4-azidobutyl)malonate (2a). To a solution of 0.598 g (0.026 mol) sodium metal in 25 mL absolute EtOH, 5.65 g diethyl acetamidomalonate

(0.026 mol) was added, following previously published procedures.³³ The mixture was stirred for 30 min at room temperature. By dropwise addition, azidobutylbromide **1a** (4.82 g, 0.027 mol) was added with stirring. The reaction mixture was stirred for 2 hours at room temperature and refluxed for 6 hours at 80 °C. After cooling overnight, the reaction mixture was concentrated to dryness, and the residue was extracted with diethyl ether. The combined ether extracts were washed with water, sat. NaHCO₃, water, and brine, and were dried over MgSO₄ and then concentrated. Silica gel chromatography (Hex:EtOAc = 1:1) gave a product (63%) as a clear, viscous oil. ¹H NMR (300 MHz, CDCl₃): δ 6.77 (1H, s), 4.24 (4H, q, *J* = 6.9 Hz), 3.26 (2H, t, *J* = 6.9 Hz), 2.31–2.37 (2H, m), 2.04 (3H, s), 1.59 (2H, p, *J* = 7.5 Hz), 1.26 (6H, t, *J* = 6 Hz), 1.16–1.27 (2H, m). ESI-MS *m/e* 315.

Diethyl 2-acetamido-2-(4-azidoethyl)malonate (2b). Similar synthetic protocol as **2a** was adopted, only azidoethylbromide **1b** served as the starting material. ¹H NMR (300 MHz, CD₃Cl₃): δ 6.76 (1H, s), 4.24 (4H, q, *J* = 7.2 Hz), 3.24 (2H, t, *J* = 6.9 Hz), 2.27–2.33 (2H, m), 2.04 (3H, s), 1.56 (2H, p, *J* = 7.5 Hz), 1.25 (6H, t, *J* = 7.2 Hz), 1.06–1.16, 1.2–1.4 (10H, m). ESI-MS *m/e* 371.

2-Azidobutyl amino acid (3a). Following standard methods³⁴, the diester **2a** (2.8 mmol) in 25 mL of 10% NaOH solution was heated to reflux for 4 hours. The solution was then neutralized with concentrated HCl and evaporated. The residue was dissolved in 25 mL of 1 M HCl and heated to reflux for 3 hours. The solvent was reduced and extraction with MeOH which afforded amino acid **3a** as the hydrochloride salt (85%). ¹H NMR (300 MHz, CD₃OD): δ 3.98 (1H, t, *J* = 6.3 Hz), 3.35 (2H, t, *J* = 7.8 Hz), 1.45–1.7, 1.85–2.05 (6H, m). MALDI-MS *m/e* 173.

2-Azidooctyl amino acid (3b). Synthesis was carried out as described above, using diester **2b** as the starting material. ^1H NMR (300 MHz, CD_3OD): δ 3.94 (1H, t, $J = 6.3$ Hz), 3.27 (2H, t, $J = 6.9$ Hz), 1.3–1.52, 1.52–1.62, 1.8–1.98 (14H, m). ESI-MS m/e 229.

Fmoc-2-Azidobutyl amino acid (Fmoc-Az4-OH). The amino acid **3a** (26.3 mmol) was dissolved in 0.45:0.55 H_2O :THF (150 mL), and NaHCO_3 (22.1 g, 263 mmol) was added, following published methods.³⁵ After the mixture was cooled to 0 °C, Fmoc-OSu (9.7 g, 28.9 mmol) was added dropwise over 5 min. The reaction mixture was allowed to come to room temperature and stirred overnight. Evaporation of THF was completed *in vacuo* and the aqueous residue was washed with diethyl ether (2×200 mL). The aqueous layer was then collected and acidified with conc. HCl to pH 2 before extraction with ethyl acetate (4×100 mL). The combined organic layers were washed with brine, dried over MgSO_4 , filtered, and concentrated. The organic residue was purified by column chromatography (2% MeOH in DCM) to yield a white powder (48% yield). ^1H NMR (300 MHz, CDCl_3): δ 7.76 (2H, d, $J = 7.5$ Hz), 7.59 (2H, d, $J = 6.9$ Hz), 7.40 (2H, t, $J = 7.5$ Hz), 7.31 (2H, t, $J = 7.5$ Hz), 5.34 (1H, d, $J = 7.8$ Hz), 4.49–4.59 (1H, m), 4.43 (2H, d, $J = 6.6$ Hz), 4.22 (1H, t, $J = 6.6$ Hz), 3.27 (2H, t, $J = 6.6$ Hz), 1.3–2.0 (6H, m). ESI-MS m/e 395.

Fmoc-2-Azidooctyl amino acid (Fmoc-Az8-OH). The amino acid **3b** was treated to Fmoc protection as described above. ^1H NMR (300 MHz, CD_3Cl_3): δ 7.75 (2H, d, $J = 7.5$ Hz), 7.57–7.61 (2H, m), 7.39 (2H, t, $J = 7.5$ Hz), 7.30 (2H, t, $J = 7.2$ Hz), 5.40 (1H, d, $J = 8.1$ Hz), 4.42–4.52 (1H, m), 4.40 (2H, d, $J = 7.2$ Hz), 4.21 (1H, t, $J = 7.2$ Hz), 3.23 (2H, t, $J = 6.9$ Hz), 1.18–1.98 (14H, m). ESI-MS m/e 450.

2.3 One-Bead One-Compound Peptide Library Construction

2.3.1 Materials. Fmoc-D-X-OH (Fmoc, fluoren-9-ylmethoxycarbonyl) (X = Ala, Arg(Pbf) (Pbf, pentamethyldihydrobenzofuran-5-sulfonyl), Asn(Trt) (Trt, trityl), Asp(OtBu) (*t*Bu, *tert*-butyl), Glu(OtBu), Gln(Trt), Gly, His(Trt), Ile, Leu, Lys(Boc) (Boc, *tert*-butyloxycarbonyl), Met, Phe, Pro, Ser(*t*Bu), Thr(*t*Bu), Trp(Boc), Tyr(*t*Bu), and Val) were purchased (Anaspec; San Jose, CA). TentaGel S-NH₂ resin (90 μm, 0.31 mmol/g) (Rapp-Polymere; Tübingen, Germany) were utilized for OBOC library construction. Amino acid coupling reactions were performed in 1-methyl-2-pyrrolidinone (NMP, 99%) with HATU (2-(7-Aza-1H-benzotriazole-1-yl)-1,1,3,3-tetramethylammonium hexafluorophosphate, ChemPep; Miami, FL) and *N,N'*-diisopropylethylamine (DIEA). For removal of N^α-Fmoc protecting groups, a solution of 20% piperidine in NMP was used. For final deprotection of the peptide libraries, trifluoroacetic acid (TFA, 98% min. titration) and triethylsilane (TES) were used. All solvents and reagents were purchased from Sigma-Aldrich (St. Louis, MO).

OBOC libraries were synthesized using a 180-degree variable-speed shaker, fitted with small sample adapter (St. John Associates; Beltsville, MD). Fritted polypropylene solid-phase synthesis tubes were used for repeated split-mix cycles. A 24-port SPE vacuum manifold system (Grace, Deerfield, IL) was used for exchanging coupling solutions and washing the resins. Fmoc-D-propargylglycine (Fmoc-D-Pra-OH) was acquired (Chem-Impex International; Wood Dale, IL) and used as the acetylene handle for construction of ligands.

Fmoc-D-propargylglycine (Fmoc-D-Pra-OH) was acquired (Chem-Impex

International; Wood Dale, IL) and used as the acetylene handle for construction of ligands.

2.3.2 Library Construction. Randomized OBOC libraries of penta- to heptapeptides were synthesized manually via standard split-and-mix solid-phase peptide synthesis methods on 90 μm polyethylene glycol-grafted polystyrene beads (TentaGel S-NH₂, 0.31 mmol -NH₂/g, 2.86 x 10⁶ beads/g, Rapp Polymere, Tübingen, Germany)¹³⁻¹⁵. Each bead is functionalized with a unique chemical entity (Figure 2.3). At least a five fold excess of beads was utilized in each library synthesis to ensure adequate representation of each library element. Nonnatural D-stereoisomers (denoted by lowercase one-letter amino acid code) were used at every possible position in the peptide sequence (See Appendix A for the structure of the D-amino acids). Acetylene and azide-containing amino acids are coupled to the N- and C-termini to serve as handles for click chemistry. The distance between the azide and alkyne during the *in situ* click experiment cannot be predicted in advance, so the incorporation of the variable length azidoalkyl linker may improve the assembly of the click product on the face of the protein.

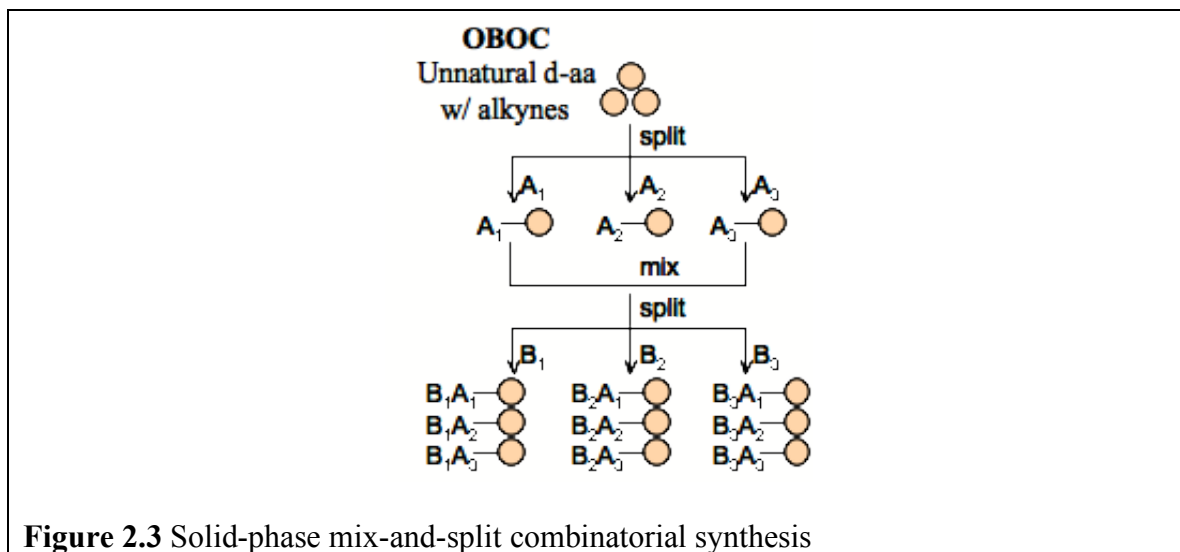


Figure 2.3 Solid-phase mix-and-split combinatorial synthesis

A standard solid-phase peptide synthesis method with 9-fluorenylmethoxycarbonyl

(Fmoc) chemistry was used.³⁶ All wash, deprotection, and coupling steps were facilitated

by 180-degree shaking of the resin. The resin was pre-swelled in *N*-methylpyrrolidinone (NMP) in a plastic disposable reaction vessel with fritted ends. The resin was separated into multiple aliquots and each aliquot was reacted with two fold molar excess (relative to resin) of a single N^{α} -Fmoc-amino acid. Amide coupling was initiated by addition of a two fold molar excess of HATU and a six fold molar excess of *N,N'*-diisopropylethylamine (DIEA). The coupling reaction was run for 15 min. Another 2 equiv N^{α} -Fmoc-amino acid, 2 equiv HATU, and 6 equiv DIEA were added, and allowed to react for 15 min (“double coupling”). In some cases, “triple coupling” with a third set of coupling reagents and N^{α} -Fmoc-amino acid was performed (Table 3.1, Libraries D, E, F, and G).

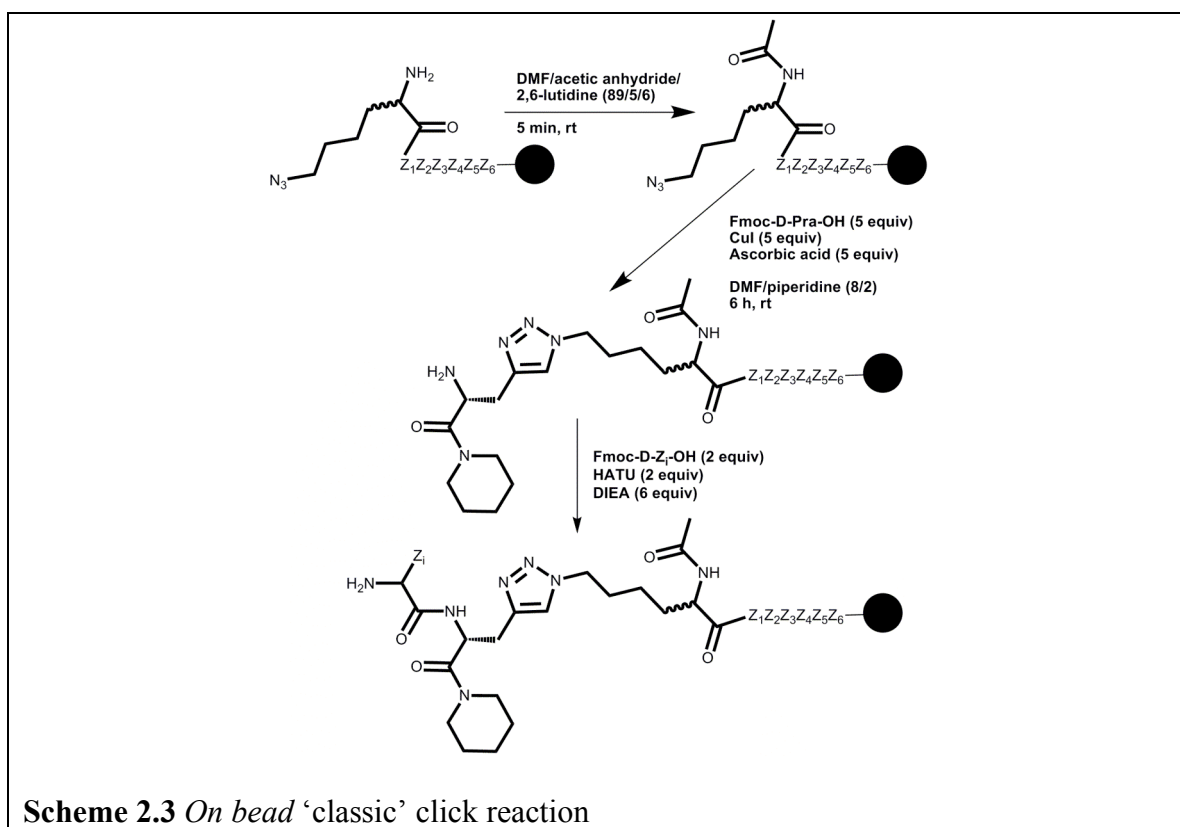
After coupling, the aliquots are thoroughly washed (5 x NMP), mixed together into a single vessel, and deprotected with 20% piperidine in NMP (30 min). The resins are thoroughly washed again (5 x NMP), dried (5 x DCM), and redivided into multiple aliquots for the next cycle of coupling. This second cycle of coupling adds another single N^{α} -Fmoc-amino acid to the growing peptide chain. The procedures of couple, wash, mix, deprotect, and split iterate until the desired length of peptide is attained.

The amino acid side-chain protecting groups are removed by incubation in 95% trifluoroacetic acid (TFA), 5% water, and triethylsilane (two fold molar excess per protected side chain) for 2 hours. The library resin was then neutralized with DMF, and washed thoroughly with DMF (5 x), water (5 x), methanol (MeOH, 5 x), and methylene chloride (DCM, 5 x)³⁷ and then dried under vacuum and stored in phosphate-buffered saline [PBS (pH 7.4)] + 0.05% NaN₃ at 25 °C.

2.4 On Bead Click Reaction

2.4.1 Materials. For peptide biligand and triligand synthesis, acetylation reagents (acetic anhydride, 2,6-lutidine, and *N,N*-dimethylformamide (DMF)) were purchased from Sigma-Aldrich (St. Louis, MO). For the *on bead* Cu(I)-catalyzed click reaction, copper(I) iodide, L-ascorbic acid, and sodium diethyldithiocarbamate trihydrate were purchased from Sigma-Aldrich (St. Louis, MO).

2.4.1 Click Reaction. For preparing biligand and triligand candidates, the Cu(I)-catalyzed azide-alkyne cycloaddition (CuAAC) on bead was completed in four general steps: (1) anchor ligand synthesis, (2) acetylation, (3) click reaction, and (4) addition of 2° ligand sequence. Scheme 2.3 illustrates these reactions (*Z* = any amino acid).



We found that the azide moiety needed to be attached to the bead and that the alkyne molecule needed to be in solution for the click reaction to work efficiently. For the

acetylation, the fully protected TentaGel S-NH₂ bead-bound anchor ligand (0.420 g, 0.13 mmol) was capped by a solution of acetic anhydride (1 mmol) in DMF, containing a catalytic amount of 2,6-lutidine.³⁸

The acetylated peptide was reacted with Fmoc-D-Pra-OH (0.218 g, 0.65 mmol) in the presence of copper(I) iodide (0.124 g, 0.65 mmol), L-ascorbic acid (0.114 g, 0.65 mmol), and DMF/piperidine (8/2) at 25 °C for 6 hours.³⁹ The resin was washed with 5 × 5 mL sodium diethyldithiocarbamate trihydrate (Et₂NCSSNa•3H₂O, 1% w/v), containing 1% DIEA (v/v) in DMF to remove excess coordinated copper.⁴⁰ Following the click reaction, the next N^α-Fmoc-amino acid was added to the peptide chain.

2.5 Bead-Based Library Screening Procedures

2.5.1 Proteins. Bovine carbonic anhydrase II (bCAII, C2522), from bovine erythrocytes, lyophilized powder, was obtained from Sigma-Aldrich (St. Louis, MO) and used as received. To prepare the protein for screening, dye-labeling was accomplished with the Alexa Fluor 647 Microscale Protein Labeling Kit (Invitrogen, Carlsbad, CA) following the manufacturer's protocol for low degree of labeling (DOL). Protein (100 μg) was incubated with 6 mol equiv Alexa Fluor 647 succinimidyl ester for 15 min at 25 °C. Excess dye was removed by BioGel P-6 size exclusion resin (Bio-Rad, Hercules, CA). The labeled protein (bCAII-Alexa647) was characterized by UV-Vis and mass spectrometry.

2.5.2 Screening. A typical peptide library screen against bCAII is described as follows. The peptide library is screened not all at once, but in several mg portions. Approximately 10–20 mg dried peptide-bead library is incubation in PBS (pH 7.4) +

0.1% Tween 20 + 0.1% bovine serum albumin (BSA) + 0.05% NaN₃ (PBSTBNaN₃) for 1 hour, with shaking, to block nonspecific protein binding.⁴¹ The library was then washed with 3 x 5 mL PBSTBNaN₃ only. *On bead* multi-ligand screens were conducted at an appropriate bCAII-Alexa Fluor 647 dilution (Table 2.1), and then washed with 3 x 5 mL PBSTBNaN₃, 3 x 5 mL PBS (pH 7.4) + 0.1% Tween 20, and finally 6 x 5 mL PBS (pH 7.4). All *in situ* screens contained an additional 2 hours preincubation of bCAII-Alexa Fluor 647 with anchor ligand (≥ 2000 equiv, relative to protein), after which the bead library was added to this mixture and the screen was continued (Table 2.1). Following *in situ* screening, beads were washed with 3 x 5 mL PBSTBNaN₃, 3 x 5 mL PBS (pH 7.4) + 0.1% Tween 20, and then 6 x 5 mL PBS (pH 7.4). We found that longer incubation times, up to 24 hours, select for more specific tight-binding events and promote dissociation of the weakly bound peptides.

Table 2.1 Screening summary; pH=7.4 and T=25°C, unless otherwise noted

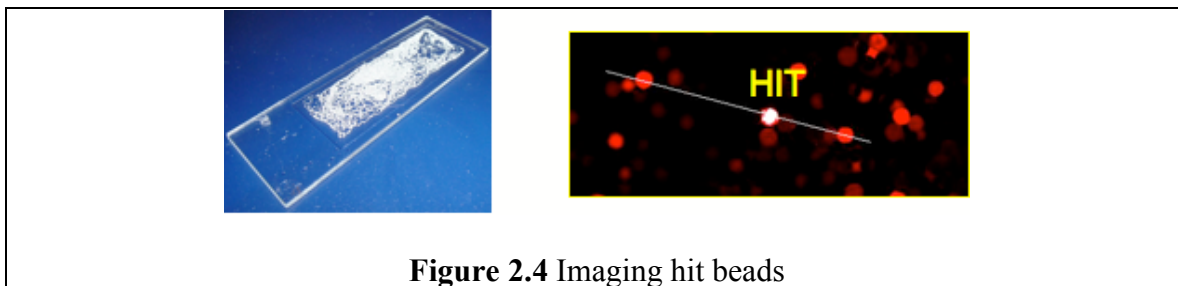
Screen	Library	[bCAII-AF647]	Time(h)	% hit beads	Buffer	Other components
An1	A	100 nM	1 h	0.02%	PBS	
An2a	B	50 nM	1 h	0.09%	PBS	
An2b	B	8 nM	24 h	2 hits	PBS	
Bi1	C	50 nM	2 h; 37° (no beads) + 48 h; 37°	0.007%	PBS + 1% DMSO (v/v)	100 μM of Iklwfk-(D-Pra)
Bi2a	D	50 nM	17 h	0.07%	PBSTBNaN ₃	
Bi2b	D	10 nM	17 h	0.008%	PBSTBNaN ₃	
Tri1	C	10 nM	2 h (no	0.007%	PBSTBNaN ₃ +	100 μM of (D-Pra)-kwlwGI-

			beads) +15 h		1% DMSO (v/v)	Tz1-kfwlkl
Tri2	E	10 nM	17 h	0.008%	PBSTBNaN ₃	
TriX	A	10 nM	17 h	0.007%	PBSTBNaN ₃ + 1% DMSO (v/v)	100 μM of (D-Pra)-kwlwGI- Tz1-kfwlkl
Tri3	F	0.5 nM	2 h (no beads) +18 h	0.005-0.01%	PBSTBNaN ₃ + 1% DMSO (v/v)	100 μM of (D-Pra)-kwlwGI- Tz1-kfwlkl
Tri4	G	0.25 nM	18 h	0.005-0.01%	PBSTBNaN ₃	

Anchor ligand screens (**An1**, **An2a**, **An2b**) were conducted using **Libraries A** and **B**. Following screening, the beads were washed with 3 x 5 mL PBS (pH 7.4), then 7 x 5 mL water.

In situ biligand and triligand screens were carried out utilizing **Libraries C** and **F**. *On bead* biligand and triligand screens were performed using **Libraries D**, **E**, and **G**. Screening conditions are provided in Table 2.1, and further details will follow.

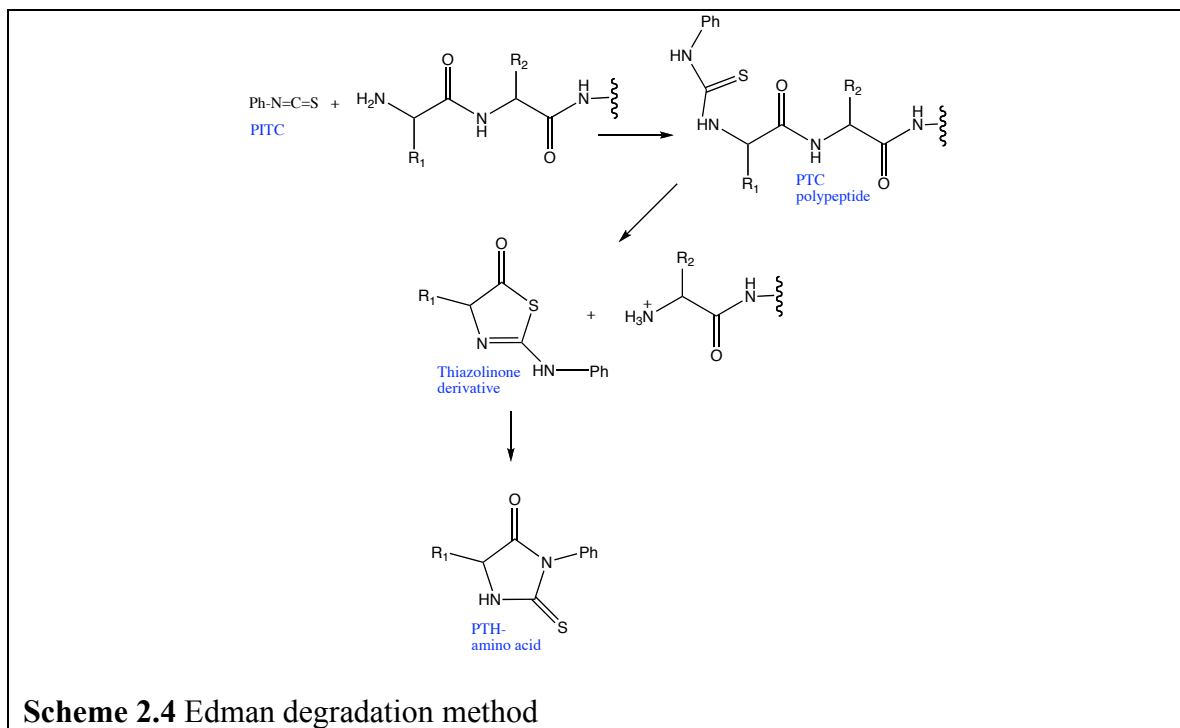
After incubation, the peptide-bead library and protein screening solution is transferred into a clean polyethylene-fritted vessel. The beads are filtered *in vacuo*, then washed with 0.1% Tween20/PBS (3 x 1 ml) followed by PBS pH 7.4 (3 x 1 ml), followed by H₂O (7 x 1 ml). The washed peptide-bead library sample is transferred onto a glass microscope slide and immediately imaged using a GenePix 4200 array scanner ($\lambda_{\text{ex}} = 635$ nm). These individual hit beads, which are white due to saturation of the PMT gain, are manually selected using a glass micropipette.



To remove bound proteins, each hit bead was incubated in 7.5 M guanidine hydrochloride (pH 2.0) for 1 hour, followed by ten rinses with water. These hits are considered lead compounds, and their sequences are analyzed by Edman degradation.

2.6 Analysis of Lead Compounds by Edman Degradation

2.6.1 Method. Edman sequencing of single hit beads was carried out on a Model 494 Procise cLC Sequencing System (Applied BioSystems, Foster City, CA). Edman sequencing requires that the peptide have a free N-terminus on α -amino acids for determination of a peptide's sequence. Edman degradation works in the following way: Phenylisothiocyanate (PITC) is reacted with an uncharged terminal amino group, under mildly alkaline conditions, to form a cyclic phenylthiocarbamoyl derivative. Then, under acidic conditions, this derivative of the terminal amino acid is cleaved as a thiazolinone derivative. The thiazolinone amino acid is then selectively extracted into an organic solvent and treated with acid to form the more stable phenylthiohydantoin (PTH)-amino acid derivative that can be identified by high-pressure liquid chromatography (Scheme 2.4). This procedure can then be repeated again to identify subsequent amino acids in the peptide sequence.



Iterative N-terminal chemical degradation cycles yielded direct positional amino acid information. Each degradation cycle produced one PTH-amino acid (PTH = phenylthiohydantoin) product that was analyzed by C_{18} HPLC and identified by retention time as compared with PTH-amino acid standards.

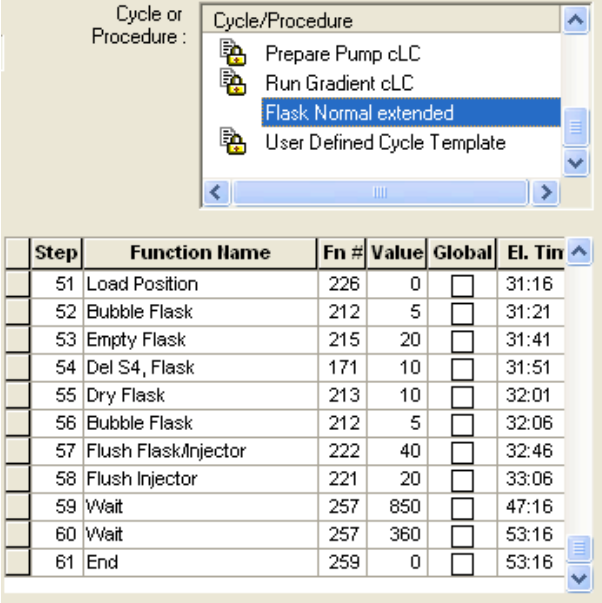
2.6.2 Custom Edman Degradation. A custom gradient was designed to allow for elution of the artificial amino acids, characterization of retention times, and confirmation of their incorporation in the *in situ* library. To allow for resolution of artificial azide-containing amino acids by Edman degradation, the Pulsed-Liquid cLC extended method was utilized (Figure 2.5). It includes a modified gradient, Normal 1 cLC extended (Figure 2.6), and a flask cycle extended by 5 min (Figure 2.7).

Cycle #	Cartridge Cycle	Flask Cycle	Gradient
Default	Cart-PL 6mmGFF cLC	Flask Normal extended	Normal 1 extended
1	None	Prepare Pump cLC	Prepare Pump cLC
2	None	Flask Blank cLC	Normal 1 extended
3	Cart Begin cLC	Flask Standard cLC	Normal 1 extended

Figure 2.5 Pulsed-Liquid cLC extended method

Time	%B	uL/min	Event	Cum. Volume A	Cum. Volume B
0.0	8	40	12	0.00	0.00
0.4	12	40	1	14.40	1.60
4.0	20	40	1	135.36	24.64
22.0	45	40	1	621.36	258.64
34.0	60	40	1	849.36	510.64
35.0	90	40	1	859.36	540.64
39.0	90	60	0	883.36	756.64
40.0	50	20	0	889.36	770.64

Figure 2.6 Normal 1 cLC extended gradient



Cycle or Procedure :

Cycle/Procedure

- Prepare Pump cLC
- Run Gradient cLC
- Flask Normal extended**
- User Defined Cycle Template

Step	Function Name	Fn #	Value	Global	El. Tin
51	Load Position	226	0	<input type="checkbox"/>	31:16
52	Bubble Flask	212	5	<input type="checkbox"/>	31:21
53	Empty Flask	215	20	<input type="checkbox"/>	31:41
54	Del S4, Flask	171	10	<input type="checkbox"/>	31:51
55	Dry Flask	213	10	<input type="checkbox"/>	32:01
56	Bubble Flask	212	5	<input type="checkbox"/>	32:06
57	Flush Flask/Injector	222	40	<input type="checkbox"/>	32:46
58	Flush Injector	221	20	<input type="checkbox"/>	33:06
59	Wait	257	850	<input type="checkbox"/>	47:16
60	Wait	257	360	<input type="checkbox"/>	53:16
61	End	259	0	<input type="checkbox"/>	53:16

Figure 2.7 Final steps of flask normal extended flask cycle

The Edman traces corresponding to elution of Az2, Az4, Az6 and Az8 are shown in Figure 2.8 and demonstrate a 6 min retention time increase for every two methylene

units added to the azidoalkyl side chain. Fmoc-Az2-OH was synthesized according to literature protocol,⁴² while Fmoc-Az6-OH was synthesized according to Scheme 2.2.

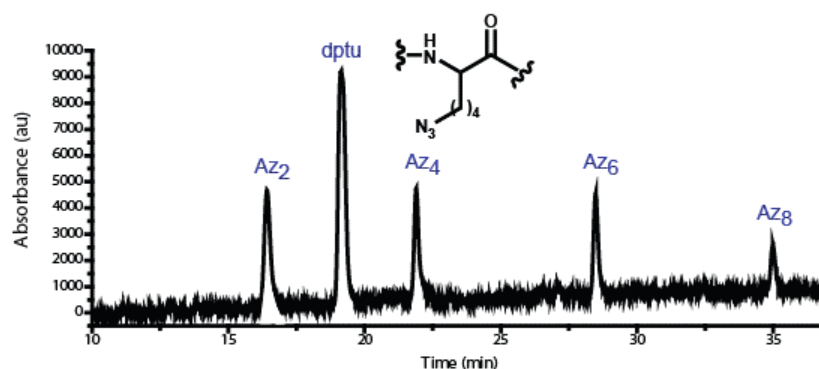


Figure 2.8 Edman traces for artificial azide-containing amino acids

Also, we performed a sequencing calibration for the *in situ* click hit using a commercially available 4-azidophenylalanine (Phe-N₃) and an alkynyl inhibitor against bCAII. The shift in retention is indicative of the click conjugation of the azide and alkyne species (Figure 2.9). Note that dptu is a side product of Edman sequencing.

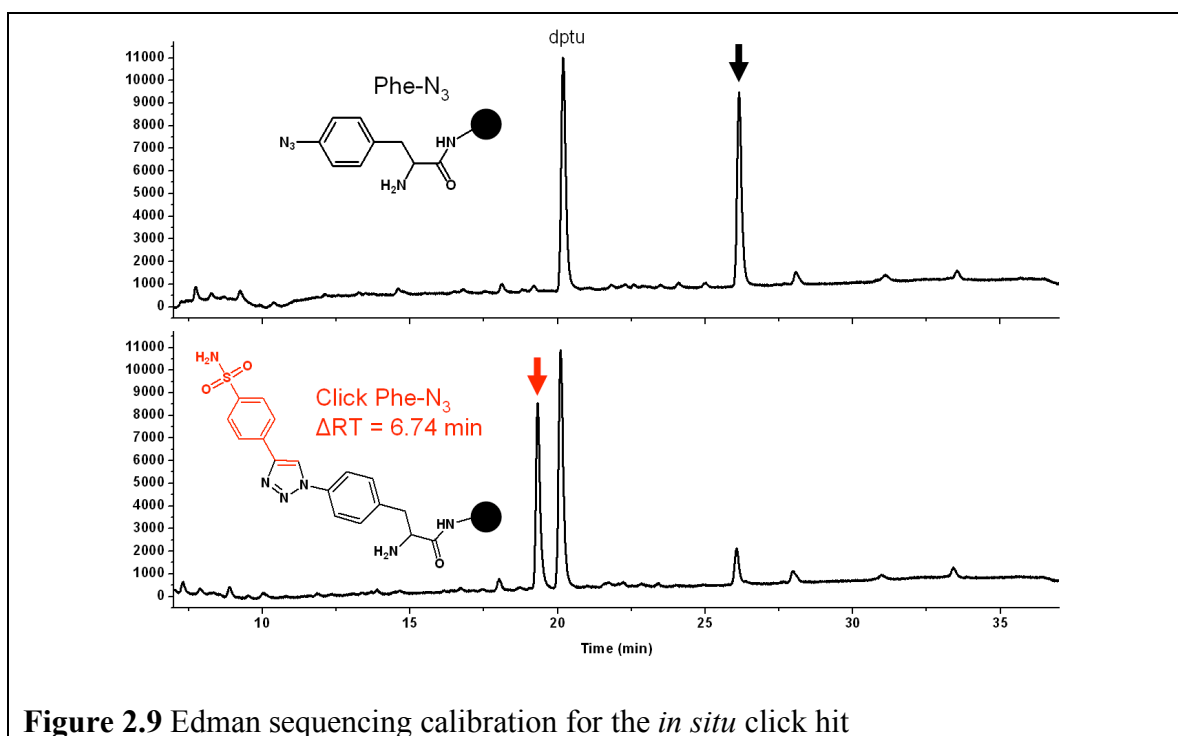


Figure 2.9 Edman sequencing calibration for the *in situ* click hit

2.7 Bulk Peptide Synthesis

Bulk synthesis of hit peptide sequences was performed on either Fmoc-Rink amide MBHA or 2-chlorotrityl chloride resins, on a typical resin scale of 0.3 g per sequence, using standard coupling chemistry. Hits were re-synthesized to contain the appropriate artificial amino acid (azide/acetylene) linkers at their termini to make them suitable for click chemistry. Biligand and triligand were synthesized in bulk and preassembled using Scheme 2.3. Crude peptides were precipitated with ether, and then purified to > 98% by HPLC (Beckman Coulter System Gold 126 Solvent Module and 168 Detector, Fullerton, CA) on a C₁₈ reversed phase semi-preparative column (Phenomenex Luna 10 μm, 250 × 10 mm). The pure peptides were used for screens, affinity measurements, and binding assays. Hit peptide sequences were also re-synthesized on TentaGel S-NH₂ on a similar resin scale, and used for *on bead* binding assays.

2.8 Conclusion

Protein capture agents are constructed from peptide ligands, each of which is constructed from a unique set of amino acids, including nonnatural amino acids and artificial amino acids. Artificial amino acids are synthesized so peptide ligands can be chemically functionalized with an azide (-N₃) or acetylene (-C≡C-H) group serving as handles for click chemistry. All of these amino acids are synthetically incorporated into peptides or polypeptides on beads using standard amino acid coupling chemistries. Using standard screening methods, the anchor, biligand, and triligand hits can be obtained and decoded by Edman degradation as shown in the last section of this chapter.

2.9 References

1. Blow, N. *Nature* **2007**, *447*, 741–744.
2. Fan, R.; Vermesh, O.; Srivastava, A.; Yen, B. K. H.; Qin, L.; Ahmad, H.; Kwong, G. A.; Liu, C.-C.; Gould, J.; Hood, L.; Heath, J. R. *Nat. Biotechnol.* **2008**, *Advance online publication*, DOI:10.1038/nbt.1507.
3. Hood, L.; Heath, J. R.; Phelps, M. E.; Lin, B. *Science* **2004**, *306*, 640–643.
4. Phelan, M. L.; Nock, S. *Proteomics* **2003**, *3*, 2123–2134.
5. Cox, J. C.; Hayhurst, A.; Hesselberth, J. R.; Bayer, T. S.; Georgiou, G.; Ellington, A. D. *Nucleic Acids Res.* **2002**, *30*, e108.
6. McCauley, T. G.; Hamaguchi, N. *Anal. Biochem.* **2003**, *319*, 244–50.
7. Lee, J. F.; Hesselberth, J. R.; Meyers, L. A.; Ellington, A. D. *Nucleic Acids Res.* **2004**, *32*, D95–D100.
8. Famulok, M.; Mayer, G.; Blind, M. *Acc. Chem. Res.* **2000**, *33*, 591–599.
9. Proske, D.; Blank, M.; Buhmann, R.; Resch, A. *Appl. Microbiol. Biotechnol.* **2005**, *69*, 367–374.
10. Thiel, K. *Nat. Biotechnol.* **2004**, *22*, 649–651.
11. Fabian, M. A.; Biggs III, W. H.; Treiber, D. K.; Atteridge, C. E.; Azimioara, M. D.; Benedetti, M. G.; Carter, T. A.; Ciceri, P.; Edeen, P. T.; Floyd, M.; Ford, J. M.; Galvin, M.; Gerlach, J. L.; Grotzfeld, R. M.; Herrgard, S.; Insko, D. E.; Insko, M. A.; Lai, A. G.; Lélias, J.-M.; Mehta, S. A.; Milanov, Z. V.; Velasco, A. M.; Wodicka, L. M.; Patel, H. K.; Zarrinkar, P. P.; Lockhart, D. J. *Nat. Biotechnol.* **2005**, *23*, 329–336.
12. Smith, G. P.; Petrenko, V. A. *Chem. Rev.* **1997**, *97*, 391–410.
13. Lam, K. S.; Lebl, M.; Krchňák, V. *Chem. Rev.* **1997**, *97*, 411–448.
14. Furka, A.; Sebestyen, F.; Asgedom, M.; Dibo, G. *Int. J. Pept. Protein Res.* **1991**, *37*, 487–493.
15. Geysen, H. M.; Mason, T. J. *Bioorg. Med Chem. Lett.* **1993**, *3*, 397–404.

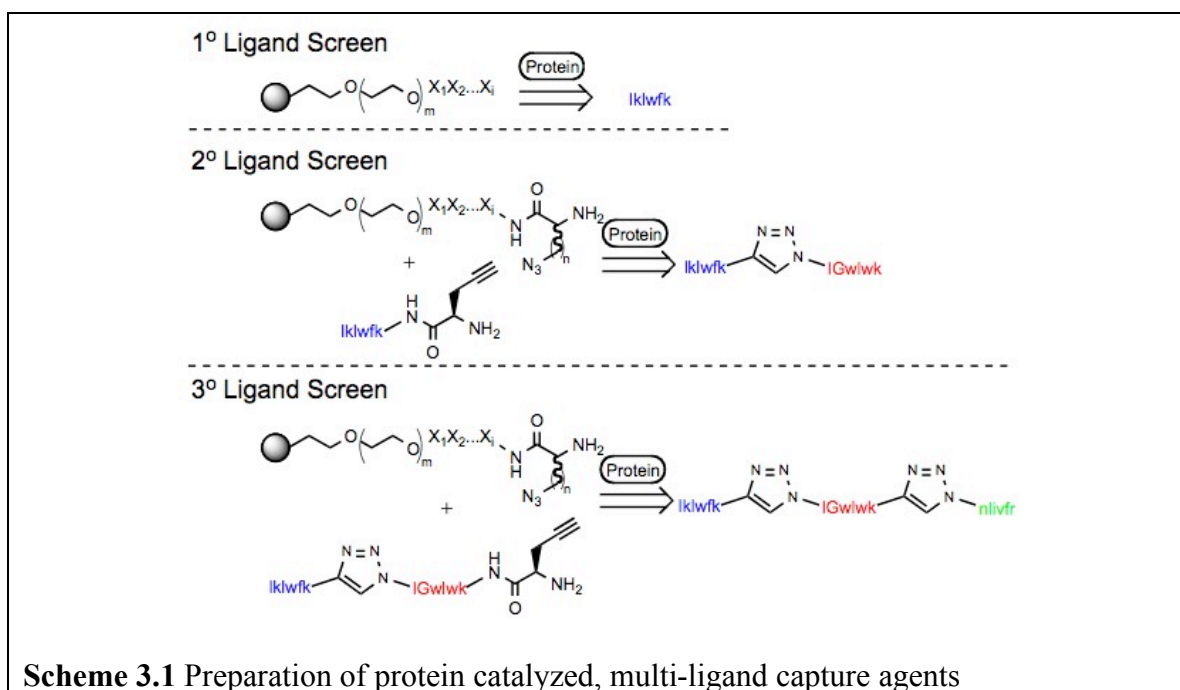
16. Lam, K. S.; Lebl, M.; Krchňák, V.; Wade, S.; Abdul-Latif, F.; Ferguson, R.; Cuzzocrea, C.; Wertman, K. *Gene* **1993**, *137*, 13–16.
17. Liu, R.; Marik, J.; Lam, K. S. *J. Am. Chem. Soc.* **2002**, *124*, 7678–7680.
18. Alluri, P. G.; Reddy, M. M.; Bachhawat-Sikder, K.; Olivos, H. J.; Kodadek, T. *J. Am. Chem. Soc.* **2003**, *125*, 13995–14004.
19. Tornøe, C. W.; Sanderson, S. J.; Mottram, J. C.; Coombs, G. H.; Meldal, M. *J. Comb. Chem.* **2004**, *6*, 312–324.
20. Lewis, W. G.; Green, L. G.; Grynszpan, F.; Radić, Z.; Carlier, P. R.; Taylor, P.; Finn, M. G.; Sharpless, K. B. *Angew. Chem. Int. Ed.* **2002**, *41*, 1053–1057.
21. Manetsch, R.; Krasinski, A.; Radić, Z.; Raushel, J.; Taylor, P.; Sharpless, K. B.; Kolb, H. C. *J. Am. Chem. Soc.* **2004**, *126*, 12809–12818.
22. Bourne, Y.; Kolb, H. C.; Radić, Z.; Sharpless, K. B.; Taylor, P.; Marchot, P. *Proc. Natl. Acad. Sci. USA* **2004**, *101*, 1449–1454.
23. Mocharla, V. P.; Colasson, B.; Lee, L. V.; Röper, S.; Sharpless, K. B.; Wong, C.-H.; Kolb, H. C. *Angew. Chem. Int. Ed.* **2005**, *44*, 116, and references therein.
24. Kehoe, J. W.; Maly, D. J.; Verdugo, D. E.; Armstrong, J. I.; Cook, B. N.; Ouyang, Y.-B.; Moore, K. L.; Ellman, J. A.; Bertozzi, C. R. *Bioorg. Med. Chem. Lett.* **2002**, *12*, 329–332.
25. Ramstrom, O.; Lehn, J. M. *Nature Rev. Drug Discov.* **2002**, *1*, 26–36.
26. Poulin-Kerstien, A. T.; Dervan, P. B. *J. Am. Chem. Soc.* **2003**, *125*, 15811–15821.
27. Jain, A.; Huang, S. G.; Whitesides, G. M. *J. Am. Chem. Soc.* **1994**, *116*, 5057–5062.
28. Mammen, M.; Choi, S. K.; Whitesides, G. M. *Angew. Chem. Int. Ed.* **1998**, *37*, 2755–2794.
29. Kodadek, T.; Reddy, M. M.; Olivos, H. J.; Bachhawat-Sikder, K.; Alluri, P. G. *Acc. Chem. Res.* **2004**, *37*, 711–718.

30. Lam, K. S.; Lake, D.; Salmon, S. E.; Smith, J.; Chen, M.-L.; Wade, S.; Abdul-Latif, F.; Knapp, R. J.; Leblova, Z.; Ferguson, R. D.; Krchňák, V.; Sepetov, N. F.; Lebl, M. *Methods (San Diego)*, **1996**, *9*, 482.
31. Simó, C.; Bachi, A.; Cattaneo, A.; Guerrier, L.; Fortis, F.; Boschetti, E.; Podtelejnikov, A.; Righetti, P. G. *Anal. Chem.* **2008**, *80*, 3547–3556.
32. Carpino, L. A.; El-Faham, A.; Minorb, C. A.; Albericio, F. *J. Chem. Soc., Chem. Commun.* **1994**, 201–203.
33. Chenault, H. K.; Dahmer, J.; Whitesides, G. M. *J. Am. Chem. Soc.* **1989**, *111*, 6354–6364.
34. van Hest, J. C. M.; Kiick, K. L.; Tirrell, D. A. *J. Am. Chem. Soc.* **2000**, *122*, 1282–1288.
35. Lee, H.-S.; Park, J.-S.; Kim, B. M.; Gellman, S. H. *J. Org. Chem.* **2003**, *68*, 1575–1578.
36. Coin, I.; Beyermann, M.; Bienert, M. *Nat. Protocols* **2007**, *2*, 3247.
37. Dixon, S. M.; Li, P.; Liu, R.; Wolosker, H.; Lam, K. S.; Kurth, M. J.; Toney, M. D. *J. Med. Chem.* **2006**, *49*, 2388.
38. Atherton, E.; Sheppard, R. C. in *Solid Phase Peptide Synthesis—A Practical Approach*, Oxford University Press, USA, **1989**, p. 136.
39. Zhang, Z.; Fan, E. *Tetrahedron Lett.* **2006**, *47*, 665–669.
40. Weterings, J. J.; Khan, S.; van der Heden, G. J.; Drijfhout, J. W.; Melief, C. J. M.; Overkleeft, H. S.; van der Burg, S. H.; Ossendorp, F.; van der Marel, G. A.; Filippov, D. V. *Bioorg. Med. Chem. Lett.* **2006**, *16*, 3258–3261.
41. Lehman, A.; Gholami, S.; Hahn, M.; Lam, K. S. *J. Comb. Chem.* **2006**, *8*, 562.
42. Roice, M.; Johannsen, I.; Meldal, M. *QSAR Comb. Sci.* **2004**, *23*, 662.

Chapter 3: Generating a High-Quality Triligand Capture Agent for bCAII

3.1 Introduction

Chapter 3 describes an effective and generalized *in situ* click chemistry catalyzed approach using peptide ligands towards a model protein biomarker, bovine carbonic anhydrase II (bCAII). Carbonic anhydrase II is from a family of metalloenzymes that catalyze the reversible hydration of carbon dioxide. This protein has been used for studying protein-ligand interactions and it is a demonstrated receptor for bivalent ligands.¹⁻⁵ In addition, expression of human carbonic anhydrase II (hCAII) is induced in the endothelium of neovessels in melanoma and renal and other cancers.⁶ Furthermore, CA II represents a major target antigen stimulating an autoantibody response in melanoma patients,⁷ and it is also potentially a therapy target for glial tumors.⁸ In this work, a triligand peptide capture agent was developed for bCAII and hCAII, which exhibited 64 and 45 nM binding affinities, respectively, by the sequential *in situ* click-catalyzed assembly of three 7-mer peptide ligands (Scheme 3.1).



A completely random OBOC library of 22-mer peptides would be impractical for constructing and identifying the protein capture agent. We further report that this triligand capture agent can detect bCAII and the hCAII from a serum consisting of multiple naturally occurring proteins. These data suggest that triligands (and higher-order multi-ligands) assembled by *in situ* click chemistry will be a great source of robust and specific capture agents for *in vitro* diagnostics. Our generalized methods should serve as the basis for inexpensive capture agent development for any protein. This is of particular interest for proteins that do not respond well to traditional capture agents.

Herein, I describe, step-by-step, the screens and results associated with developing an anchor ligand, biligand, and triligand. Binding affinity and selectivity measurements are also covered in this chapter. Appendix B gives the complete structures of biligands and triligands, along with mass spectrum analysis. Attached to Appendix C is our recent literature paper: “Iterative *In Situ* Click Chemistry Creates Antibody-Like Protein-Capture Agents,” that can be further reviewed.

3.2 Peptide Library Construction

One-bead one-compound (OBOC) peptide libraries were synthetically constructed and discussed in Section 2.3. Table 3.1 shows the specific libraries that were fabricated and used for screening against bCAII.

Table 3.1 Libraries used in this study[†]

	Formula	Components	# of unique sequences
A	$X_1X_2X_3X_4X_5$	$x_i = 19$ D-amino acids (no D-Cys)	2,476,099
B	$X_1X_2X_3X_4X_5X_6$	$x_i = r, k, l, w, f, h, y$	117,649
C	$Az_n-X_2X_3X_4X_5X_6-Az_n$	$x_i = 19$ D-amino acids (no D-Cys) $Az_n = 1/3$ Az4 , $1/3$ Az8 , $1/3$ nothing	22,284,891
D	$X_1X_2X_3X_4X_5X_6-Tz1-kfwlkl$	$x_i = k, l, w, f, i, g, v$	117,649
Tz1 = triazole formed between Az4 (on terminal k) and D-Pra (on x_6)			
E	$X_7X_6X_5X_4X_3X_2-Tz2-kwlwGl-Tz1-kfwlkl$	$x_i = d, r, s, w, G, f, l$	117,649
Tz1 = triazole formed between Az4 (on terminal k) and D-Pra (on l) Tz2 = triazole formed between Az4 (on terminal x_2) and D-Pra (on k)			
F	$Az4-X_2X_3X_4X_5X_6X_7$	$x_2 = r, n, l, i;$ $x_3 = w, f, l, i;$ $x_4 = r, w, f, l, i;$ $x_5 = w, f, v, l;$	3200
G	$X_7X_6X_5X_4X_3X_2-Tz2-kwlwGl-Tz1-kfwlkl$	$x_6 = r, w, f, l, k;$ $x_7 = f, r$	3200

[†] Randomized positions are denoted by x (for D-amino acids) and Az_n (for azide-containing artificial amino acids).

3.3 Screening and Results for Anchor Ligand

The first peptide, or anchor ligand, was selected from a 2-generation library screen (**An1**, **An2**, **An2b**, **Table 3.1**). Using the OBOC combinatorial library methodology, a randomized library of pentapeptides consisting of 2,476,099 D-peptide compounds was synthesized manually by a split-and-mix synthesis approach as previously discussed in Chapter 2. An approximately ten fold excess of beads was utilized to fabricate the peptide library. This pentapeptide library was expected to afford enough diversity to discriminate between weak and strong binders, and the sample size was large enough to ensure that

there will be some lead compounds. The library was also simple enough to manually prepare on the bench-top, and was readily modified with azide-containing amino acids.

3.3.1 First-Generation Screen for Anchor Ligand. For the first screen (**An1**), **Library A** was screened with 100 nM bCAII protein, labeled with Alexa Fluor 647 succinimidyl ester (Figure 3.1).

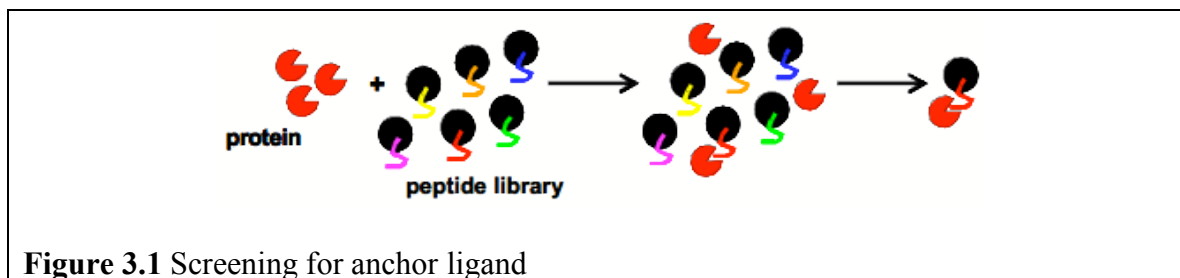
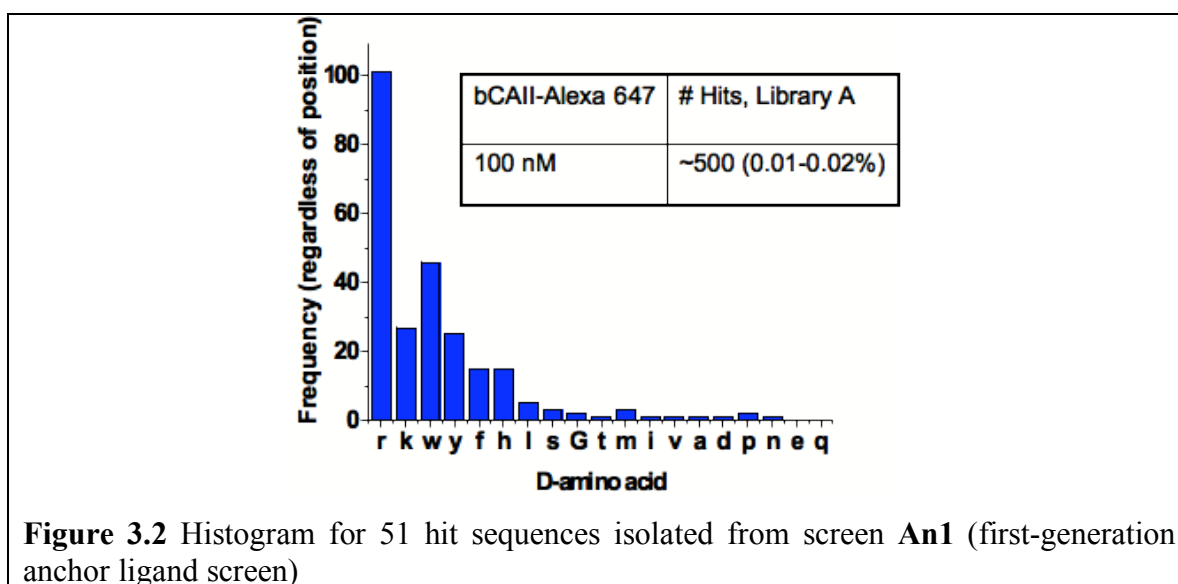


Figure 3.1 Screening for anchor ligand

The red Alexa Fluor 647 dye was chosen for protein labeling due to the low autofluorescence of the TentaGel bead at these wavelengths. The dye was conjugated to the bCAII protein at low level (< 3 fluorophores/protein) to minimize interference of the fluorophore with real binding interactions. Thus, the “hit” beads were identified by their fluorescence. The brightest fluorescent beads ($< 0.02\%$ of library) were manually separated from the non-hit beads. After removing the protein from the beads using 7.5 M guanidine hydrochloride (pH 2.0), the hit peptide-beads were sequenced by Edman degradation⁹ (Table 3.2) and analyzed by a histogram correlating the frequency of amino acid occurrence vs amino acid identity (Figure 3.2). The results suggest that basic/charged (k, r) and aromatic residues (y, f, w) are important amino acids in an anchor ligand for bCAII.

Table 3.2 First-generation anchor ligand screen **An1** (100 nM) results

	X ₁	X ₂	X ₃	X ₄	X ₅		X ₁	X ₂	X ₃	X ₄	X ₅
hit1	r	r	y	h	r	hit27	w	r	--	y	r
hit2	m/v	r	w	k	r	hit28	h	r	w	r	r
hit3	k	r	w	y	y	hit29	w	y	r	k	r
hit4	w	k	k	k	w	hit30	l	r	f	r	r
hit5	h	f	f	f	r	hit31	w	k	r	k	k
hit6	s	r	--	r	r	hit32	r	r	r	w	s/m
hit7	r	r	w	h	y	hit33	r	r	k	f	w
hit8	r	k	w	w	w	hit34	r	r	w	r	y
hit9	r	w	s	f	r	hit35	w	r	h	y	k
hit10	r	r	G	w	r	hit36	r	r	y	f	r
hit11	G	f	r	r	w	hit37	w	r	k	w	r
hit12	r	t	r	r	w	hit38	w	y	--	r	r
hit13	m	r	w	k	r	hit39	y	r	r	r	h
hit14	y	r	k	r	w	hit40	y	r	r	r	w
hit15	a	--	--	--	--	hit41	p	f	y	w	r
hit16	r	r	i	r	w	hit42	k	y	w	r	k
hit17	--	--	k/l	w	--	hit43	r	y	w	h	k
hit18	r	w	--	--	r	hit44	r	w	h	w	n
hit19	k/l	r	--	w	r	hit45	r	h	f	h	h/f
hit20	w	r	f	r	y	hit46	r	r	--	h	r
hit21	d/p	y	y	r	r	hit47	r	y	r	r	r
hit22	r	y	w	k	k	hit48	y	f	h	h/w	w
hit23	k/l	r	r	r	w	hit49	r	r	r	w	y
hit24	y	r	r	k	w	hit50	w	r	r	r	r/--
hit25	r	k/l	f	y	r	hit51	r	w	k	f	h
hit26	r	w	w	k	r						

**Figure 3.2** Histogram for 51 hit sequences isolated from screen **An1** (first-generation anchor ligand screen)

3.3.2 Re-Screening for Anchor Ligand with a Focused Library. A second, more focused library (**Library B, Table 3.1**) of 117,649 D-peptide compounds was constructed from the most commonly occurring amino acids (r, k, l, w, f, h, y), as identified from screen **An1**, but expanded into a 6-mer peptide, and screened under 50 nM bCAII (**An2a**) and 8 nM bCAII (**An2b**) conditions. The results of the second-generation anchor ligand screens are shown in Tables 3.3 and 3.4. The hit rates were 0.09% and 0.05% for 50 nM and 8 nM, respectively.

Table 3.3 Second-generation anchor ligand screen **An2a** (50 nM) results

	X ₁	X ₂	X ₃	X ₄	X ₅	X ₆
hit1	y	r	w	f	k	f
hit2	h/r	h/r	f	l	l/r	r
hit3	f	r	f	y	y	r
hit4	h/r	f	f	k	l	--
hit5	k	l	f	l	k	l
hit6	l	f	l	w	l	k
hit7	f	f	f	r	y	--
hit8	h/r	f	f	f	r	--
hit9	r	w	w	l	k	f
hit10	h/r	f	f	r	y	y
hit11	l	k	l	f	l	k
hit12	f	r	r	w	w	k
hit13	h/r	y	f	f	k	l
hit14	l	k	f	f	f	k
hit15	h/r	f	f	r	r	--

Table 3.4 Second-generation anchor ligand screen **An2b** (8nM) results

	X ₁	X ₂	X ₃	X ₄	X ₅	X ₆
hit1	h	l	y	f	l	r
hit2	l	k	l	w	f	k

The more stringent screen yielded two hits, **hlyflr** and **lklwfk**. From these two candidates, one peptide (**lklwfk**) was arbitrarily chosen as the starting point for an anchor ligand for use in the multi-ligand screens.

3.4 Binding Measurements for Anchor Ligand by Fluorescence Polarization

The anchor peptide **lklwfk** was then functionalized with an acetylene ($-C\equiv C-H$) at the C-terminus and produced in bulk quantities (see Section 2.7 for details) for affinity measurements by fluorescence polarization (using a fluoresceinated peptide). The N-terminus of the anchor ligand was labeled with fluorescein isothiocyanate (FITC) following published protocols.¹⁰ After resin cleavage, the crude fluoresceinated anchor ligand was precipitated with ether and then purified to > 98% by C_{18} reversed-phase HPLC.

Luminescence spectra were recorded by Fluorolog2 spectrofluorimeter (Jobin Yvon, Longjumeau, France) in the Beckman Institute Laser Resource Center (Pasadena, CA). All samples contained 6 μM fluoresceinated anchor ligand and varying concentrations of bCAII (0.2 μM to 800 μM) in PBS (pH 7.4) + 3% (v/v) DMSO. Stock protein and anchor ligand concentrations were verified by UV-Vis using ϵ_{280} (bCAII) = 57,000 $M^{-1}cm^{-1}$ or ϵ_{494} (FITC, 0.1 N NaOH) = 68,000 $M^{-1}cm^{-1}$ for fluoresceinated anchor ligand. Samples were excited at 488 nm (2 nm band-pass), and luminescence spectra were obtained between 500 nm and 700 nm (4 nm band-pass). All measurements were taken at 2 nm intervals with 0.5 s integration times at 25 °C. All luminescence spectra were subjected to background subtraction.

The ratio of sensitivities (G) for the vertically and horizontally plane-polarized light in the system was calculated by the equation $G=I_{HH}/I_{HV}$ using the I_{HH} and I_{HV} luminescence spectra obtained from a peptide-only sample. The luminescence spectra

I_{VV} and I_{VH} were integrated, and the fluorescence polarization value (P) was obtained by applying Equation 1.

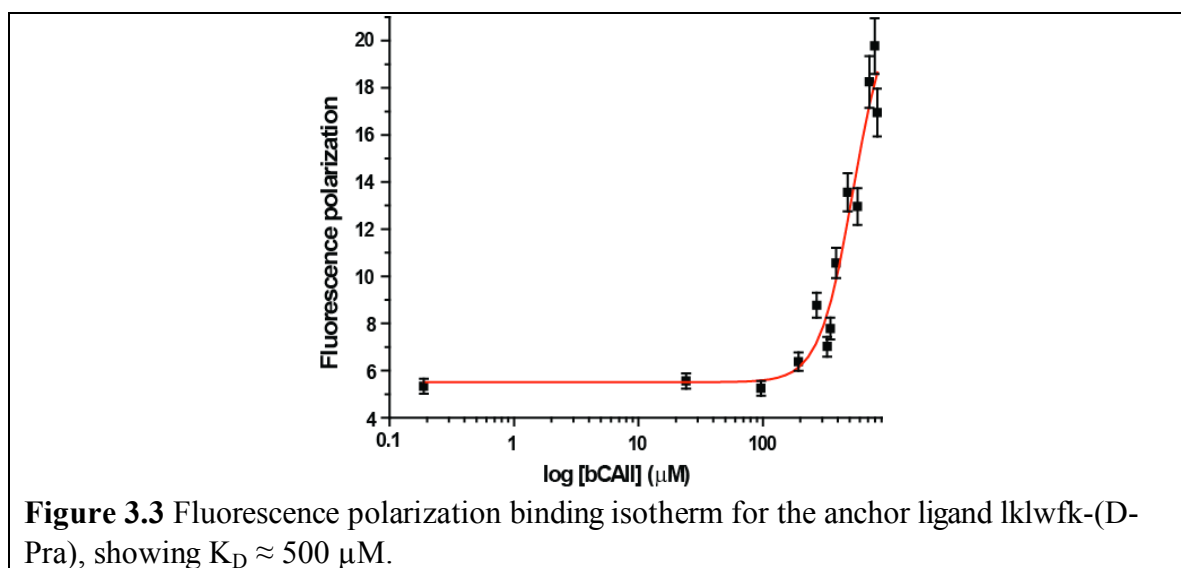
$$P = \frac{I_{VV} - GI_{VH}}{I_{VV} + GI_{VH}} \quad (1)$$

The polarization values were fitted with a sigmoidal curve using the logistical equation (Origin 6.1, Northampton, MA),

$$y = \frac{A_1 - A_2}{1 + (x/x_0)^p} + A_2 \quad (2)$$

where A_1 = initial y value, A_2 = final y value, p = power, and x_0 = center.

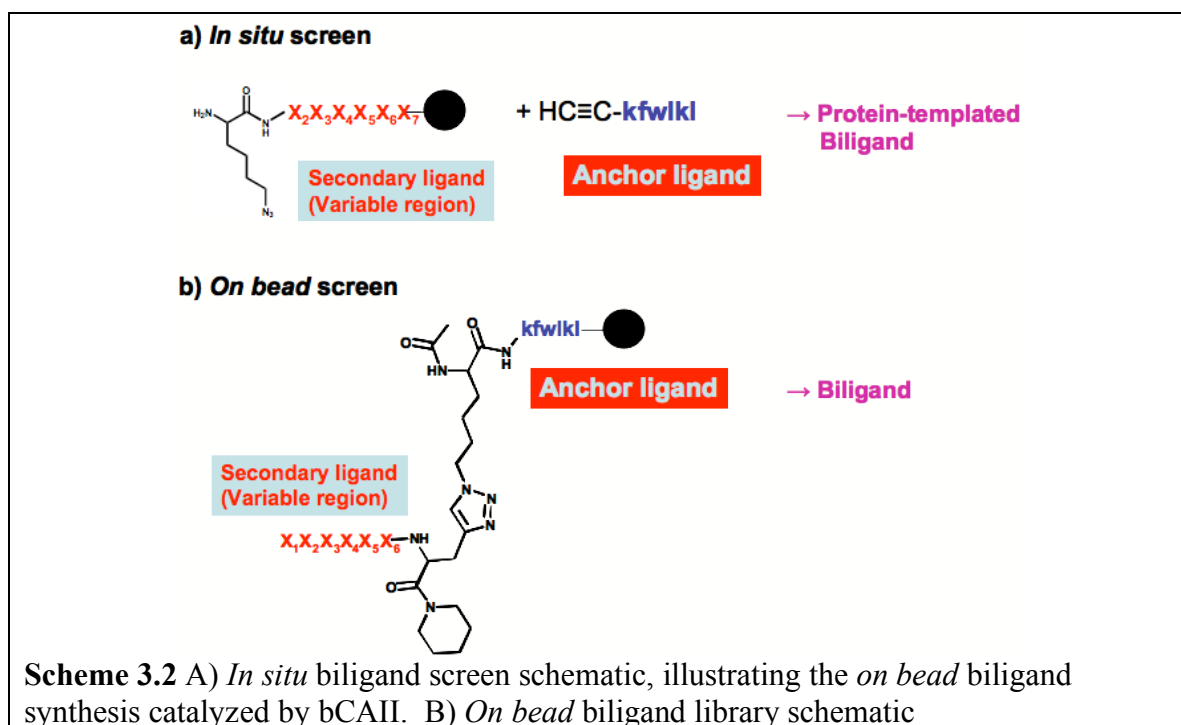
By this method, a 500 μM affinity was measured for the fluoresceinated anchor ligand lklwfk-(D-Pra) (Figure 3.3). However this value is an estimate, since weak affinities are hard to quantify.



Surface plasmon resonance (SPR) was also used to measure the affinity of bCAII with lklwfk-(D-Pra), and a similarly low affinity was recorded (at least $> 10 \mu\text{M}$, data not shown).

3.5 In Situ Click and On Bead Biligand Screens and Results

A biligand is constructed of a 2° ligand that is covalently attached, via a 1,2,3-triazole linkage, to the anchor ligand. Two screening strategies, namely *in situ* (Scheme 3.2A) and *on bead* (Scheme 3.2B) screens, were utilized to screen for biligand candidates.



3.5.1 First-Generation In Situ Biligand Screen. Based upon the *in situ* click chemical reactions reported by the Sharpless group,¹¹⁻¹⁷ the anchor ligand and protein are in solution, and the library of 2° ligands is on the bead. Only those 2° ligands that bind with bCAII *and* are in close proximity with the anchor peptide, *and* are in the correct orientation, will react to form the 1,2,3-triazole product. In the *in situ* click biligand screen (**Bi1**), a solution of 50 nM bCAII-Alexa Fluor 647 was pre-incubated with the anchor ligand, 100 μM **iklwfk-(D-Pra)**, for 2 hours at 37 °C in PBS (pH 7.4) + 1%

DMSO (v/v). The anchor/protein solution was added and incubated with a large and comprehensive, azide-modified OBOC **Library C** (22,284,891 element, 4× sampled, Table 3.1) for 48 hours at 37 °C, with shaking to form an *in situ* biligand. For this screen, excess anchor ligand is supplied so that it is noncovalently attached to its binding site on every protein molecule. The bCAII protein target acts as a catalyst for the click reaction by orienting the anchor ligand and the secondary ligand correctly with respect to each other and the protein surface. The screened beads were washed with 3 × 5 mL PBS (pH 7.4), then 7 × 5 mL water. The beads were imaged for fluorescence using the protocol outlined before. Hits, representing potential biligands formed *in situ*, were manually selected by micropipette and processed with guanidine hydrochloride to remove bound protein. These beads were then sequenced by Edman degradation.

The hit beads (0.007% hit rate) from the *in situ* screen (Scheme 3.2A) were sequenced to identify 2° ligand candidates, from which a biligand could be separately prepared. The results from Edman degradation of the 23 *in situ* hits are presented in Table 3.5.

Table 3.5 *In situ* biligand screen **Bi1** (50 nM) results

	Az _n	x ₂	x ₃	x ₄	x ₅	x ₆	Az _n
hit1	Az4	k	i	w	i	G	
hit2	Az8	r	l	w	v	G	Az4
hit3	Az8	r	r	r	k	r	Az8
hit4	Az4	l	l	v	i	k	Az4
hit5	Az4	m	i	l	i	k	
hit6	Az8	i	i	i	m	r	Az4
hit7	Az8	i	i	i	w	r	Az8
hit8	Az4	n	v	i	i	f	
hit9	Az4	i	f	l	v	k	Az8
hit10	Az4	k	i	w	i	G	Az8
hit11	Az4	r	r	k	f	r	Az8
hit12	Az4	r	v	w	l	r	Az8
hit13	Az8	k	y	r	r	r	Az4

hit14	Az8	r	r	k	v	w	Az4
hit15	Az4	i	f	l	v	k	Az8
hit16		k	r	k	r	f	Az4
hit17	Az8	k	i	w	i	k	
hit18	Az8	y	r	k	f	k	
hit19	Az4	i	f	f	r	v	Az8
hit20		a	r	k	k	y	Az4
hit 21		r	k	r	t	i	Az4
hit 22	Az8	k	m	v	f	k	Az4
hit23	Az4	l	i	m	k	i	Az4

An extremely high level of sequence homology is observed. Three almost identical peptides, **Az_nkiwiGAz_n**, are highlighted above. Note also that all of the peptides contain at least one azido group, although, statistically, over 1/3 of the OBOC library does not contain azido groups at the 1 or 7 positions. The high sequence homology, coupled with the persistence of azido groups in the peptide, provides strong evidence that the *in situ* OBOC screen worked to produce a biligand.

3.5.2 First-Generation *On Bead* Biligand Screen. In the second approach, the anchor ligand and cognate library of 2^o ligands are preassembled as complete biligands *on bead*. The protein is screened against the library of biligands in a stringent screen, in order to choose the best biligands. *On bead* (Scheme 3.2B) biligand screens (**Bi2a** and **Bi2b**) were carried out utilizing a focused biligand library (**Library D**; 117,649 peptides, Table 3.1) that was prepared based upon the sequencing results from screen **Bi1**. The 1,2,3-triazole linkage in this library was prepared using the classical click reaction between artificial amino acid **Az4** and **D-Pra** described earlier in Chapter 2. **Az4** was chosen as the optimal azide linker length based on sequence homology found among the *in situ* biligand hits. This library was limited to a smaller size to ensure high purity of full-length biligand sequence on every bead. To block nonspecific protein binding, the library was first incubated in PBS (pH 7.4) + 0.1% Tween 20 + 0.1% bovine serum

albumin (BSA) + 0.05% NaN₃ (PBSTBNaN₃) for 1 hour, with shaking.¹⁸ Following this pre-blocking step, the library was washed with 3 × 5 mL PBSTBNaN₃. The bCAII-Alexa Fluor 647, at 50 nM (**Bi2a**) and 10 nM (**Bi2b**) in 4 mL PBSTBNaN₃, was incubated with the library for 17 hours at 25 °C, with shaking. The screened beads were washed with 3 × 5 mL PBSTBNaN₃, then 3 × 5 mL PBS (pH 7.4) + 0.1% Tween 20, and finally 6 × 5 mL PBS (pH 7.4). The beads were imaged for fluorescence, and the hits were selected by micropipette. After washing the hits to remove bound protein, their sequences were determined by Edman degradation (Tables 3.6 and 3.7).

Table 3.6 *On bead* biligand screen **Bi2a** (50 nM) results

	X ₁	X ₂	X ₃	X ₄	X ₅	X ₆
hit1	f	k	l	w	i	k
hit2	v	w	l	w	G	G
hit3	f	w	f	w	G	G
hit4	k	w	f	w	G	G
hit5	f	k	l	w	l	k
hit6	k	w	f	w	G	G
hit7	w	w	i	w	G	G
hit8	k	G	w	l	w	G
hit9	k	l	w	i	w	G
hit10	l	w	i	w	G	l
hit11	f	k	G	f	l	i
hit12	f	w	i	w	G	k
hit13	l	w	l	w	G	i
hit14	i	i	v	l	w	k
hit15	l	i	i	f	v	
hit16	v	k	f	i	l	l
hit17	l	G	f	f	w	i
hit18	k	k	l	k	k	l
hit19	f	k	l	w	i	k
hit20	w	i	w	G	G	f
hit 21	f	f	l	l	v	k
hit 22	k	f	k	f	w	k
hit23	l	i	k	l	f	v
hit24	l	w	f	w	G	v
hit25	f	w	f	w	G	i
hit26	G	w	f	w	G	v
hit27	G	w	i	w	G	k

Table 3.7 *On bead* biligand screen **Bi2b** (10 nM) results

	X ₁	X ₂	X ₃	X ₄	X ₅	X ₆
hit1	k	w	i	w	G	w
hit2	k	w	i	w	G	v
hit3	k	w	l	w	G	l
hit4	k	w	i	w	G	l
hit5	k	w	i	w	G	w
hit6	k	w	l	w	G	l
hit7	G	w	i	w	G	i
hit8	k	i	f	k	i	f

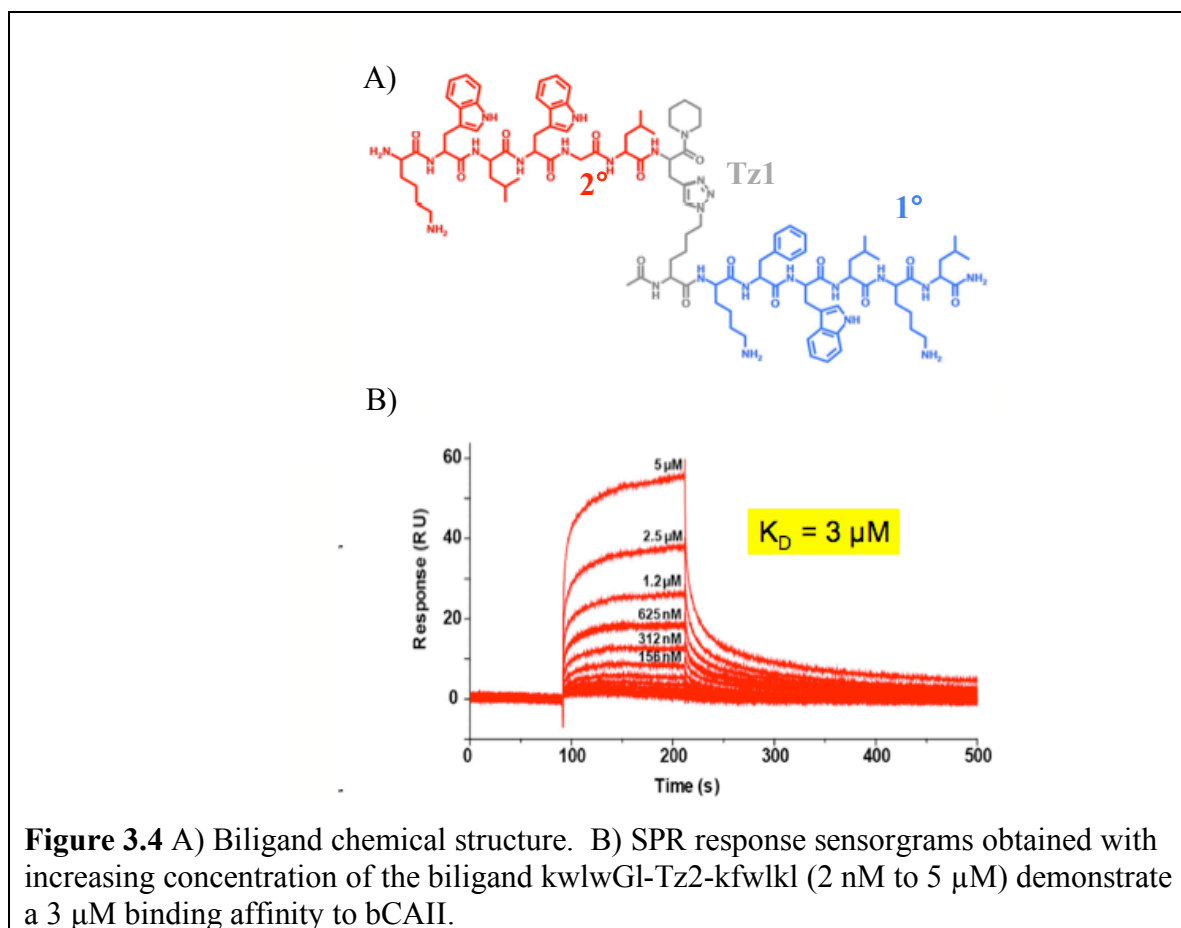
The *on bead* **Bi2a** and **Bi2b** screens (0.07% and 0.008% hit rates, respectively) again yielded a striking sequence homology, suggesting the consensus sequence **kwx₃wGx₆** (where x₃ = hydrophobic amino acid, x₆ = any amino acid). Two secondary ligand candidates from the *on bead* screen were repeated several times, namely **kwlwGI** and **kwiwGw**.

From the *on bead* and *in situ* screens, three candidate biligands— **kwlwGI-Tz2-kfwlkl**, **kwiwGw-Tz4-kfwlkl**, and **lklwfk-Tz5-kiwiG** [where **Tz4** = triazole formed between **Az4** (on terminal k) and **D-Pra** (on w), and **Tz5** = triazole formed between **Az4** (on terminal k) and **D-Pra** (on k)]— were synthesized in bulk on 2-chlorotriyl chloride (1.6 mmol/g) resin (Anaspec, San Jose, CA) using Scheme 2.3. The biligand was released either as the fully deprotected peptide by cleavage with 95:5 TFA:water (+ 2 mol equiv TES per side chain protecting group), or as the fully protected peptide by cleavage with 99:1 DCM:TFA (García-Martín et al. 2007).

3.6 Binding Measurements for Biligand by Surface Plasmon Resonance (SPR)

Immobilization and biligand sensing experiments were performed on a Biacore T100 SPR (California Institute of Technology Protein Expression Center, Pasadena, CA). Two flow cells of the biosensor surface (Biacore CM5) were immobilized with bCAII following standard procedures using NHS/EDC and 0.25 mg/mL bCAII prepared in 10 mM sodium acetate (pH 5.0) buffer.¹² The remaining two flow cells were left underivatized, to correct for changes in bulk refractive index and to assess nonspecific binding. Biligand samples were injected in a concentration series (5 μ M to 2 nM) at 100 μ L/min flow rate for 120–180 s across the four flow cells.

All three biligands— **kwlwGI-Tz2-kfwlkl**, **kwiwGw-Tz4-kfwlkl**, and **lklwfk-Tz5-kiwiG**— were synthesized in bulk (as described above) and their binding affinities for bCAII were measured using SPR. The binding responses reveal 10^{-6} M affinity for the biligands toward bCAII proving that the bead-based *in situ* screen and the *on bead* biligand library screen converge on similar biligand sequences with similar affinities. The SPR data for the best-binding biligand **kwlwGI-Tz2-kfwlkl** is shown in Figure 3.4B, and its chemical structure is pictured in Figure 3.4A. The biligand affinity fit of $K_D \approx 3$ μ M is two orders of magnitude greater than the affinity for the 1^o ligand alone, meeting our goal of affinity enhancement.



3.7 In Situ Click and On Bead Triligand Screens and Results

A triligand capture agent was identified in a similar way to the biligand, but with two exceptions. First, a modified form of the best-binding biligand **(D-Pra)-kwlwGI-Tz2-kfwlkl** served as the anchor peptide. Second, within the constraints of the OBOC libraries we could reasonably prepare, we attempted a direct comparison of *in situ* (**Tri1**) and *on bead* (**Tri2**) first-generation screens. The notable difference between these screens was the chemical diversity of the OBOC libraries.

3.7.1 First-Generation In Situ Triligand Screen. For the first generation *in situ* screen **Tri1**, a solution of 10 nM bCAII-Alexa Fluor 647 was pre-incubated with 100 μ M biligand anchor **(D-Pra)-kwlwGI-b-kfwlkl** for 2 hours at 25 $^\circ$ C in PBSTBNaN₃ (pH 7.4)

+ 1% DMSO (v/v). After blocking the library in PBSTBNaN₃ (pH 7.4) for 1 hour, with shaking, the anchor/protein solution was added to the bead library **C** (4 g, ~ 2,250,000 beads) and incubated for 15 hours at 25 °C, with shaking, to form an *in situ* triligand. Notice that the same, comprehensive 2×10^7 element OBOC **Library C** that was utilized in screen **Bi1** was applied again here, demonstrating the versatility of this type of general library. The screened beads were washed with 3×5 mL PBSTBNaN₃, then 3×5 mL PBS (pH 7.4) + 0.1% Tween 20, and finally 6×5 mL PBS (pH 7.4). The beads were then imaged for fluorescence. Hits, representing potential triligands formed *in situ*, were selected manually by micropipette. The selected beads were washed to remove bound protein and the sequences of these hits were obtained by Edman degradation (Table 3.8).

Table 3.8 First-generation *in situ* triligand screen **Tri1** (10 nM) results

	Az _n	x ₂	x ₃	x ₄	x ₅	x ₆	Az _n
hit1	Az4	n	i	i	i	v	
hit2	Az4	i	i	l	l	k	Az4
hit3	Az4	n	i	i	v	l	
hit4	Az4	n	m	i	f	l	Az4
hit5	Az4	n	v	l	v	l	
hit6	Az4	n	l	i	l	f	Az4
hit7	Az4	n	l	i	l	f	Az4
hit8	Az8	r	l	w	i	r	Az4
hit9	Az4	n	l	i	v	f	Az4
hit10	Az4	r	m	w	v	k	Az8
hit11	Az4	i	i	l	l	k	Az8
hit12	Az4	i	l	v	v	r	Az4
hit13	Az4	n	l	l	f	l	Az4
hit14	Az4	n	i	i	v	y	
hit15		m	k	r	k	k	Az8
hit16	Az4	i	l	i	r	w	Az4
hit17	Az8	i	i	v	f	r	Az8
hit18	Az8	y	f	t	r	r	
hit19	Az4	n	m	i	i	v	Az4
hit20	Az8	i	l	i	a	k	Az4
hit21	Az4	i	l	l	r	w	
hit22	Az8	i	v	v	f	r	Az4
hit23	Az4	l	l	l	v	k	Az4
hit24	Az4	k	v	w	i	k	Az4

3.7.2 First-Generation *On Bead* Triligand Screen. For the *on bead* screen **Tri2**, the difficulty of manually synthesizing a high-purity 22-mer OBOC library meant that we limited the library to a smaller number of amino acids (d, r, s, w, G, f, l), chosen to represent as high a chemical diversity as possible for a limited library size ($\sim 10^5$ – 10^6 peptides). Screens were conducted using **Library E** (40 mg, $\sim 120,000$ beads, Table 3.1) in a polypropylene fritted tube. To block nonspecific protein binding, the library was first incubated in PBSTBNaN₃ (pH 7.4) for 1 hour, with shaking. Following this pre-blocking step, the library was washed with 3×5 mL PBSTBNaN₃. The bCAII-Alexa Fluor 647, at 10 nM dilution in 4 mL PBSTBNaN₃, was incubated with the library for 17 hour at 25 °C, with shaking. The screened beads were washed with 3×5 mL PBSTBNaN₃, then 3×5 mL PBS (pH 7.4) + 0.1% Tween 20, and finally 6×5 mL PBS (pH 7.4). The beads were imaged for fluorescence, and the hits were selected by micropipette. After washing the hits to remove bound protein, their sequences were determined by Edman degradation (Table 3.9).

Table 3.9 First-generation *on bead* triligand screen **Tri2** (10 nM) results

	X ₂	X ₃	X ₄	X ₅	X ₆	X ₇
hit1	r	l	w	l	r	f
hit2	r	l	w	l	r	l
hit3	r	f	f	f	r	f
hit4	r	l	f	l	r	f
hit5	l	f	f	w	f	r
hit6	l	w	f	f	f	r
hit7	l	f	l	w	f	r
hit8	l	w	l	f	f	r
hit9	l	f	f	w	l	r
hit10	r	r	r	l	w	r
hit11	r	l	w	l	r	f
hit12	w	r	r	r	r	w
hit13	r	f	r	f	r	w
hit14	f	w	f	f	w	r

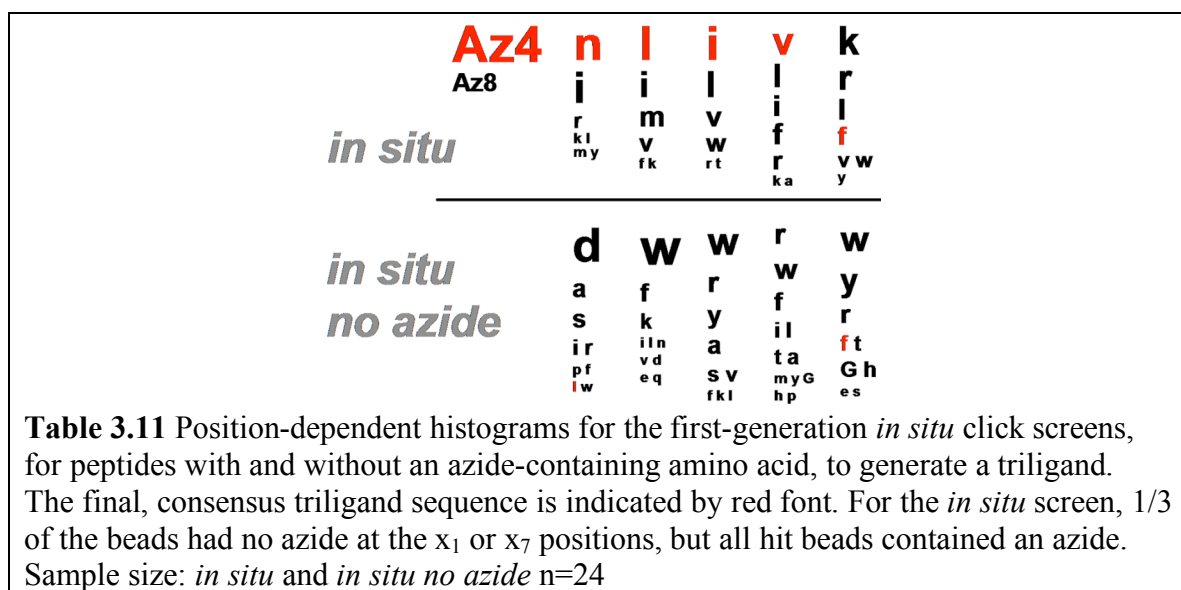
There was also a high sequence homology among the triligand sequences. The *in situ* screen **Tri1** yielded a 0.007% hit rate that suggested sequences **Az4-nlilfx₇** and **Az4-nlivfx₇** (where x₇ = any amino acid). The *on bead* screen **Tri2** resulted in a 3° ligand candidate, **Az4-rlwlrx₇**, whose motif was repeated three times. Since the *on bead* **Tri2** screen was by no means comprehensive, it is not surprising that a somewhat different 3° ligand consensus was reached.

3.7.3 Azide-Free *In Situ* Triligand Screen. To further understand the effect of the azide-acetylene interaction on the *in situ* results, a third *in situ* screen (**TriX**) was conducted under otherwise identical conditions as screen **Tri1**, except for the substitution of azide-rich **Library C** with the azide-free **Library A**, thus prohibiting the formation of a triazole linkage. While this control *in situ* screen **TriX** displayed a nearly identical hit rate (0.007%), a completely different sequence homology was reached as **(d/a/s)wwx₄x₅** (where x₄,x₅ = any amino acid) (Table 3.10 and 3.11). The remaining hit sequences from screen **TriX** display significant variation and high numbers of repeating arginine residues, indicative of nonspecific anionic-cationic interactions.¹⁹ This argues the importance of the azide-acetylene interaction in the *in situ* library selection for choosing a specific ligand, whose specificity is a consequence of the *in situ* click conjugation.

Table 3.10 Azide-free *in situ* triligand screen **TriX** results (control)

	x₁	x₂	x₃	x₄	x₅
hit1	w	f	r	r	r
hit2	s	w	v	w	G
hit3	p	v	y	f	w
hit4	d	d	y	w	G
hit5	i	w	a	y	w
hit6	d	n	w	G	f
hit7	a	w	w	a	t
hit8	r	f	r	r	f
hit9	d	w	w	h	t
hit10	r	f	r	w	r

hit11	d	e	w	p	h
hit12	a	w	w	l	w
hit13	a	w	w	a	y
hit14	d	k	k	i	y
hit15	d	w	s	i	e
hit16	s	w	w	f	y
hit17	d	w	l	r	y
hit18	s	w	a	f	y
hit19	d	l	f	l	w
hit20	d	w	a	t	w
hit21	f	k	y	r	s
hit22	d	q	r	w	r
hit23	i	w	s	t	h
hit24	l	i	v	m	w



3.7.4 Re-Screening for Triligand Ligand with Focused Libraries. Second-generation *in situ* (screen **Tri3**) and *on bead* (screen **Tri4**) triligand screens were conducted using **Libraries F** and **G**, respectively (Table 3.1). Each **Library F** and **Library G** included *all* the high-homology amino acids isolated by the first-generation triligand screens. The second-generation screens were used to determine whether a single

triligand capture agent could be deduced by screening a single, highly focused triligand library.

Both triligand screening strategies allowed for isolation of hits at much lower bCAII-Alexa Fluor 647 concentrations, as low as 500 pM for the *in situ* library and 250 pM for the *on bead* library, compared to the biligand screens. In the second-generation *in situ* click triligand screen, a solution of 500 pM bCAII-Alexa Fluor 647 was pre-incubated with 100 μ M Biligand Anchor **(D-Pra)-kwlwGI-b-kfwlkl** for 2 hours at 25 °C in PBSTBNaN₃ (pH 7.4) + 1% DMSO (v/v). After blocking the library in PBSTBNaN₃ (pH 7.4) for 1 hour, with shaking, the anchor/protein solution was added to the focused bead **Library F** (3200 D-peptide compounds, 1 mg, ~ 3200 beads) and incubated for 18 hours at 25 °C, with shaking, to form a triligand.

In the second-generation *on bead* triligand screen, screens were conducted using the focused **Library G** (1 mg, ~ 3200 beads) for 18 hours at 25 °C, with shaking. **Library G** was constructed using exactly the same constituent amino acids as **Library F**, but with the biligand anchor covalently attached to the end of the library via the Cu(I)-catalyzed click reaction. In both cases, the screened beads were washed with 3 \times 5 mL PBSTBNaN₃, then 3 \times 5 mL PBS (pH 7.4) + 0.1% Tween 20, and finally 6 \times 5 mL (PBS pH 7.4). The beads were then imaged for fluorescence. Hits, representing potential triligands formed *in situ*, were selected manually by micropipette. The selected beads were then processed to remove bound protein, and the sequences of these hits were obtained by Edman degradation (Tables 3.12 and 3.13).

Table 3.12 Second-generation *in situ* triligand screen **Tri3** (500 pM) results

	X ₂	X ₃	X ₄	X ₅	X ₆	X ₇
hit1	n	l	l	v	f	r
hit2	n	l	i	v	l	r
hit3	n	i	i	l	l	r
hit4	i	l	f	l	f	r
hit5	n	l	i	v	l	r
hit6	n	i	i	l	w	r
hit7	n	l	i	v	f	r
hit8	n	l	i	v	f	r

Table 3.13 Second-generation *on bead* triligand screen **Tri4** (250 pM) results

	X ₂	X ₃	X ₄	X ₅	X ₆	X ₇
hit1	n	l	i	v	f	r
hit2	n	l	i	v	f	r
hit3	n	i	i	v	f	r
hit4	n	i	i	v	f	r
hit5	n	i	i	l	l	r
hit6	n	l	i	v	l	r
hit7	n	l	i	v	f	r

Both the *in situ* (**Tri3**) and *on bead* (**Tri4**) screens yielded a single 3° ligand sequence of **Az4-nlivfr**. The fact that this same consensus sequence was identified by both an *on bead* and an *in situ* screen (each designed to sample the same chemical space, albeit via different paths) provides further confirmation of the equivalence of the two types of screens.

The triligand— **rfviln-Tz2-kwlwGl-Tz1-kfwlkl**— was synthesized by the click reaction between the fully protected biligand anchor (0.274 g, 0.1 mmol, > 98% HPLC) and bead-bound 3° ligand **Az4-nlivfr** (0.1 g, 0.07 mmol) using copper iodide (0.021 g, 0.1 mmol) and L-ascorbic acid (0.020 g, 0.1 mmol) in DMF/piperidine (8/2) at 25 °C (Scheme 2.3).

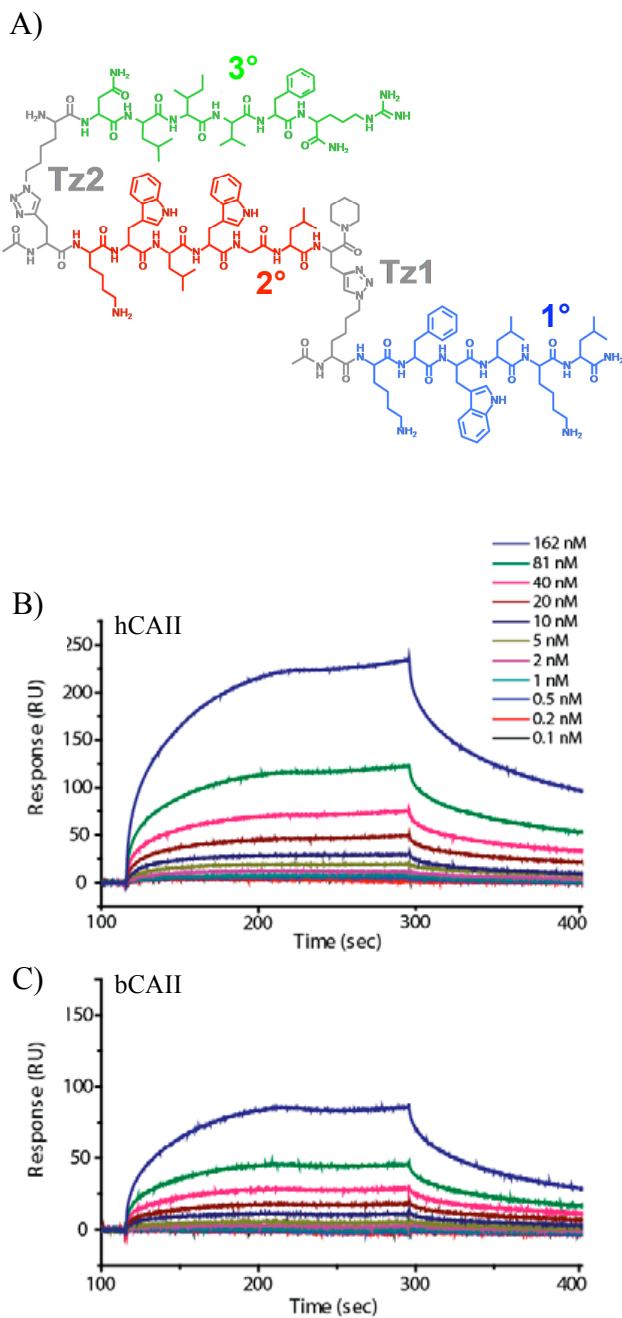
3.8 Binding Measurements for Triligand using SPR

3.8.1 Protein. Human carbonic anhydrase II (hCAII, C6165), from human erythrocytes, lyophilized powder, was purchased from Sigma-Aldrich (St. Louis, MO) and used in affinity and selectivity studies. Both bCAII and hCAII were tested by SDS gel electrophoresis, and confirmed to display a single band corresponding to 29,000 Da.

3.8.2 SPR. The triligand, **rfvilm-Tz2-kwlwGI-Tz1-kfwlkl**, (chemical structure shown in Figure 3.5A) was synthesized in bulk and its binding affinity for both bCAII and hCAII was measured using SPR. These affinity measurements utilized a Biacore T100 SPR (California Institute of Technology Protein Expression Center, Pasadena, CA). One flow cell of the biosensor surface (Biacore CM5) was immobilized with bCAII following standard procedures using 0.25 mg/mL bCAII prepared in 10 mM sodium acetate (pH 5.0) buffer and a 1:1 solution of 0.1 mM NHS and 0.4 mM EDC.²⁰ Similarly, a second flow cell was immobilized with hCAII following standard procedures using 0.25 mg/mL hCAII prepared in 10 mM sodium acetate (pH 5.5) buffer. An immobilization level of 5000 RU was achieved using a flow rate of 100 μ L/min over 420 s. The remaining two flow cells were left underivatized, to correct for changes in bulk refractive index and to assess nonspecific binding. The running buffer was prepared to contain 10 mM HEPES + 150 mM NaCl + 0.05% Tween20 + 3% DMSO, and this buffer was used for all experiments.

Prior to the peptide analyte experiment, 8 'startup' cycles (running buffer alone) were completed to ensure that the instrument had a stable baseline. Response data were then collected for biligand samples over increasing concentrations (2 nM to 5 μ M) at 100 μ L/min flow rate, 120–180 s contact time, and 300 s dissociation phase across the four

flow cells. Similarly, response data were collected for anchor ligands (300 nM to 9.4 μ M) and triligand (0.1 nM to 162 nM) over increasing analyte concentrations. After subtracting the background response from the underivatized flow cell, the analyte response data was fitted for 1:1 binding affinity using the BiaEvaluation software.



Figures 3.5B and 3.5C show the SPR results for the triligand to be $K_D \approx 45$ nM (hCAII) and $K_D \approx 64$ nM (bCAII). This represents a fifty fold affinity enhancement over the biligand. The triligand was also shown to not bind to the enzymatically active site of bCAII by an activity assay using 4-nitrophenyl acetate (4-NPA) as chromogenic substrate (data not shown here).²¹

3.9 Dot Blot Selectivity/Sensitivity Assays in Serum

The sensitivity and selectivity of the multi-ligand (biligand and triligand) capture agents for b(h)CAII in complex environments were demonstrated through the use of dot blot experiments in 10% porcine serum. For these tests, Biotin-PEG-NovaTag resin (0.48 mmol/g; Novabiochem) was utilized for bulk synthesis of C-terminal biotin-labeled multi-ligands. After resin cleavage, the crude biotinylated multi-ligand was precipitated with ether and then purified to > 98% by C_{18} reversed-phase HPLC. Antigens (bCAII and hCAII) were prepared as 2 mg/mL stocks in PBS (pH 7.4). A dilution series of antigen was applied to a nitrocellulose membrane, typically ranging from 20 μ g to 0.4 pg per spot. The membrane was blocked at 4 °C overnight in 5% milk in Tris-buffered saline (TBS) [25 mM Tris, 150 mM NaCl, 2 mM KCl (pH 7.4)]. The membrane was then washed with 3 x 5 min TBS (pH 7.4). The biotinylated triligand was prepared at 1 μ M in 10% porcine serum in TBS (pH 7.4) + 0.1% DMSO and incubated over the membrane overnight at 4 °C. After washing with TBS (pH 7.4) for 1 hour, 1:3000 Streptavidin-HRP (AbCam, Cambridge, MA) prepared in 0.5% milk/TBS (pH 7.4) was added to the membrane and incubated for 1 hour. After washing with TBS (pH 7.4) for 1 hour, chemiluminescent reagents (SuperSignal West Pico Chemiluminescent Enhancer and

Substrate Solutions, Pierce, Rockford, IL) were incubated over the membrane and then immediately developed on film to determine binding.

Figure 3.6A illustrates that the triligand is a suitable capture agent for detection of ~ 20 ng antigen from 10% serum, and that the capture agent was specific for both the bovine and human forms of the enzyme. Since bCAII and hCAII are 81.2% identical in sequence, similar binding sites are expected (PDB ID: 1CA2, 1V9E). The commercial anti-bCAII was capable of detecting lower antigen (~ 1 ng). However, this result cannot be directly compared to the triligand result, as this antibody is labeled with significantly more biotins per molecule (15–20 biotins/antibody), while the triligand is labeled with only 1 biotin per molecule. When the biligand anchor (D-Pra)-kwlwGI-Tz2-kfwlkl was used as the capture agent in 0.1% serum, the sensitivity was reduced more than ten fold (Figure 3.6B).

For comparison, the dot blot was completed in parallel using a commercial antibody as the capture agent. The polyclonal rabbit anti-bCAII IgG, biotin conjugate (Rockland Immunochemicals, Gilbertsville, PA) was prepared at 1:4000 dilution and incubated as described above. Both the triligand and commercial antibody were tested for cross-reactivity with 1 µg human IL-2 (BD Biosciences, San Jose, CA) and 1 µg human TNF α (eBioscience, San Diego, CA), and no binding was detected (Figure 3.6C). We also tested BSA as the antigen and similarly found no cross-reactivity.

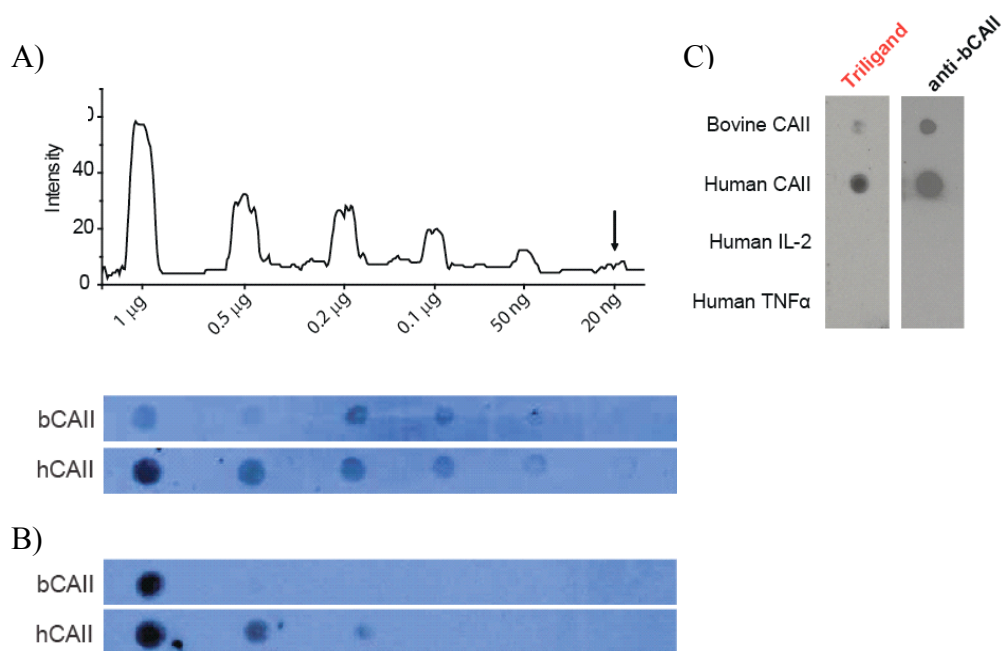


Figure 3.6 A) Dot blot illustrating the limit of detection by the triligand for bCAII and hCAII in 10% serum. B) When the biligand anchor is used as the capture agent in 0.1% serum, the sensitivity is reduced > ten fold. C) Dot blot illustrating the selectivity of the triligand, compared to a commercial antibody

3.10 Conclusion

This thesis demonstrated the development of a peptide capture agent with high affinity and selectivity against CAII through the conjugation of modest affinity peptides using *in situ* click chemistry. An affinity enhancement due to *in situ* click conjugation was apparent starting from the level of the biligand screens. Even for a weakly binding anchor ligand ($K_D \approx 500 \mu\text{M}$), biligand screens yielded high hit homologies and affinities between 3 and 10 μM . Both types of biligand screens, *in situ* and *on bead*, demonstrated this effect, suggesting that although the mechanism of the selection is different, the hits identified are essentially equivalent. When the peptide ligand becomes larger than a 10–15mer, the OBOC library size is practically limited to < 1 million sequences, and the *in situ* screen becomes the only way to sample increasing diversity and length.

Comprehensive *in situ* libraries are also quite valuable in their versatility, as they can be used in more than one screen and with more than one protein target, if synthesized at a large enough scale to accommodate multiple experiments. At the triligand level, a similar concept was explored. While the *in situ* library was still comprehensive, it utilized the basis of the biligand anchor to direct the assembly of the triligand. Based on analysis of sequence homology, we discovered that the final triligand capture agent reflects *in situ* assembly, as the *on bead* triligand library was not comprehensive. The final triligand peptide capture agent was demonstrated to bind to bCAII and hCAII with affinities of $K_D \approx 64$ nM and $K_D \approx 45$ nM, respectively, and it was proven to be a selective binder for the enzyme as illustrated by dot blot. The small size of the triligand peptide capture agent is expected to increase sensitivity of CAII detection in surface-based diagnostic assays.

The advantage of this approach is multifold. First, each multi-ligand is comprised of two or more ligands, and each ligand is a peptide-like molecule, comprised of natural, artificial, or nonnatural amino acids and other organic molecule building blocks. Chemical and biochemical stability, water solubility, thermal stability, and other desired characteristics can be custom designed into the multi-ligand. Also, multi-ligand capture agents produced in this way do not denature, as antibodies do, since their affinity and selectivity are not contingent upon their folded structure. Next, as the number of ligands comprising the multi-ligand protein capture agent is increased, the selectivity and affinity of the multi-ligand for the protein of interest rapidly increases. Tetraligands, pentiligands, etc., are all possible using the same concepts. Moreover, the target protein itself is utilized as a catalyst to assemble its own multi-ligand capture agent. The

individual ligands themselves are specifically designed for this catalytic process. No previous knowledge is needed of the capture agent and the protein of interest. Furthermore, amino acid building blocks are readily available, and chemical synthesis of peptides in relatively large quantities using conventional amide coupling chemistries is not difficult. This implies that the peptide capture agents may be produced in multi-gram quantities at low cost. Since straightforward chemistries are implemented at every stage in the process, we expect to use this as a general and robust platform for high-throughput capture agent discovery making an *in vitro* diagnostic device possible and inexpensive.

3.11 References

1. Mocharla, V. P.; Colasson, B.; Lee, L. V.; Röper, S.; Sharpless, K. B.; Wong, C.-H.; Kolb, H. C. *Angew. Chem. Int. Ed.* **2005**, *44*, 116–120.
2. Krishnamurthy, V. M.; Kaufman, G. K.; Urbach, A. R.; Gitlin, I.; Gudiksen, K. L.; Weibel, D. B.; Whitesides, G. M. *Chem. Rev.* **2008**, *108*, 946–1051.
3. Jude, K. M.; Banerjee, A. L.; Haldar, M. K.; Manokaran, S.; Roy, B.; Mallik, S.; Srivastava, D. K. Christianson, D. W. *J. Am. Chem. Soc.* **2006**, *128*, 3011–3018.
4. Melkko, S.; Scheuermann, J.; Dumelin, C. E.; Neri, D. *Nat. Biotechnol.* **2004**, *22*, 568–574.
5. Wilkinson, B. L.; Bornaghi, L. F.; Houston, T. A.; Innocenti, A.; Supuran, C. T.; Poulsen, S.-A. *J. Med. Chem.* **2006**, *49*, 6539–6548.
6. Parkkila, S.; Rajaniemi, H.; Parkkila, A.-K.; Kivelä, J.; Waheed, A.; Pastoreková, S.; Pastorek, J.; Sly, W. S. *Proc. Natl. Acad. Sci. USA* **2000**, *97*, 2220–2224.
7. Yoshiura, K.; Nakaoka, T.; Nishishita, T.; Sato, K.; Yamamoto, A.; Shimada, S.; Saida, T.; Kawakami, Y.; Takahashi, T. A.; Fukuda, H.; Imajoh-Ohmi, S.; Oyaizu, N.; Yamashita, N. *Clin. Cancer Res.* **2005**, *11*, 8201–8207.
8. Haapasalo, J.; Nordfors, K.; Järvelä, S.; Bragge, H.; Rantala, I.; Parkkila, A.-K.; Haapasalo, S. *Neuro-Oncol.* **2007**, *9*, 308–313.
9. Laursen, R. A. *Eur. J. Biochem.* **1971**, *20*, 89–102.
10. Yin, H.; Litvinov, R. I.; Vilaire, G.; Zhu, H.; Li, W.; Caputo, G. A.; Moore, D. T.; Lear, J. D.; Weisel, J. W.; DeGrado, W. F.; Bennett, J. S. *J. Biol. Chem.* **2006**, *281*, 36732–36741.
11. Lewis, W. G.; Green, L. G.; Grynszpan, F.; Radić, Z.; Carlier, P. R.; Taylor, P.; Finn, M. G.; Sharpless, K. B. *Angew. Chem. Int. Ed.* **2002**, *41*, 1053–1057.
12. Manetsch, R.; Krasiński, A.; Radić, Z.; Raushel, J.; Taylor, P.; Sharpless, K. B.; Kolb, H. C. *J. Am. Chem. Soc.* **2004**, *126*, 12809–12818.

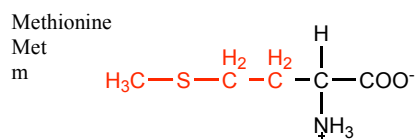
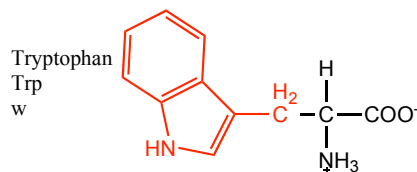
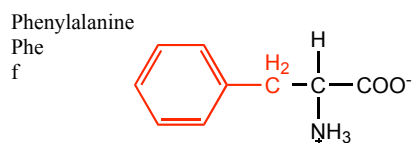
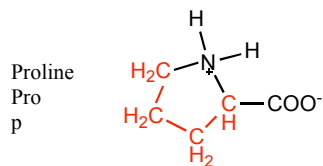
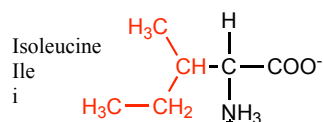
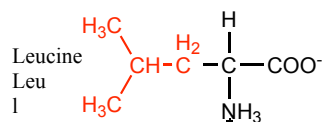
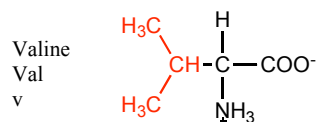
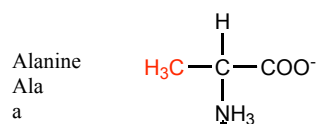
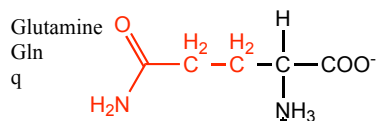
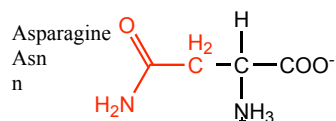
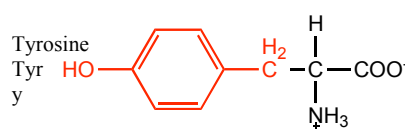
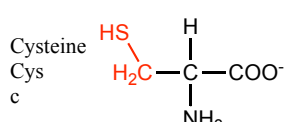
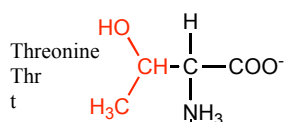
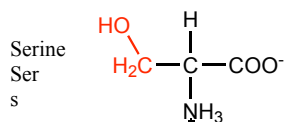
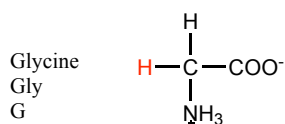
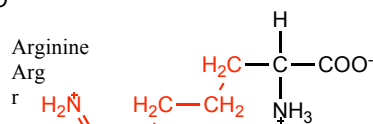
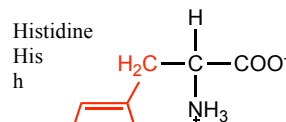
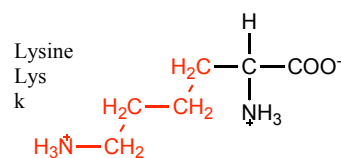
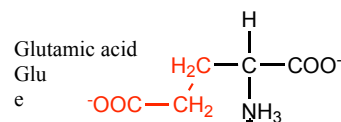
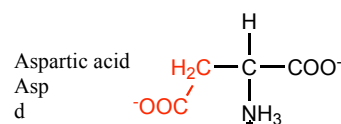
13. Bourne, Y.; Kolb, H. C.; Radić, Z.; Sharpless, K. B.; Taylor, P.; Marchot, P. *Proc. Natl. Acad. Sci. USA* **2004**, *101*, 1449–1454.
14. Mocharla, V. P.; Colasson, B.; Lee, L. V.; Röper, S.; Sharpless, K. B.; Wong, C.-H.; Kolb, H. C. *Angew. Chem. Int. Ed.* **2005**, *44*, 116–120.
15. Krasinski, A.; Radić, Z.; Manetsch, R.; Raushel, J.; Taylor, P.; Sharpless, K. B.; Kolb, H. C. *J. Am. Chem. Soc.* **2005**, *127*, 6686–6692.
16. Whiting, M.; Muldoon, J.; Lin, Y. C.; Silverman, S. M.; Lindstrom, W.; Olson, A. J.; Kolb, H. C.; Finn, M. G.; Sharpless, K. B.; Elder, J. H.; Fokin, V. V. *Angew. Chem. Int. Ed.* **2006**, *45*, 1435–1439.
17. Brik, A.; Muldoon, J., Lin, Y. C.; Elder, J. H.; Goodsell, D. S.; Olson, A. J.; Fokin, V. V.; Sharpless, K. B.; Wong, C. H. *ChemBioChem* **2003**, *4*, 1246–1248.
18. Lehman, A.; Gholami, S.; Hahn, M.; Lam, K. S. *J. Comb. Chem.* **2006**, *8*, 562.
19. Aina, O. H.; Liu, R.; Sutcliffe, J. L.; Marik, J.; Pan, C.-X.; Lam, K. S. *Mol. Pharm.* **2007**, *4*, 631–651.
20. Papalia, G. A.; Leavitt, S.; Bynum, M. A.; Katsamba, P. S.; Wilton, R.; Qiu, H.; Steukers, M.; Wang, S.; Bindu, L.; Phogat, S.; Giannetti, A. M.; Ryan, T. E.; Pudlak, V. A.; Matusiewicz, K.; Michelson, K. M.; Nowakowski, A.; Pham-Baginski, A.; Brooks, J.; Tieman, B. C.; Bruce, B. D.; Vaughn, M.; Baksh, M.; Cho, Y. H.; De Wit, M.; Smets, A.; Vandersmissen, J.; Michiels, L.; Myszka, D. G. *Anal. Biochem.* **2006**, *359*, 94.
21. Pocker, Y.; Stone, J. T. *Biochemistry* **1967**, *6*, 668–678.

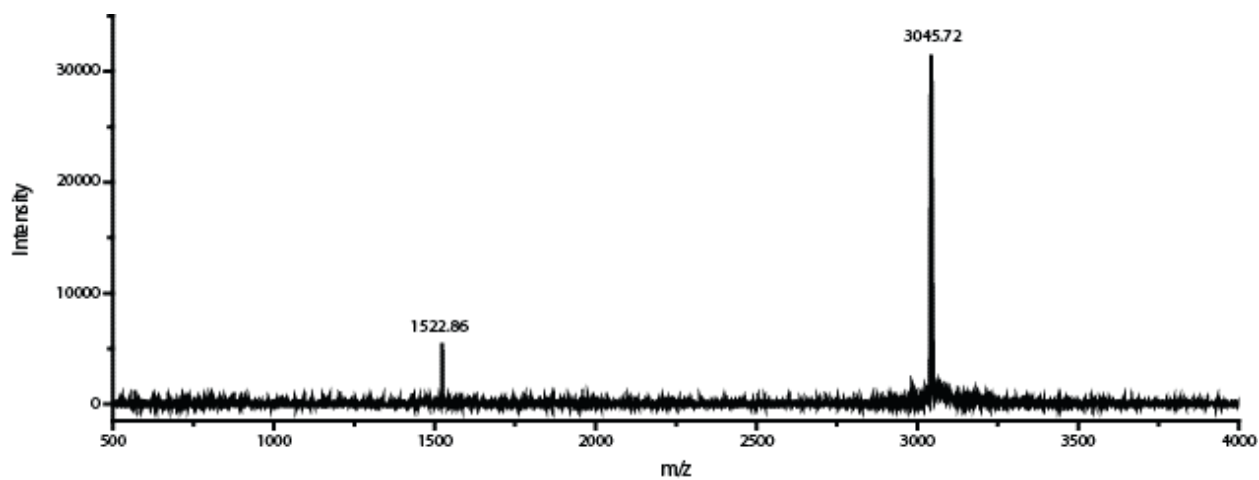
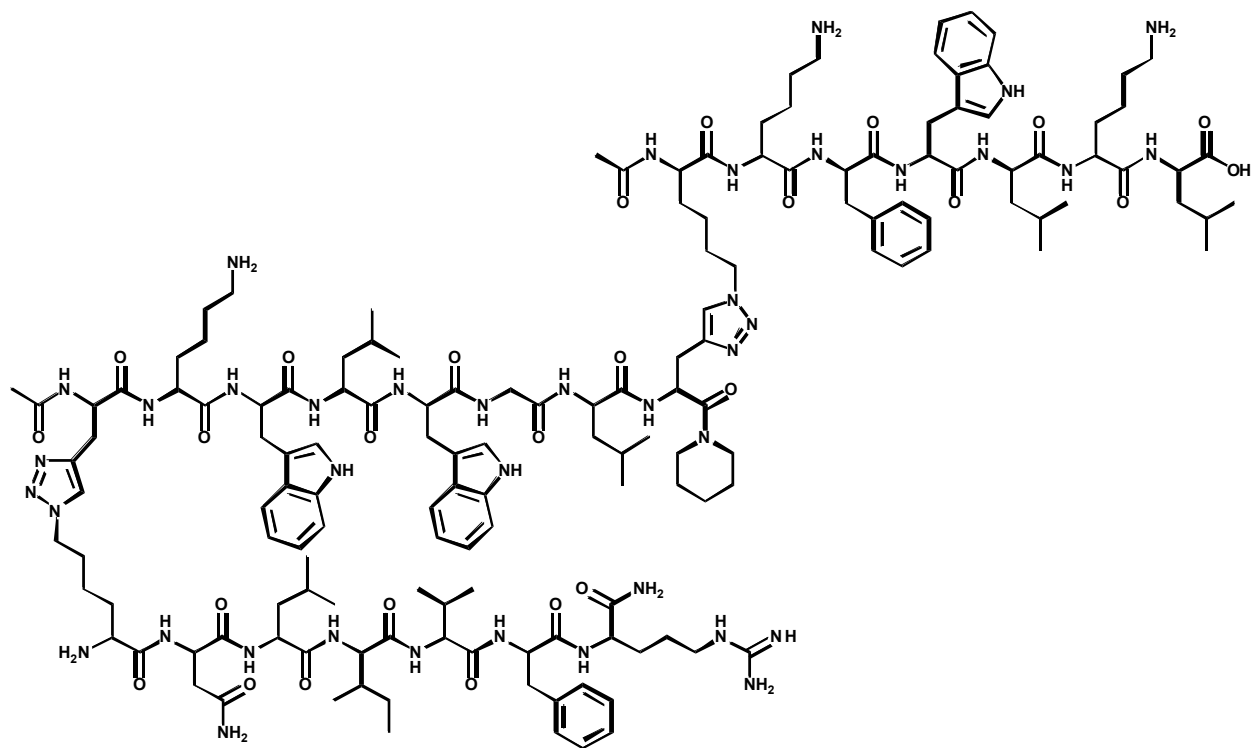
3.12 Future Directions

A method for developing multi-ligand based protein capture agents that can potentially replace the current standard, antibodies, is described and demonstrated in this thesis. The approach is now being applied towards the development of branched capture agents. Branched peptides can emulate the effect of the variable region within a folded immunoglobulin (antibody), while maintaining a fairly low molecular weight (which reduces cost and production time). Branched multi-ligand capture agents, like linear capture agents, can exhibit stability in various environments in which antibodies and natural polypeptides are not stable.

Protein catalyzed multi-ligand capture agents can potentially be utilized for standard assays in either laboratory or clinical settings. The standard assays fall into two classes: label-free and sandwich assays. In both assays, antibodies are the mostly commonly utilized protein capture agents. Multi-ligand capture agents will be tested as a replacement for antibodies in such traditional antibody-based assays. Prior to the selection process, multi-ligand capture agents can be designed with functional groups that promote specific surface attachment and orientation that would be compatible with these assay formats. Creating capture agents for detecting and/or separating one or more targets in a complex sample (e.g., blood) with high affinity and specificity will allow diagnosis, patient monitoring, and selection of treatment options to patients. Multiparameter assays can also be performed with the multi-ligand capture agents for proteomic analysis, tissue analysis, serum diagnostics, biomarker, serum profiling, multiparameter cell sorting, single cell studies, etc. We are currently translating our

approach to many cancer relevant protein biomarkers, including proteins with post-translational modifications such as phosphorylation and glycosylation.

Appendix A.**Group I. Amino Acids with Apolar R Groups****Group II. Amino Acids with Uncharged R Groups****Group III. Amino Acids with Charged R Groups****Figure A1.** Structures of the twenty d-amino acids (side groups are denoted in red)

Appendix B. Complete Structures of Biligands and Triligands**Figure B1.** Triligand (Mol. Wt. 3045.72)

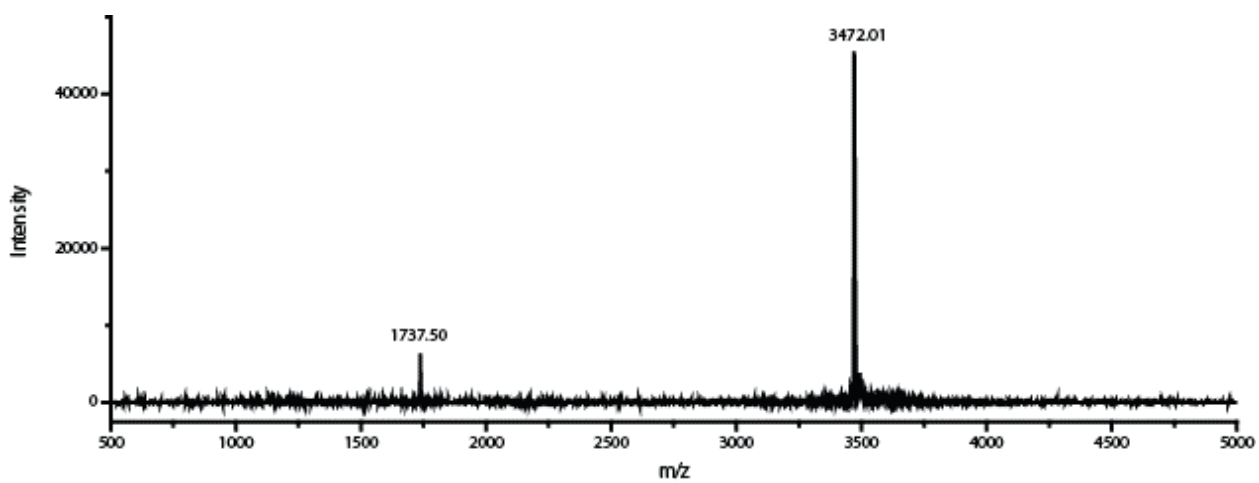
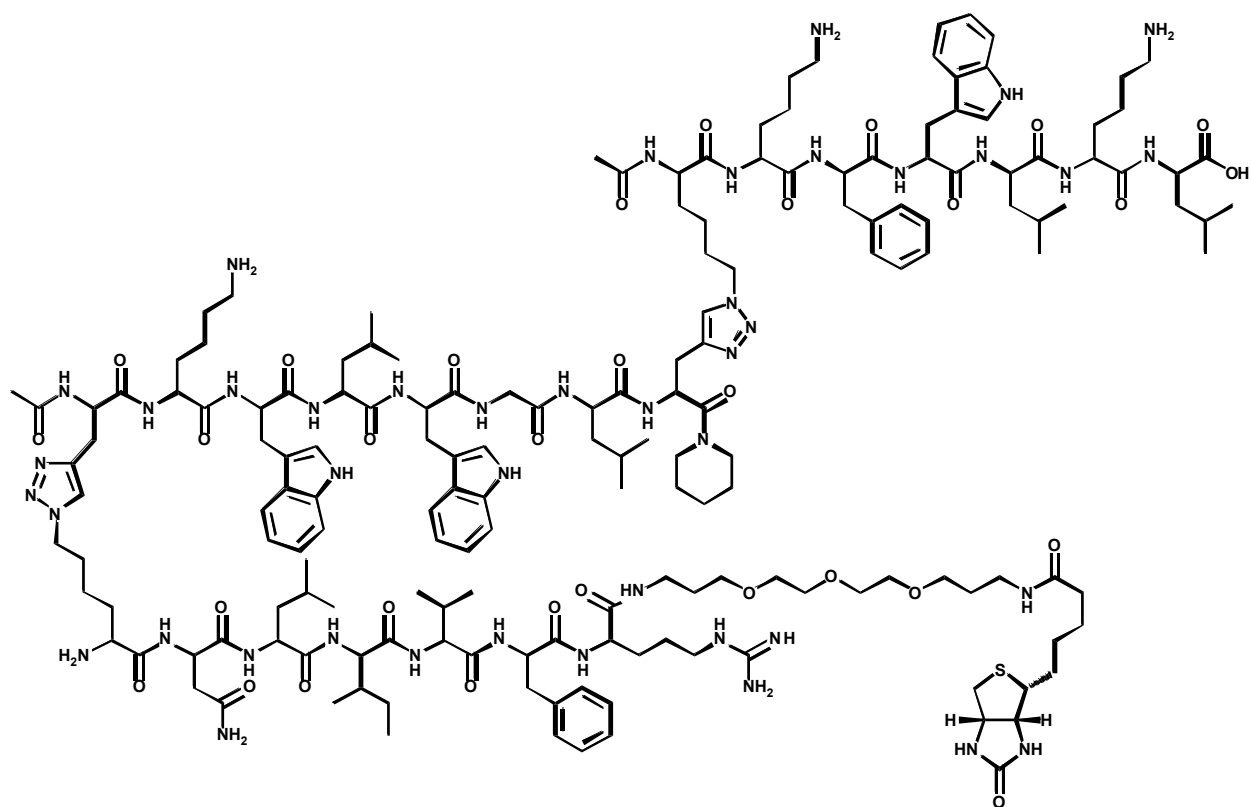


Figure B2. Triligand, biotin conjugate (Mol. Wt. 3475.29)

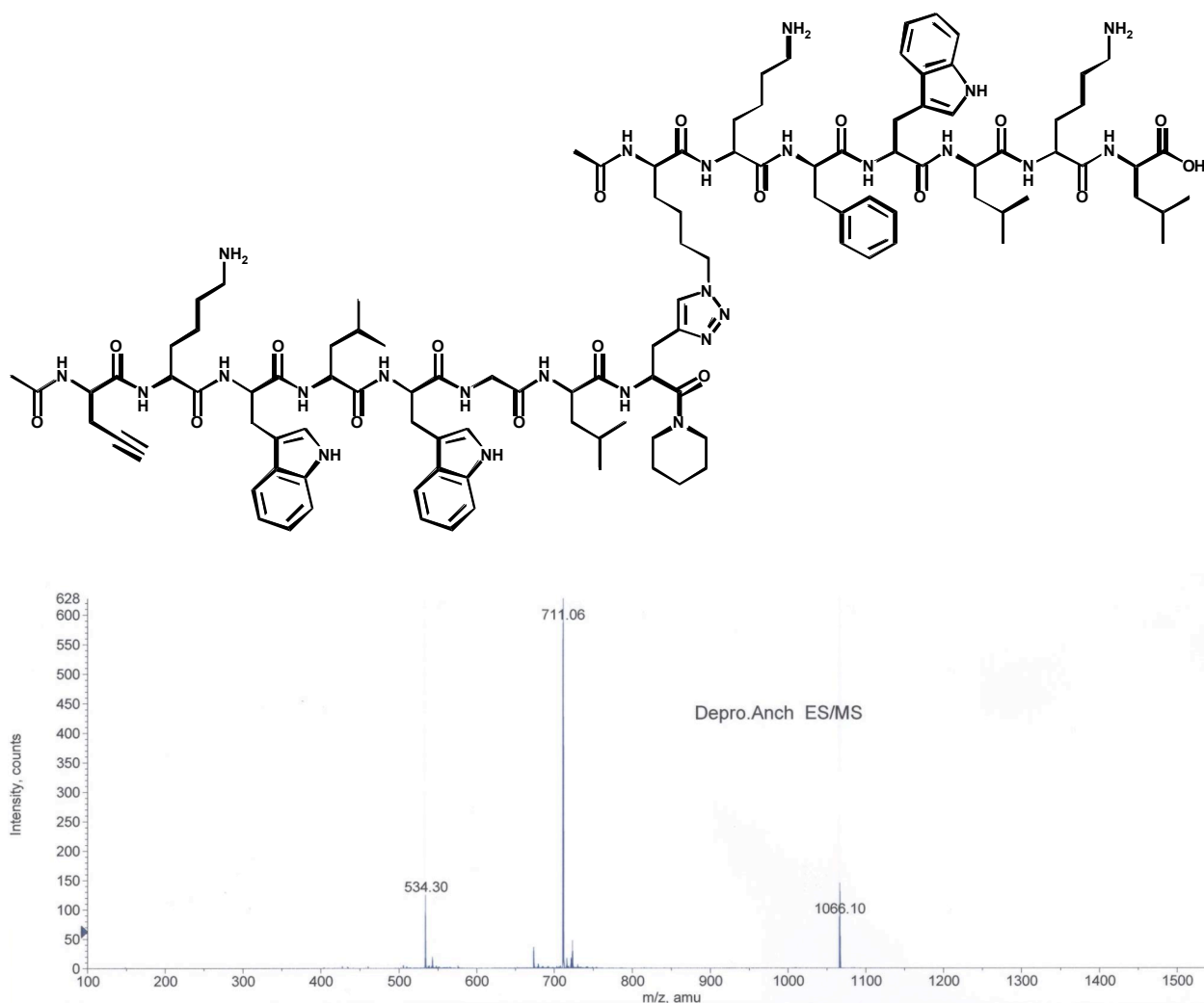


Figure B3. Biligand Anchor, deprotected (Mol. Wt.: 2131.61)

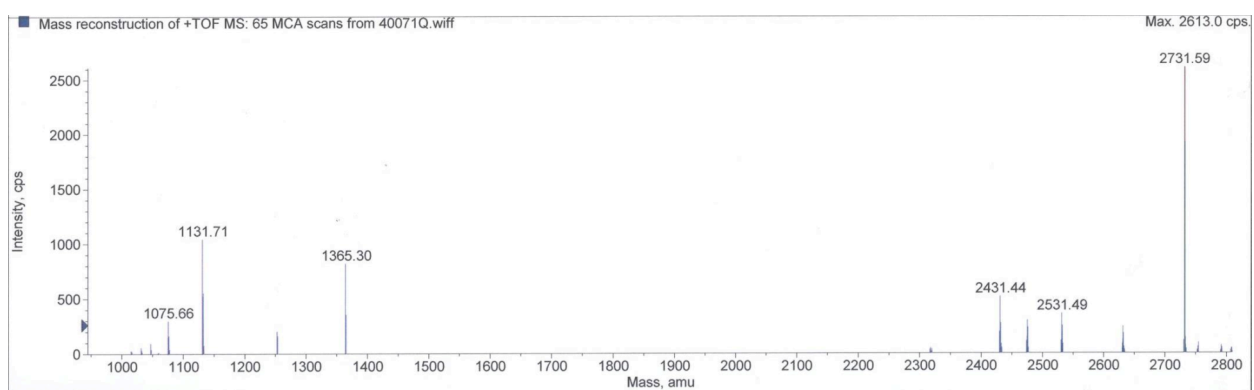
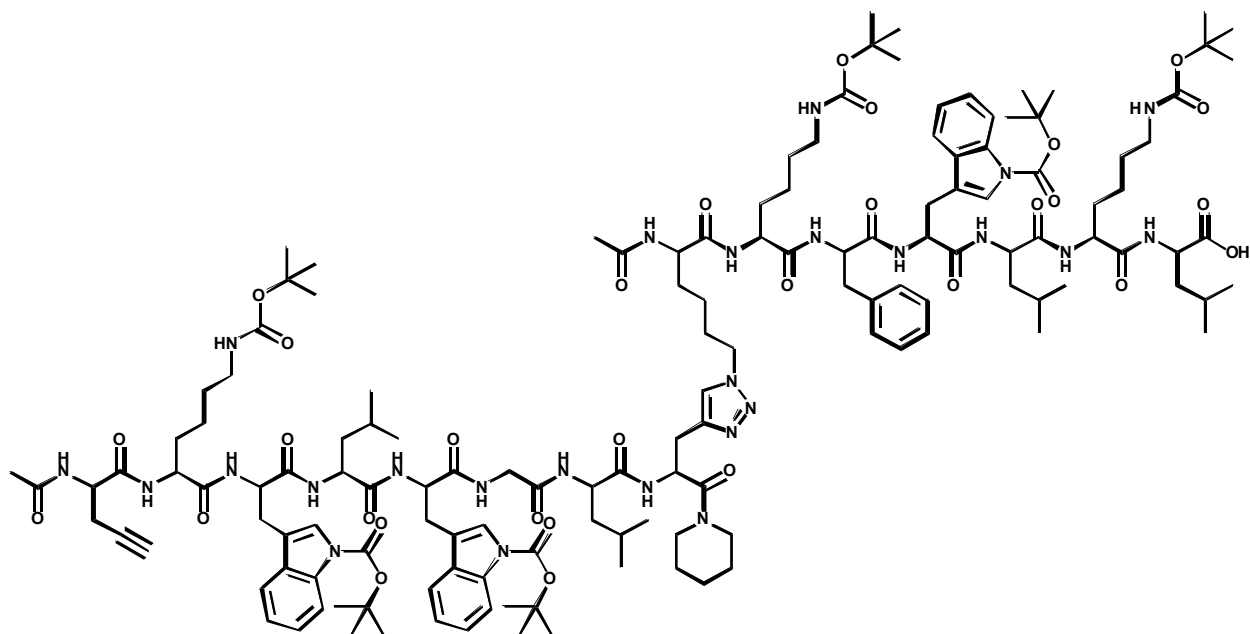


Figure B4. Biligand Anchor, fully protected (Mol. Wt.: 2732.30)

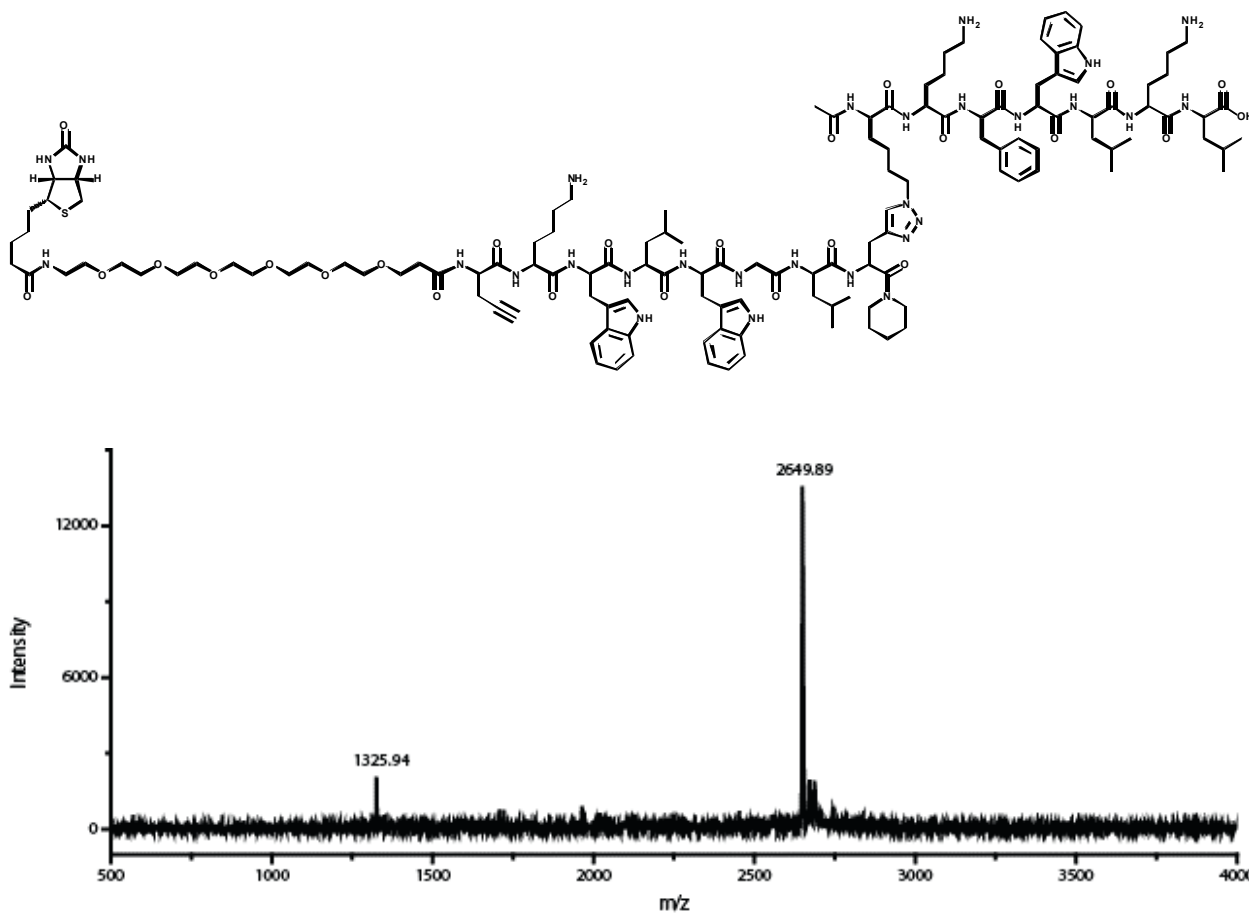


Figure B5. Biligand Anchor, biotin conjugate (Mol. Wt.: 2651.26)

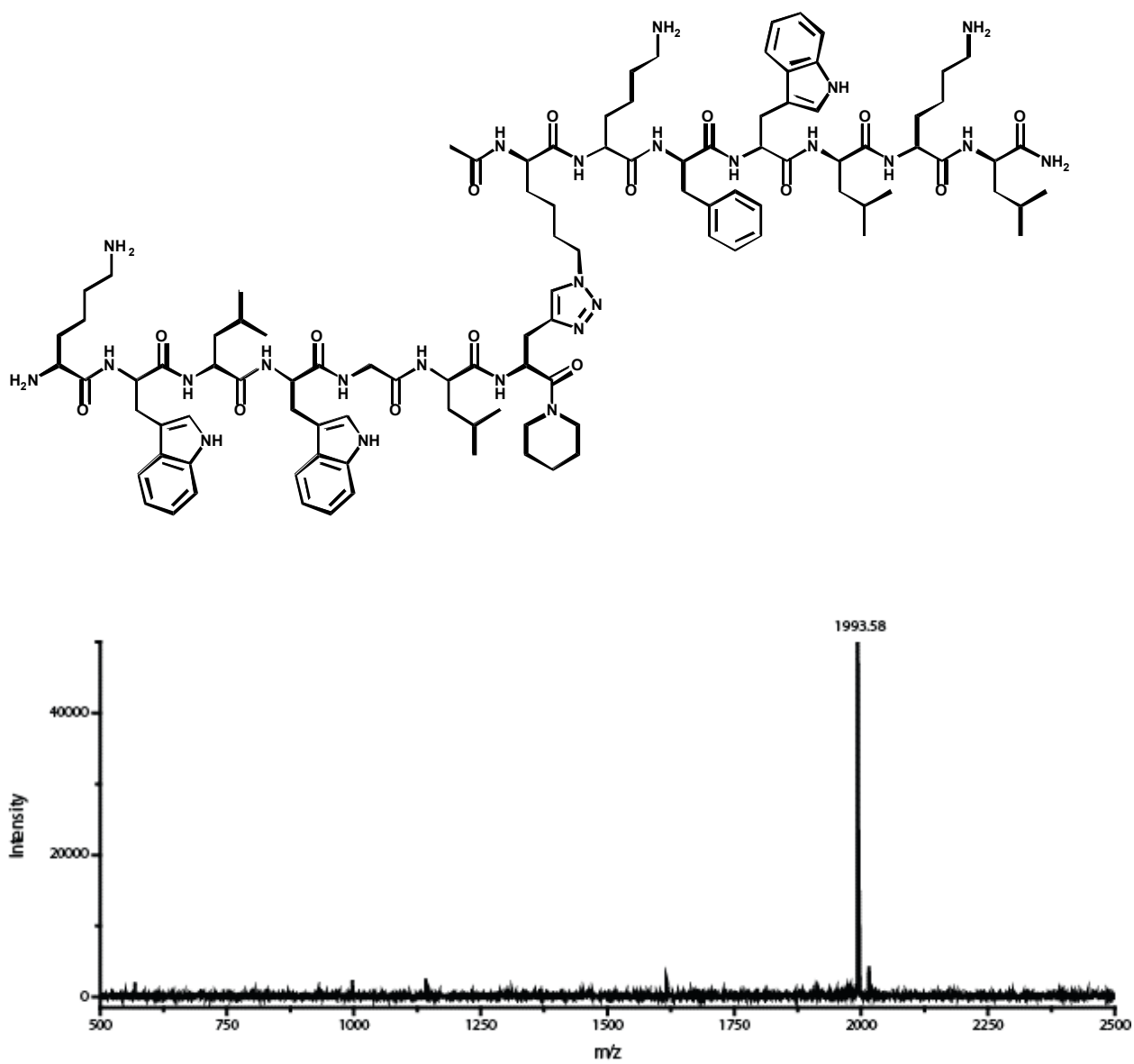


Figure B6. Biligand kwlwGl-Tz2-kfwlkl (Mol. Wt.: 1993.49)

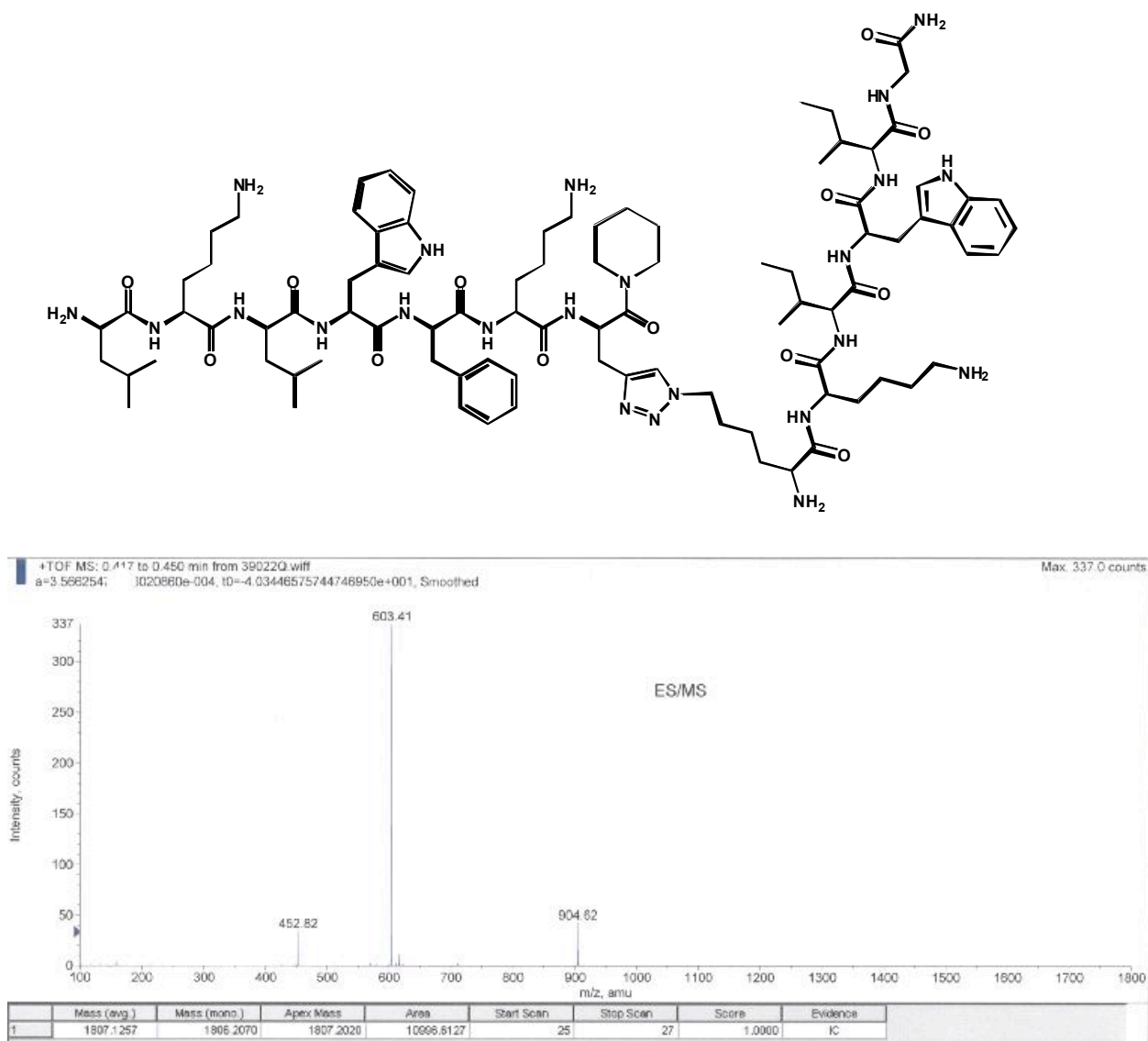


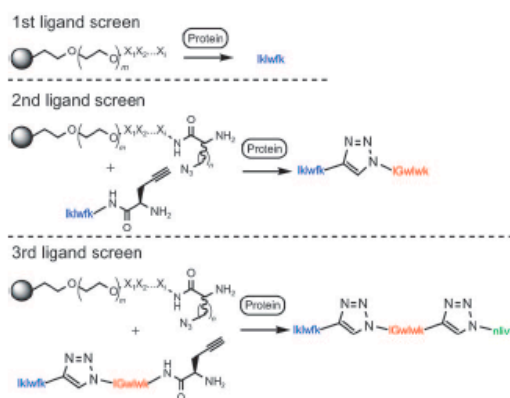
Figure B7. Biligand lklwfk-Tz5-kiwiG (Mol. Wt.: 1807)

Affinity Agents

Iterative In Situ Click Chemistry Creates Antibody-like Protein-Capture Agents**

Heather D. Agnew, Rosemary D. Rohde, Steven W. Millward, Arundhati Nag, Woon-Seok Yeo, Jason E. Hein, Suresh M. Pitram, Abdul Ahad Tariq, Vanessa M. Burns, Russell J. Krom, Valery V. Fokin, K. Barry Sharpless, and James R. Heath*

Most protein-detection methods rely upon antibody-based capture agents.^[1] A high-quality antibody exhibits high affinity and selectivity for its cognate protein. However, antibodies are expensive and can be unstable towards dehydration, pH variation, thermal shock, and many other chemical and biochemical processes.^[2–3] Several alternative protein-capture agents, including oligonucleotide aptamers and phage-display peptides, have been reported, each of which has advantages as well as significant limitations.^[4–10] A further alternative is the use of one-bead-one-compound (OBOC) peptide or peptide-mimetic libraries.^[11–13] An advantage of OBOC libraries is that chemical stability, water solubility, and other desired properties may be designed into the compounds. However, OBOC libraries contain typically only 10^4 – 10^6 elements, and so significant trade-offs are made between peptide length and library chemical diversity. Herein we report the use of in situ click chemistry as a screening approach towards the construction of multi-ligand protein-capture agents (Scheme 1). We harnessed the method to produce a triligand capture agent against human and bovine carbonic anhydrase II (h(b)CAII) as a model system.



Scheme 1. Representation of an in situ screen based on click chemistry for the preparation of a multiligand protein-capture agent. 1st: A comprehensive OBOC peptide library on TentaGel (TG) beads (X_i : variable region) is incubated together with a fluorescently labeled protein target. Hit beads are identified on the basis of their fluorescence intensity. 2nd: A hit peptide from the 1st screen is employed as the anchor ligand and incubated in the presence of the OBOC peptide library, in which the peptides are now appended with an azide linker ($n = 4, 8$). 3rd: The process is repeated, but with the biligand from the 2nd screen as the new anchor unit to enable the rapid identification of higher-order multiligand capture agents.

In situ click chemistry has been utilized previously for the rapid identification of small-molecule enzymatic inhibitors.^[16–20] These studies implemented libraries of small-molecule building blocks functionalized with either azide or acetylene groups. During the screening of the target protein with the molecular libraries, the protein plays an active role in the selection and covalent assembly of a new inhibitor. In these systems, the protein accelerates the Huisgen 1,3-dipolar cycloaddition by holding the two fragments—azide and acetylene—in proximity. The protein exhibits exquisite selectivity; it only promotes the formation of a 1,2,3-triazole (Tz) between those library elements that can be brought into a precise relative molecular orientation on the protein surface. The result is a biligand inhibitor with an affinity that approaches the full product of the affinities of the individual molecular components. Furthermore, the triazole itself can contribute to the binding affinity observed for this inhibitor.

The advances we report herein are manifold. First, the production of the capture agent does not require prior

[*] H. D. Agnew, R. D. Rohde, Dr. S. W. Millward, A. Nag, Dr. W.-S. Yeo,^[1] A. A. Tariq, V. M. Burns, R. J. Krom, Prof. J. R. Heath
Division of Chemistry and Chemical Engineering
California Institute of Technology
1200 East California Boulevard, Pasadena, CA 91125 (USA)
Fax: (+1) 626-395-2355
E-mail: heath@caltech.edu
Homepage: <http://www.its.caltech.edu/~heathgrp>
Dr. J. E. Hein, Dr. S. M. Pitram, Prof. V. V. Fokin, Prof. K. B. Sharpless
Department of Chemistry and
The Skaggs Institute for Chemical Biology
The Scripps Research Institute
10550 North Torrey Pines Road, La Jolla, CA 92037 (USA)

[*] Current address: Department of Bioscience and Biotechnology
Konkuk University, Seoul, 143-701 (Korea)

[**] This research was supported by the National Cancer Institute, grant No. 5U54 CA119347 (J.R.H.), the W. M. Keck Foundation (K.B.S.), and a subcontract from the MITRE Corporation (J.R.H.). Postdoctoral and graduate fellowships were provided by the NSF and PEO (H.D.A.), the Gates Foundation (R.D.R.), the NSERC (J.E.H.), and the NCI (S.W.M.). We also acknowledge H. C. Kolb, S. S. Lee, J. Cha, J. Lim, S. Tan, S. Y. Yeo, A. Srivastava, M. Barrientos, E. Johnson Chavarria, A. Stuparu, J. Vielmetter, and C. S. Parker for useful discussions and assistance.

Supporting information for this article is available on the WWW under <http://dx.doi.org/10.1002/anie.200900488>.

Communications

knowledge of affinity agents against the target protein. Our anchor ligand was a relatively weakly binding short heptapeptide comprised of non-natural D-amino acids and a terminal, acetylene-containing amino acid (D-propargylglycine, D-Pra). It was identified by using a standard, two-generation OBOC screen against bCAII; the peptide sequence on the hit beads was identified by Edman degradation (see the Supporting Information). This first anchor ligand, lklwfk-(D-Pra), exhibited an approximately 500 μM affinity for bCAII (see the Supporting Information). The second advance is that the in situ click screen (Scheme 1) samples a very large chemical space. Our OBOC library consisted of short-chain peptides and was comprehensive. We utilized five copies of a 2×10^7 -element library of D stereoisomers: $\text{Az}_n\text{-x}_2\text{-x}_3\text{-x}_4\text{-x}_5\text{-x}_6\text{-Az}_n$ (Az_n = azide-containing amino acids ($n=4, 8$); x_i = any D-amino acid except Cys). Az_n building blocks were prepared by published methods (see the Supporting Information).^[21–23]

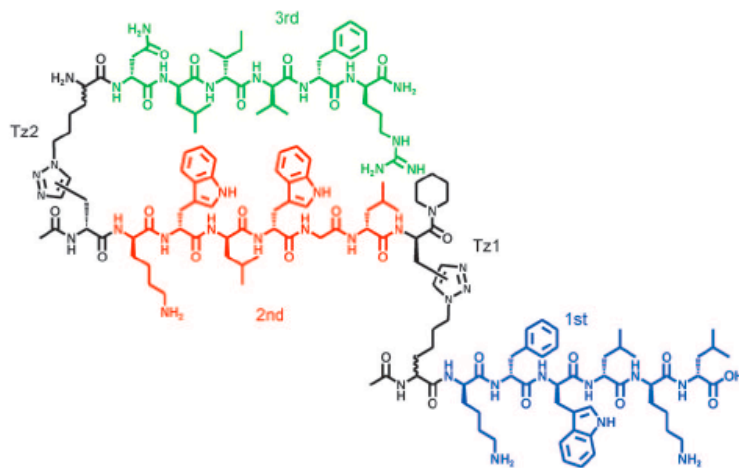
The third advance is that the process can be repeated. Once a biligand has been identified, that biligand can serve as the anchor ligand. The same OBOC library is employed to identify a triligand, and so forth (Scheme 1). Upon the addition of each ligand to the capture agent, the affinity and the selectivity of the capture agent for its cognate protein increase rapidly. With lklwfk-(D-Pra) as the anchor ligand, we used the screen in Scheme 1, followed by a more focused screen against a much smaller OBOC library, to identify the biligand (D-Pra)-kwlwGl-Tz1-kfwlkl against bCAII. This biligand exhibited a 3 μM binding affinity for bCAII, as measured by surface plasmon resonance (SPR). With this biligand as the new anchor unit, we repeated the screen in Scheme 1, followed again by a focused screen in situ, to identify a triligand, rfviln-Tz2-kwlwGl-Tz1-kfwlkl (Scheme 2), which exhibited 64 and 45 nM binding affinities against bCAII and hCAII, respectively, as determined by SPR.^[24] The triligand can be prepared in bulk quantities by

standard solid-phase synthesis of the individual heptapeptides followed by ligation through the copper(I)-catalyzed azide–alkyne cycloaddition (CuAAC).^[25] Details of all screening conditions and OBOC libraries are in the Supporting Information.

In the case of previously reported screens based on in situ click chemistry, the triazole product, or biligand inhibitor, was identified by chromatographic separation followed by mass spectrometry.^[16–20] In the screen in Scheme 1, the triazole product represents a very small fraction of the peptide on the bead, and so only the variable region of the peptide is identified during the peptide-sequencing step. Thus, we sought to confirm the validity of the in situ screen in multiple ways.

For triligand screens, we generated a histogram to chart the position-dependent frequency of amino acids observed on the hit beads (Figure 1). On the basis of this histogram, we constructed two focused OBOC libraries. The first library contained only the 3rd-ligand variable region and was used in an in situ screen. The second library contained the same 3rd-ligand variable region and was coupled by CuAAC (Tz2; Scheme 2), to the biligand. This on-bead triligand screen and the in situ screen both yielded the same consensus sequence. This result confirmed the equivalence of the two screen types. We also carried out a third in situ screen in which the Az_n (azide-containing) amino acid was not included in the OBOC library. The formation of a triazole linkage was thus prohibited. This screen generated a very different, and much less homologous, set of hit sequences (Figure 1). This result confirmed the importance of the triazole linkage in the formation of a multiligand species.

Finally, we developed an enzyme-linked colorimetric assay for detecting the on-bead, protein-templated multiligand inhibitor (Figure 2a). For this assay, we prepared a biotin conjugate of the biligand anchor (biotin-(EG)₂-(D-Pra)-kwlwGl-Tz1-kfwlkl; EG = ethylene glycol), which was then employed in an in situ OBOC screen (Scheme 1) with beads appended with the single consensus 3rd ligand $\text{Az}_4\text{-nlivfr}$. After the screen, alkaline phosphatase–streptavidin (AP–SA) was introduced to bind to any potential bead-bound biotinylated triligand. Excess AP–SA was removed, and the beads were incubated with 5-bromo-4-chloro-3-indoyl phosphate (BCIP), a chromogenic substrate for AP (Figure 2b; see the Supporting Information for details).^[26] The purple color is a positive indicator for an on-bead triligand. The triligand was only formed in the presence of the protein b(h)CAII, and not when the protein substrate was transferrin (Tf), bovine serum albumin (BSA), or absent. Similarly, the



Scheme 2. Triligand capture agent for the protein b(h)CAII. The triazoles (Tz1, Tz2) can be either 1,4 (*anti*) or 1,5 (*syn*) isomers since the protein-templated reaction can produce both products.

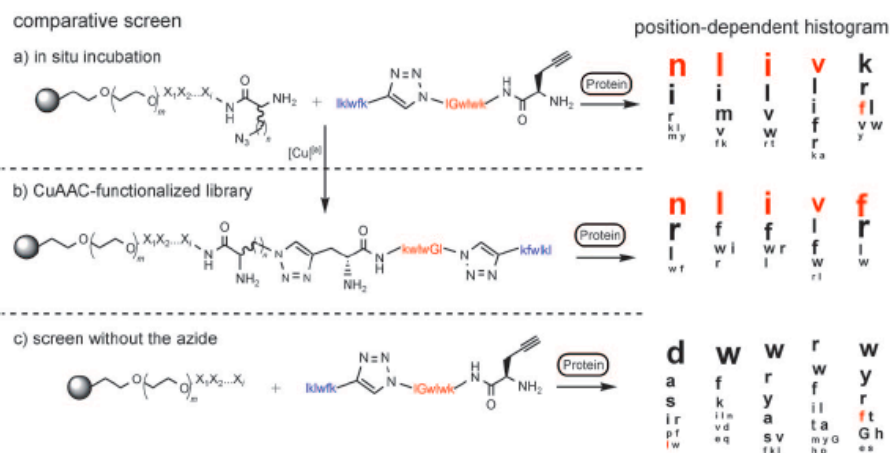


Figure 1. Position-dependent histograms for the first-generation in situ click screens (for peptides with (a) and without (c) an azide-containing amino acid) to generate a triligand. a) For the in situ screen, a third of the beads had no azide group at the x_1 and x_2 positions, but all hit beads contained an azide group. b) First- and second-generation CuAAC-library screens yielded independent validation of the result obtained in the in situ screens. The final, consensus triligand sequence is indicated by red font. c) In the absence of the azide functionality, completely different hit sequences were obtained. Sample size: in situ, 25 hits; in situ, no azide, 24 hits; CuAAC library, 21 hits. [a] See the Supporting Information for CuAAC conditions.

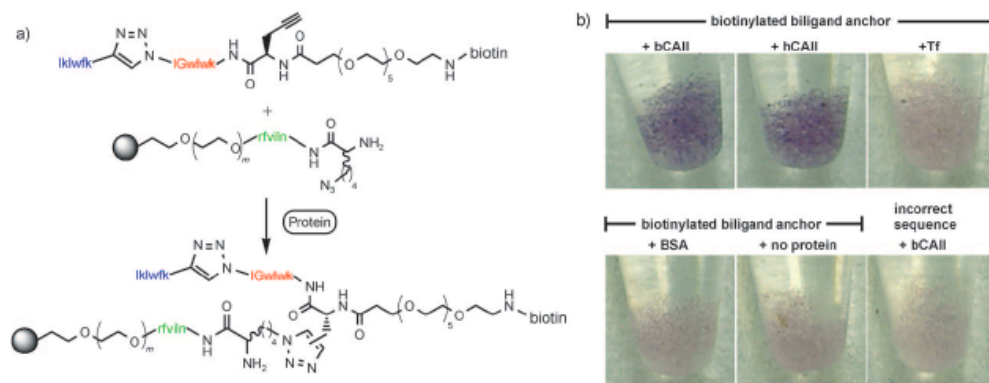


Figure 2. a) Scheme for the in situ click assay for on-bead triazole formation with a biotinylated biligand anchor (biotin-(EG)₅-(D-Pra)-kwlwGI-Tz1-kfwk). b) After treatment with AP-SA then BClP, purple beads are a positive indicator of triazole formation. The triligand was only formed by the in situ process in the presence of b(h)CAII, and not when the protein was TF, BSA, or absent. The on-bead triligand was not observed when the biligand anchor sequence was incorrect.

on-bead triligand was not obtained when the incorrect biligand anchor sequence was used.

For the first-generation biligand and triligand screens, a striking result was the extremely high sequence homology that was observed for the hit beads. For example, for the first 17 hit beads sequenced from the initial biligand in situ screen (with five copies of a 2×10^7 -element OBOD library), two peptides were identical, and a third peptide differed by only a single amino acid (see the Supporting Information). For the initial triligand screen (against the same library), the most commonly observed amino acids by position (Figure 1) reflect the consensus sequence identified in the second-generation

(focused) screen almost exactly. Such sequence homology is unique to the in situ screens and suggests that these screens generate highly selective hits. Thus, multiligand capture agents identified in this way should exhibit high selectivity. In a dot-blot experiment, b(h)CAII was detected selectively by the triligand in 10 % porcine serum with a detection limit of 20 ng of the protein (Figure 3; see the Supporting Information for details). The sequence identity of the proteins bCAII and hCAII is greater than 80 % (PDB ID: 1CA2, 1V9E).

The protein bCAII is also known to have intrinsic esterase activity. It catalyzes the hydrolysis of 4-nitrophenyl acetate (4-

Communications

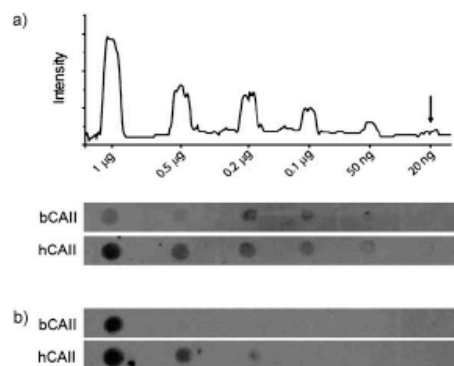


Figure 3. a) Dot blot illustrating the limit of detection by the triligand for b(h)CAII in 10% porcine serum. b) When the biligand anchor (o-Pra)-kwlwGI-Tz1-kfwlkl was used as the capture agent in 0.1% serum, the sensitivity was reduced more than 10-fold.

NPA) to the chromophore 4-nitrophenol (4-NP).^[27] Thus, we utilized the 4-NPA assay to determine whether the triligand binds to the active site (see the Supporting Information). The triligand did not interfere with the enzyme activity of bCAII; it apparently binds away from the active site, or at least does not interfere with the normal catalysis of the active site. Such off-site, yet highly selective, binding is common for natural antibodies raised against proteins and binds well for the scope of the technique we have described.

We are currently exploring the limits of the binding affinity that can be attained with these multiligand inhibitors and developing multiligand capture agents against other proteins so as to demonstrate the generality and/or limitations of this approach.

Received: January 26, 2009

Published online: ■■■ ■■■, 2009

Keywords: click chemistry · combinatorial chemistry · inhibitors · peptides · protein-capture agents

- [1] C. A. K. Borrebaeck, *Immunol. Today* **2000**, *21*, 379.
- [2] T. Kodadek, M. M. Reddy, H. J. Olivos, K. Bachhawat-Sikder, P. G. Alluri, *Acc. Chem. Res.* **2004**, *37*, 711.
- [3] N. Blow, *Nature* **2007**, *447*, 741.
- [4] G. P. Smith, V. A. Petrenko, *Chem. Rev.* **1997**, *97*, 391.

- [5] J. C. Cox, A. Hayhurst, J. Hesselberth, T. S. Bayer, G. Georgiou, A. D. Ellington, *Nucleic Acids Res.* **2002**, *30*, 108e.
- [6] T. G. McCauley, N. Hamaguchi, M. Stanton, *Anal. Biochem.* **2003**, *319*, 244.
- [7] J. F. Lee, J. R. Hesselberth, L. A. Meyers, A. D. Ellington, *Nucleic Acids Res.* **2004**, *32*, 95D.
- [8] L. Gold, B. Polisky, O. Uhlenbeck, M. Yarus, *Annu. Rev. Biochem.* **1995**, *64*, 763.
- [9] P. E. Burmeister, S. D. Lewis, R. F. Silva, J. R. Preiss, L. R. Horwitz, P. S. Pendergrast, T. G. McCauley, J. C. Kurz, D. M. Epstein, C. Wilson, A. D. Keefe, *Chem. Biol.* **2005**, *12*, 25.
- [10] D. Proské, M. Blank, R. Buhmann, A. Resch, *Appl. Microbiol. Biotechnol.* **2005**, *69*, 367.
- [11] K. S. Lam, M. Lebl, V. Krchnák, *Chem. Rev.* **1997**, *97*, 411.
- [12] A. Furka, F. Sebestyén, M. Asgedom, G. Dibo, *Int. J. Pept. Protein Res.* **1991**, *37*, 487.
- [13] H. M. Geysen, T. J. Mason, *Bioorg. Med. Chem. Lett.* **1993**, *3*, 397.
- [14] P. G. Alluri, M. M. Reddy, K. Bachhawat-Sikder, H. J. Olivos, T. Kodadek, *J. Am. Chem. Soc.* **2003**, *125*, 13995.
- [15] a) M. M. Reddy, K. Bachhawat-Sikder, T. Kodadek, *Chem. Biol.* **2004**, *11*, 1127; b) D. G. Udugamasooriya, S. P. Dineen, R. A. Brekken, T. Kodadek, *J. Am. Chem. Soc.* **2008**, *130*, 5744.
- [16] W. G. Lewis, L. G. Green, F. Grynszpan, Z. Radić, P. R. Carlier, P. Taylor, M. G. Finn, K. B. Sharpless, *Angew. Chem.* **2002**, *114*, 1095; *Angew. Chem. Int. Ed.* **2002**, *41*, 1053.
- [17] R. Manetsch, A. Krasinski, Z. Radić, J. Rauschel, P. Taylor, K. B. Sharpless, H. C. Kolb, *J. Am. Chem. Soc.* **2004**, *126*, 12809.
- [18] Y. Bourne, H. C. Kolb, Z. Radić, K. B. Sharpless, P. Taylor, P. Marchot, *Proc. Natl. Acad. Sci. USA* **2004**, *101*, 1449.
- [19] V. P. Mocharla, B. Colasson, L. V. Lee, S. Röper, K. B. Sharpless, C.-H. Wong, H. C. Kolb, *Angew. Chem.* **2005**, *117*, 118; *Angew. Chem. Int. Ed.* **2005**, *44*, 116.
- [20] M. Whiting, J. Muldoon, Y.-C. Lin, S. M. Silverman, W. Lindstrom, A. J. Olson, H. C. Kolb, M. G. Finn, K. B. Sharpless, J. H. Elder, V. V. Fokin, *Angew. Chem.* **2006**, *118*, 1463; *Angew. Chem. Int. Ed.* **2006**, *45*, 1435.
- [21] H. K. Chenault, J. Dahmer, G. M. Whitesides, *J. Am. Chem. Soc.* **1989**, *111*, 6354.
- [22] J. C. M. van Hest, K. L. Kiick, D. A. Tirrell, *J. Am. Chem. Soc.* **2000**, *122*, 1282.
- [23] H.-S. Lee, J.-S. Park, B. M. Kim, S. H. Gellman, *J. Org. Chem.* **2003**, *68*, 1575.
- [24] Although we have not yet been able to determine which regioisomer of the in situ click product was formed, the authentic triligand synthesized by CuAAC to test affinity and selectivity was definitely the 1,4-triazole.
- [25] V. V. Rostovtsev, L. G. Green, V. V. Fokin, K. B. Sharpless, *Angew. Chem.* **2002**, *114*, 2708; *Angew. Chem. Int. Ed.* **2002**, *41*, 2596.
- [26] G. Liu, K. S. Lam in *Combinatorial Chemistry—A Practical Approach* (Ed.: H. Fenniri), Oxford University Press, USA, **2000**, pp. 43–44.
- [27] Y. Pocker, J. T. Stone, *Biochemistry* **1967**, *6*, 668.